

ISSN 1881-7831 Online ISSN 1881-784X

DD & T

Drug Discoveries & Therapeutics

Volume 10, Number 6
December, 2016



www.ddtjournal.com

DD & T

Drug Discoveries & Therapeutics



ISSN: 1881-7831
Online ISSN: 1881-784X
CODEN: DDTRBX
Issues/Year: 6
Language: English
Publisher: IACMHR Co., Ltd.

Drug Discoveries & Therapeutics is one of a series of peer-reviewed journals of the International Research and Cooperation Association for Bio & Socio-Sciences Advancement (IRCA-BSSA) Group and is published bimonthly by the International Advancement Center for Medicine & Health Research Co., Ltd. (IACMHR Co., Ltd.) and supported by the IRCA-BSSA and Shandong University China-Japan Cooperation Center for Drug Discovery & Screening (SDU-DDSC).

Drug Discoveries & Therapeutics publishes contributions in all fields of pharmaceutical and therapeutic research such as medicinal chemistry, pharmacology, pharmaceutical analysis, pharmaceuticals, pharmaceutical administration, and experimental and clinical studies of effects, mechanisms, or uses of various treatments. Studies in drug-related fields such as biology, biochemistry, physiology, microbiology, and immunology are also within the scope of this journal.

Drug Discoveries & Therapeutics publishes Original Articles, Brief Reports, Reviews, Policy Forum articles, Case Reports, News, and Letters on all aspects of the field of pharmaceutical research. All contributions should seek to promote international collaboration in pharmaceutical science.

Editorial Board

Editor-in-Chief:

Kazuhisa SEKIMIZU
The University of Tokyo, Tokyo, Japan

Co-Editors-in-Chief:

Xishan HAO
Tianjin Medical University, Tianjin, China
Munehiro NAKATA
Tokai University, Hiratsuka, Japan

Chief Director & Executive Editor:

Wei TANG
The University of Tokyo, Tokyo, Japan

Senior Editors:

Guanhua DU
Chinese Academy of Medical Science and Peking Union Medical College, Beijing, China
Xiao-Kang LI
National Research Institute for Child Health and Development, Tokyo, Japan
Masahiro MURAKAMI
Osaka Ohtani University, Osaka, Japan
Yutaka ORIHARA
The University of Tokyo, Tokyo, Japan
Tomofumi SANTA
The University of Tokyo, Tokyo, Japan
Hongbin SUN
China Pharmaceutical University, Nanjing, China

Fengshan WANG
Shandong University, Ji'nan, China

Managing Editor:

Hiroshi HAMAMOTO
The University of Tokyo, Tokyo, Japan

Web Editor:

Yu CHEN
The University of Tokyo, Tokyo, Japan

Proofreaders:

Curtis BENTLEY
Roswell, GA, USA
Thomas R. LEBON
Los Angeles, CA, USA

Editorial and Head Office:

Pearl City Koishikawa 603,
2-4-5 Kasuga, Bunkyo-ku,
Tokyo 112-0003, Japan
Tel.: +81-3-5840-9697
Fax: +81-3-5840-9698
E-mail: office@ddtjournal.com

Drug Discoveries & Therapeutics

Editorial and Head Office

Pearl City Koishikawa 603, 2-4-5 Kasuga, Bunkyo-ku,
Tokyo 112-0003, Japan

Tel: +81-3-5840-9697, Fax: +81-3-5840-9698
E-mail: office@ddtjournal.com
URL: www.ddtjournal.com

Editorial Board Members

Alex ALMASAN (Cleveland, OH)	Rodney J. Y. HO (Seattle, WA)	Xingyuan MA (Shanghai)	Yuhong XU (Shanghai)
John K. BUOLAMWINI (Memphis, TN)	Hsing-Pang HSIEH (Zhunan, Miaoli)	Ken-ichi MAFUNE (Tokyo)	Bing YAN (Ji'nan, Shandong)
Jianping CAO (Shanghai)	Yongzhou HU (Hangzhou, Zhejiang)	Sridhar MANI (Bronx, NY)	Yun YEN (Duarte, CA)
Shousong CAO (Buffalo, NY)	Yu HUANG (Hong Kong)	Tohru MIZUSHIMA (Tokyo)	Yasuko YOKOTA (Tokyo)
Jang-Yang CHANG (Tainan)	Hans E. JUNGINGER (Marburg, Hesse)	Abdulla M. MOLOKHIA (Alexandria)	Takako YOKOZAWA (Toyama, Toyama)
Fen-Er CHEN (Shanghai)	Amrit B. KARMARKAR (Karad, Maharashtra)	Yoshinobu NAKANISHI (Kanazawa, Ishikawa)	Rongmin YU (Guangzhou, Guangdong)
Zhe-Sheng CHEN (Queens, NY)	Toshiaki KATADA (Tokyo)	Weisan PAN (Shenyang, Liaoning)	Guangxi ZHAI (Ji'nan, Shandong)
Zilin CHEN (Wuhan, Hubei)	Gagan KAUSHAL (Philadelphia, PA)	Rakesh P. PATEL (Mehsana, Gujarat)	Liangren ZHANG (Beijing)
Shaofeng DUAN (Lawrence, KS)	Ibrahim S. KHATTAB (Kuwait)	Shivanand P. PUTHLI (Mumbai, Maharashtra)	Lining ZHANG (Ji'nan, Shandong)
Chandradhar DWIVEDI (Brookings, SD)	Shiroh KISHIOKA (Wakayama, Wakayama)	Shafi qur RAHMAN (Brookings, SD)	Na ZHANG (Ji'nan, Shandong)
Mohamed F. EL-MILIGI (6th of October City)	Robert Kam-Ming KO (Hong Kong)	Adel SAKR (Cairo)	Ruiwen ZHANG (Amarillo, TX)
Hao FANG (Ji'nan, Shandong)	Nobuyuki KOBAYASHI (Nagasaki, Nagasaki)	Gary K. SCHWARTZ (New York, NY)	Xiu-Mei ZHANG (Ji'nan, Shandong)
Marcus L. FORREST (Lawrence, KS)	Norihiro KOKUDO (Tokyo, Japan)	Yuemao SHEN (Ji'nan, Shandong)	Yongxiang ZHANG (Beijing)
Takeshi FUKUSHIMA (Funabashi, Chiba)	Toshiro KONISHI (Tokyo)	Brahma N. SINGH (New York, NY)	
Harald HAMACHER (Tübingen, Baden-Württemberg)	Chun-Guang LI (Melbourne)	Tianqiang SONG (Tianjin)	(As of February 2016)
Kenji HAMASE (Fukuoka, Fukuoka)	Minyong LI (Ji'nan, Shandong)	Sanjay K. SRIVASTAVA (Amarillo, TX)	
Junqing HAN (Ji'nan, Shandong)	Xun LI (Ji'nan, Shandong)	Chandan M. THOMAS (Bradenton, FL)	
Xiaojiang HAO (Kunming, Yunnan)	Jikai LIU (Kunming, Yunnan)	Murat TURKOGLU (Istanbul)	
Kiyoshi HASEGAWA (Tokyo)	Xinyong LIU (Ji'nan, Shandong)	Hui WANG (Shanghai)	
Waseem HASSAN (Rio de Janeiro)	Yuxiu LIU (Nanjing, Jiangsu)	Quanxing WANG (Shanghai)	
Langchong HE (Xi'an, Shaanxi)	Hongxiang LOU (Jinan, Shandong)	Stephen G. WARD (Bath)	

Reviews

- 276 - 284 **Nitric oxide donor hybrid compounds as promising anticancer agents.**
Qin-ge Ding, Jie Zang, Shuai Gao, Qianwen Gao, Wenwen Duan, Xiaoyang Li, Wenfang Xu, Yingjie Zhang
- 285 - 291 **The role of growth factors in nerve regeneration.**
Mehmet Emin Önger, Burcu Delibaş, Aysin Pinar Türkmen, Erkan Erener, Berrin Zuhall Altunkaynak, Süleyman Kaplan
- 292 - 299 **A review of complementary therapies for chemotherapy induced gastrointestinal mucositis.**
Raja A.H Kuchay

Original Articles

- 300 - 306 **Generic selection criteria for safety and patient benefit [VI]: Comparing the physicochemical and pharmaceutical properties of brand-name, generic, and OTC felbinac tapes.**
Yuko Wada, Yukie Takaoka, Mitsuru Nozawa, Miho Goto, Ken-ichi Shimokawa, Fumiyoshi Ishii
- 307 - 313 **Fabrication of Janus particles composed of poly (lactic-co-glycolic) acid and hard fat using a solvent evaporation method.**
Akihiro Matsumoto, Satoshi Murao, Michiko Matsumoto, Chie Watanabe, Masahiro Murakami
- 314 - 322 **The serum/PDGF-dependent "melanogenic" role of the minute level of the oncogenic kinase PAK1 in melanoma cells proven by the highly sensitive kinase assay.**
Pham Thi Be Tu, Binh Cao Quan Nguyen, Shinkichi Tawata, Cheong-Yong Yun, Eung Gook Kim, Hiroshi Maruta
- 323 - 328 **Effect of astigmatism on refraction in children with high hyperopia**
Hao Hu, Jinhui Dai, Minjie Chen, Lanting Chen, Lingli Jiang, Ran Lin, Ling Wang

CONTENTS

(Continued)

- 329 - 333 **The use of mannitol in HIV-infected patients with symptomatic cryptococcal meningitis.**
Zhiliang Hu, Yongfeng Yang, Jian cheng, Cong Cheng, Yun Chi, Hongxia Wei

Case Report

- 334 - 337 **A newborn with hemorrhagic meningoencephalitis due to *Proteus mirabilis*.**
Yesim Coskun, Ipek Akman, Canan Yildirim, Mustafa Kemal Demir

Letter

- 338 - 339 **Biotin treatment causing erroneous immunoassay results: A word of caution for clinicians.**
Raashda Ainuddin Sulaiman

Guide for Authors

Copyright

Nitric oxide donor hybrid compounds as promising anticancer agents

Qin-ge Ding, Jie Zang, Shuai Gao, Qianwen Gao, Wenwen Duan, Xiaoyang Li, Wenfang Xu*, Yingjie Zhang*

Department of Medicinal Chemistry, School of Pharmaceutical Sciences, Shandong University, Ji'nan, Shandong, China.

Summary Nitric oxide (NO) plays important roles in cardiovascular regulation, nerve transmission delivery and immune responses. In the last semicentury, it has been proved that though low concentration of NO is tumor-promoting, high concentration of NO could exhibit multiple antitumor effects, which led to the research and development of kinds of NO donors and NO donor hybrid compounds as antitumor agents. Herein, the recent development of NO donor hybrid compounds is briefly reviewed.

Keywords: NO releasing agents, antitumor, NOSs, furoxan, NO-NSAIDs

1. Introduction

Nitric oxide (NO), identified in the 1980s as a vasoactive small molecule, can regulate various pathological and physiological processes in cardiovascular, nerve transmission delivery and immune systems (1,2). Besides, NO also plays roles in other physiological functions such as cellular redox and anti-pathogenic responses (3-6).

The functions of NO are dependent on the interaction with cell factors. Two signal pathways have been discussed for mechanisms of NO. In the NO/sGC/cGMP pathway, endogenous NO synthesized by NO synthases (NOSs) activates soluble guanylate cyclase (sGC) in cells such as muscles, neurons and leukocytes. Active sGC catalyzes the synthesis of cyclic GMP (cGMP) (7). Then cGMP activates three effector molecules: the cGMP-dependent protein kinase G (PKG), cGMP-regulated phosphodiesterases, and cGMP-gated ion channels (8). These effectors lead to a cascade of effects including smooth muscle relaxation, inflammatory pain and platelet anticoagulation (9).

In the cGMP-independent pathway, the functions of NO are based on NO-mediated protein modification, including *i*) binding to metal centers; *ii*) nitrosylation of thiol and amine groups; *iii*) nitration of tyrosine, tryptophan, amine, carboxylic acid, and phenylalanine groups; and *iv*) oxidation of thiols (both cysteine and methionine residues) and tyrosine (10).

2. NO-donor hybrid compounds as anti-cancer agents

Because of the promising antitumor effects of NO (11), numerous NO-releasing agents (also called NO-donors) have been developed as antitumor agents, including organic nitrates, synthetic peroxyxynitrite (12), 3-morpholinopyridone (13), furoxans and benzofuroxans and hydroxylamines (14). Increasing research showed that NO donors were effective on various malignant tumors, such as myeloma, breast cancer, ovarian cancer, prostate cancer and pancreatic cancer (15-17). Moreover, it is worth noting that more and more NO-donor hybrids have been designed, synthesized and evaluated as antitumor agents (Table 1), which will be discussed in the following part of this review.

2.1. NO-nucleoside hybrids

Novel NO-releasing 5-FU hybrid (compound 1a, Figure 1) was designed by Cai TB *et al.* with an aim to reduce the toxicity of nucleoside agents. This hybrid showed stronger cytotoxicity on tumor cells and less toxicity

Released online in J-STAGE as advance publication December 18, 2016.

*Address correspondence to:

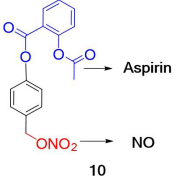
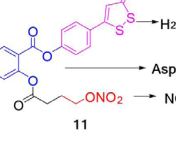
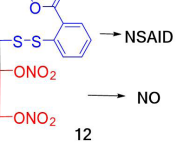
Dr. Yingjie Zhang and Dr. Wenfang Xu, Department of Medicinal Chemistry, School of Pharmacy, Shandong University, 44, West Culture Road, 250012, Ji'nan, Shandong, China.

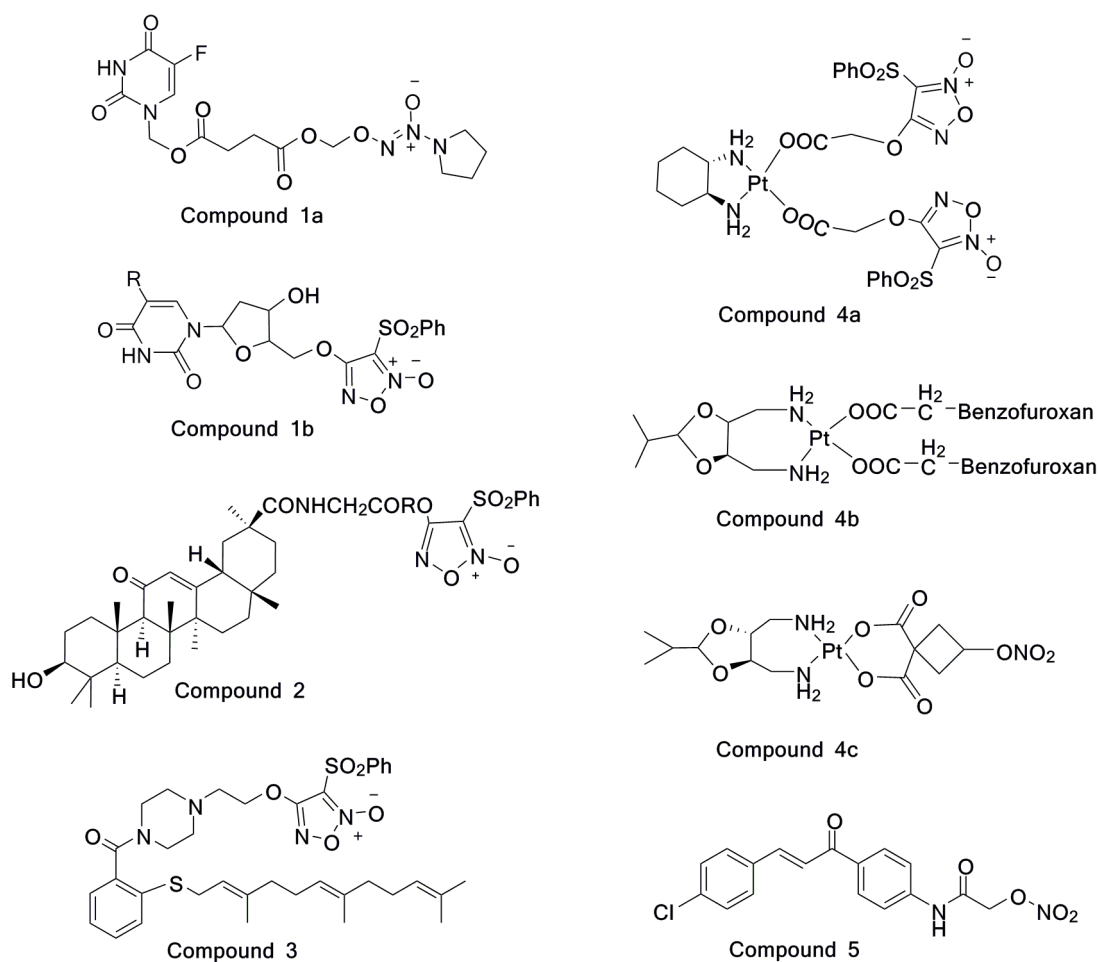
E-mail: zhangyingjie@sde.edu.cn

Table 1. NO-donor hybrids dependent on different antitumor agents

Compound NO.	NO-donor type	Ligand agents	Structure	Cell lines	Ref.
1a	NONOates	5-FU		DU-145, HeLa	18
1b	Furoxan	Nucleoside		143B, EMT-6, KBALB-STK, KBALB, 143B-LTK, Hs578Bst	19
2	Furoxan	Glycyrrhethinic acid		HCC cells	20
3	Furoxan	Farnesylthiosalicylic acid (FTS)		HCC cells	21
4	Furoxan	Platinum		SGC-7901, MCF-7, HepG2, HCT-116	23,24
5	Furoxan	Chalcone		60 human tumor cell lines: molt-4, HL-60, A549...	25,26
6	Furoxan	Oridonin		K562, MGC-803, Bel-7402	28,29
	NONOates	Oridonin		Bel-7402	30
7	Diazeniumdiolate	Oleanolic Acid		HepG2, HCC, H22.	31
8	Furoxan	HDACis		HEL	35,36
9	Furoxan	Tamibarotene		NB4, HL-60	37

Table 1. NO-donor hybrids dependent on different antitumor agents (continued)

Compound NO.	NO-donor type	Ligand agents	Structure	Cell lines	Ref.
10	Nitrate ester	Aspirin		HT 29	40
11	Nitrate ester	H2S- Aspirin		HT-29	41,42
12	Nitrate ester	NSAID		RKO, Caco-2, HT-29, RAW 264.7, SW480	43

**Figure 1. The structure of NO donor hybrids with chemotherapeutic drugs (compound 1-5).**

on normal cells than its parent agent 5-FU in prostate and HeLa cancer cells (18). The latter research from Moharram S *et al.* showed that a NO-nucleoside hybrid

(compound 1b, Figure 1) with the ability to release NO and nucleoside simultaneously leading to high cellular cytotoxic effects by inducing DNA alkylation (19).

2.2. The GA-NO-donor hybrids

The glycyrrhetic acid (GA) and its derivative glycyrrhizin acid both showed protective activity on hepatocytes. Dependent on the researches of Lai Y *et al.*, the hybrid (compound 2) of glycyrrhetic acid and furoxan (Figure 1) showed selective NO-releasing activity in HCC cells (20). Compound 2 induced selective cytotoxicity against human HCC cells with little untoward effect on normal hepatocytes due to the cytotoxicity of NO against liver tumor cells and the protective effects of GA on normal hepatocytes.

2.3. Nitric oxide-releasing derivatives of farnesylthiosalicylic acid

Farnesylthiosalicylic acid (FTS) was a Ras inhibitor that inhibited tumor cell proliferation. But its therapeutic efficacy was limited because of its high cytotoxicity on normal cells (21).

A combination of FTS and furoxan led to a kind of

furoxan hybrid derivative 3 (Figure 1), which showed highly selective cytotoxicity against HCC through cooperative effects of high levels of NO and FTS but not in normal liver cells. The evaluation of phosphorylation of AKT and ERK showed that compound 3 induced stronger inhibition of Akt/ERK phosphorylation than FTS due to the production of NO (21).

2.4. NO donors-Pt hybrids

Platinum-based antitumor drugs, such as cisplatin, carboplatin and oxaliplatin have been widely used in clinical cancer therapy (22). The research of

Zhao J *et al.* found that hybrids of furoxan and Pt (4a, 4b, 4c, Figure 1) were more effective against gastric carcinoma cell line SGC-7901 and colonic carcinoma cell line HCT-116 *in vitro* compared with carboplatin, oxaliplatin alone or a combination of oxaliplatin and furoxan (23). Moreover, it was demonstrated that the hybrids had better stability and less adverse effects than Platinum agents (24).

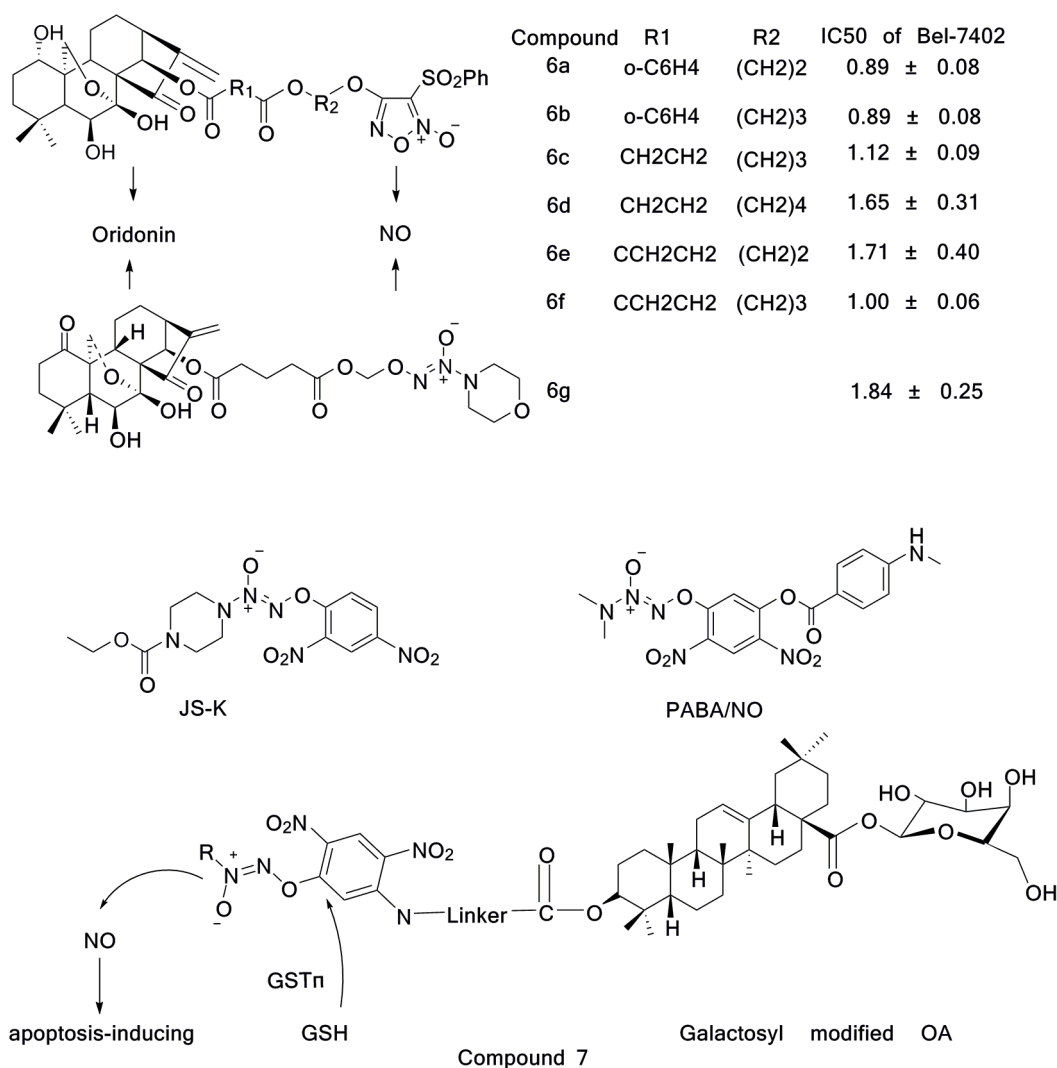


Figure 2. The structure of furoxan-origonin (compound 6) and NO-OA hybrids (compound 7).

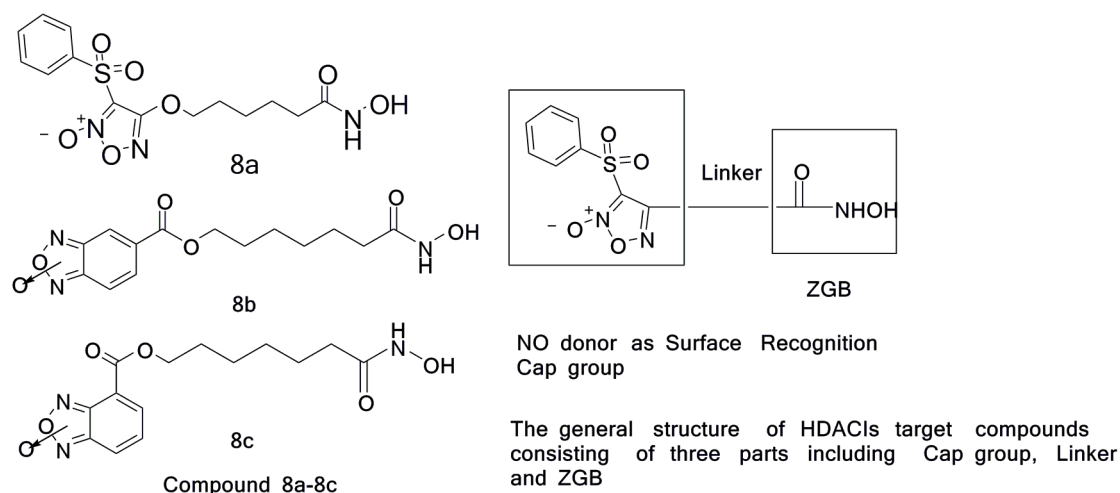


Figure 3. The structure of NO-HDACis (compound 8) and general structure of HDACis.

2.5. NO donors-Pt hybrids

The NO-chalcone hybrid compound 5 (Figure 1) exhibited significant activity against colorectal and melanoma cancers (25). The nitrate ester chimaera 5 exhibited moderate broad-spectrum antitumor activity against nine kinds of tumors, and showed high selectivity toward colon cancer, which proved that a NO donor could enhance selectivity of chalcone (26).

2.6. NO-Oridonin hybrids

Oridonin is a commercially available natural diterpenoid, and it has attracted much more attentions because of its anti-tumor activity (27). Li D *et al.* demonstrated that furoxan-oridonin hybrids showed improved anti-proliferative activity against several tumor cell lines due to their NO-releasing ability (28). The hybrids showed stronger activity when R1 was an aromatic group (6a, 6b, Figure 2) rather than an alkyl group. The anti-proliferative activity was stronger when R2 contained three carbons (29).

Dependent on previous studies, researchers synthesized a series of novel NO-releasing oridonin derivatives coupling diazeniumdiolates with oridonin (30). The hybrids inhibited tumor cell proliferation with IC_{50} ranging from 1.84 to 17.01 μ M. The antitumor activity was positively correlated to the NO releasing ability of these hybrids. Stimulated by the antitumor properties of compounds 6a-6f, the hybrid 6g was a synthesized combination of oridonin and diazeniumdiolate, which exhibited stronger inhibition of Bel-7402 cells than oridonin, diazeniumdiolates and their combination after 72 h treatment (30).

2.7. NO-OA hybrids

Fu J *et al.* synthesized a series of hybrids based on

oleanolic acid (OA) and O_2 -(2,4-dinitrophenyl)-diazoniumdiolate (31). It was anticipated that those hybrids could exhibit selective cytotoxicity to tumor cells because they could only be activated to release NO in GST π overexpressed tumor cells. It was revealed that compound 7, which was much more stable than JS-K and PABA/NO in the absence of GST π (Figure 2), exhibited strong antitumor potency and low toxicity *in vivo* (32). Treatment with compound 7 (38.3 μ M/kg) inhibited H22 tumor growth stronger than 5-FU (153.8 μ M/kg).

2.8. NO-HDACis

Histone deacetylases inhibitors (HDACis) are a family of compounds that could induce cancer cell cycle arrest, differentiation, and apoptosis (33,34). Several HDAC inhibitors (HDACis) have been recently approved by the FDA or CFDA for cancer therapy, including SAHA, LBH589, PXD101 and chidamide for cancer therapy.

The classical structure of HDACis consists of three parts: surface recognition domain, linker and zinc binding group (ZBG). Our laboratory integrated NO donors into the surface recognition domain of HDACis to get two series of NO-donor HDACI hybrids with favorable anti-tumor activity (Figure 3) (35,36). The NO-donor of 8a is furoxan and the NO-donor of 8b and 8c is benzofuroxan. The most potent compound 8a had better *in vitro* and *in vivo* antitumor activity against HEL than the approved HDAC inhibitor SAHA.

2.9. NO-Tamibarotene hybrids

Tamibarotene (AM80), approved in Japan as a selective RAR α agonist, was used for relapsed or refractory acute promyelocytic leukemia (APL). Compared with all-trans retinoic acid (ATRA), tamibarotene could cause higher differentiation and lower drug resistance in APL

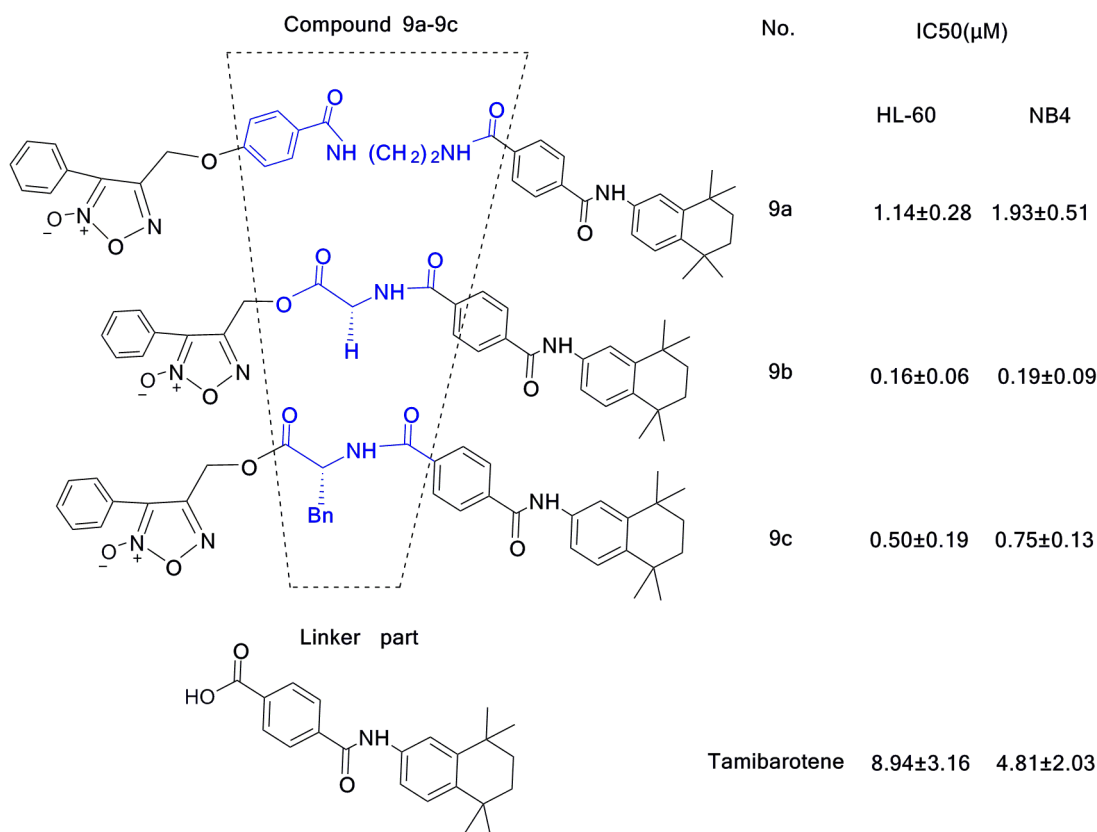


Figure 4. The structure of NO donor hybrids with tamibarotene (compound 9).

cells.

Our laboratory designed a series of novel tamibarotene derivatives by bridging tamibarotene with NO donors with various linkers (Figure 4) (37). The studies showed that these compounds (9a, 9b, 9c) exhibited stronger anti-leukemic activity than tamibarotene. Furthermore, the preliminary structure-activity relationships (SAR) analysis showed that biological activities could be enhanced by introduction of amino acids in the linker part of these hybrids.

2.10. NO-aspirin

Aspirin (ASA), a kind of non-steroidal anti-inflammatory drug (NSAIDs), showed potency in inhibiting colorectal cancer (38). Studies showed that the use of NO-releasing NSAIDs could reduce the gastrointestinal risk (39). Williams JL *et al.* synthesized a NO-NSAID hybrid (compound 10) combining aspirin and nitrate ester based NO donor (Figure 5), and compared its anti-proliferative activity in HT-29 colon tumor cells with NO-ibuprofen *in vitro* (40). Results showed that the IC₅₀ values of compound 10 (NO-aspirin) and NO-ibuprofen were 1 μM and 42 μM, respectively, while the IC₅₀ values of both aspirin and ibuprofen were over 1,000 μM. The subsequent mechanism studies showed that after 48 h treatment with 100 μM of NO-aspirin, PCNA (proliferating cell

nuclear antigen) expression was reduced by 54.5% and more than 83.9% of tumor cells were blocked at G0/G1 phases. In conclusion, these data demonstrated that the NO-NSAIDs are more potent than traditional NSAIDs in anti-proliferation and apoptosis induction against colon cancer (40).

2.11. NBS-1120

NBS-1120 (compound 11, Figure 5), standing for a series of compounds which linked NO-donor nitrate ester and H₂S-aspirin in one molecule, also called NOSH-aspirins, could release gasotransmitters NO and H₂S simultaneously (41).

The lower recurrence of colon cancer and less adverse effects of 11 than parent agent aspirin were recognized. Compound 11 showed anti-inflammatory and anti-proliferative abilities on HT-29 colon tumor cells *in vitro*. It caused G0/G1 cell cycle arrest, inhibited tumor growth and increased apoptosis at high concentrations (42). In animal tests, compound 11 reduced tumor volume (96% reduction) and tumor mass (97% reduction) at 50 mg/kg, whereas aspirin inhibited tumor volume (70% reduction) and tumor mass (65% reduction) at the same dosage. Less lipid peroxidation and more SOD activity were observed in animals treated by 11. These effects might decrease the side effects of compound 11 in the gastric mucosal tissue.

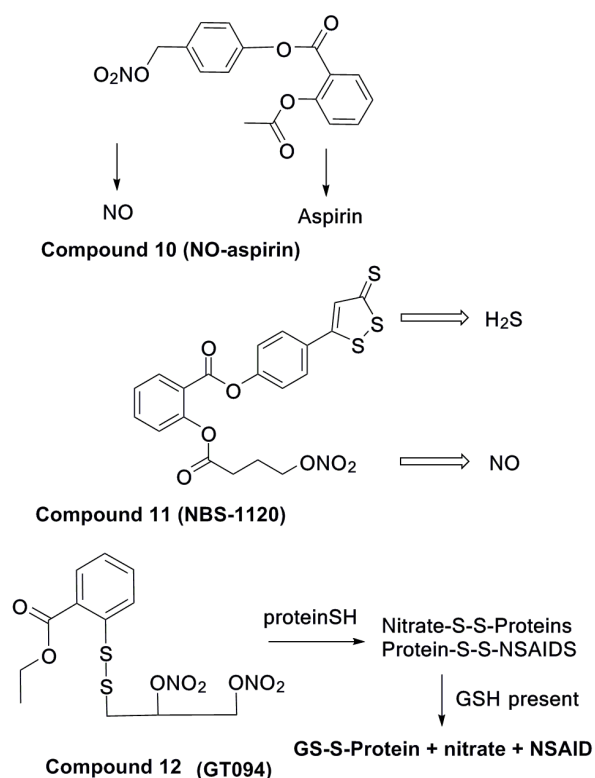


Figure 5. The structure of NO donor hybrids with NSAIDs (compound 10-12).

These results collectively showed that NOSH-aspirin derivatives were superior to aspirin in both efficacy and safety as chemotherapeutics.

2.12. GT-094

Compound 12 (GT-094) was a novel NO hybrid combining nitrate ester and NSAID *via* disulfide (Figure 5) (43). Studies showed that compound 12 inhibited tumor cell growth in both Caco-2 and HT-29 cells (43). Through a 28-week study, Hagos GK *et al.* found compound 12 could reduce weight and multiplicity of tumors in rats contrasted with the NO donor azoxymethane. Moreover, 12 could reduce iNOS expression more potently than azoxymethane alone.

Significant inhibition of proliferation has been shown in RKO and SW480 cancer cells after 24 h treatment with compound 12. Compound 12 down-regulated expressions of pro-survival genes such as hepatocyte growth factor receptor (c-Met), epidermal growth factor receptor (EGFR), Bcl-2, and vascular endothelial growth factor receptors (VEGFR1 and VEGFR1). It also decreased the overexpression of Sp1, Sp3 and Sp4 in colon cancer cells by down-regulating microRNA-27a (miR-27a) and up-regulating ZBTB10 (44).

3. Conclusion

It has been validated with increasing evidence that high

concentration of NO could exhibit potent antitumor activities. Moreover, NO donors combined with other antitumor agents exhibited synergetic or additional antitumor effects, which stimulated research and development of NO donor hybrids as novel anticancer agents. Due to the multiple biological effects of NO in cardiovascular, nerve transmission and immune systems, further research should focus on characterizing the pharmacokinetics profiles and systemic toxicity of these NO donor hybrids to identify promising antitumor leads with higher potency and less side effects.

Acknowledgements

This work was supported by Major Project of Science and Technology of Shandong Province (2015ZDJS04001), Young Scholars Program of Shandong University (YSPSDU, Grant NO. 2016WLJH33).

References

- Ignarro LJ, Buga GM, Wood KS, Byrns RE, Chaudhuri G. Endothelium-derived relaxing factor produced and released from artery and vein is nitric oxide. *Proc Natl Acad Sci U S A.* 1987; 84:9265-9269.
- Ignarro LJ, Napoli C, Loscalzo J. Nitric oxide donors and cardiovascular agents modulating the bioactivity of nitric oxide: An overview. *Circul Res.* 2002; 90:21-28.
- Geller DA, Billiar TR. Molecular biology of nitric oxide synthases. *Cancer Metastasis Rev.* 1998; 17:7-23.
- Quinn AC, Petros AJ, Vallance P. Nitric oxide: An endogenous gas. *Br J Anaesth.* 1995; 74:443-451.
- Jones ML, Ganopolsky JG, Labbé A, Wahl C, Prakash S. Antimicrobial properties of nitric oxide and its application in antimicrobial formulations and medical devices. *Appl Microbiol Biotechnol.* 2010; 88:401-407.
- Bogdan C. Nitric oxide and the immune response. *Nat Immunol.* 2001; 2:907-916.
- Dangel O, Mergia E, Karlisch K, Groneberg D, Koesling D, Friebe A. Nitric oxide-sensitive guanylyl cyclase is the only nitric oxide receptor mediating platelet inhibition. *J Thromb Haemost.* 2010; 8:1343-1352.
- Friebe A, Koesling D. Regulation of nitric oxide-sensitive guanylyl cyclase. *Circul Res.* 2003; 93:96-105.
- Switzer CH, Cheng RY, Ridnour LA, Glynn SA, Ambs S, Wink DA. Ets-1 is a transcriptional mediator of oncogenic nitric oxide signaling in estrogen receptor-negative breast cancer. *Breast Cancer Res.* 2012; 14:1-13.
- Gow AJ, Farkouh CR, Munson DA, Posencheg MA, Ischiropoulos H. Biological significance of nitric oxide-mediated protein modifications. *Am J Physiol Lung Cell Mol Physiol.* 2004; 287:262-268.
- Mocellin S. Nitric oxide: Cancer target or anticancer agent? *Curr Cancer Drug Targets.* 2009; 9:214-236.
- Robinson KM, Beckman JS. Synthesis of peroxynitrite from nitrite and hydrogen peroxide. *Methods Enzymol.* 2005; 396:207-214.
- Feelisch M, Ostrowski J, Noack E. On the mechanism of NO release from sydnonimines. *J Cardiovasc Pharmacol.* 1989; 14 (Suppl 11):S13-S22.
- Miranda KM, Dutton AS, Ridnour LA, Foreman CA,

- Ford E, Paolucci N, Katori T, Tocchetti CG, Mancardi D, Thomas DD. Mechanism of aerobic decomposition of Angeli's salt (sodium trioxodinitrate) at physiological pH. *J Am Chem Soc.* 2005; 127:722-731.
15. Kiziltepe T. JS-K has potent anti-angiogenic activity *in vitro* and inhibits tumour angiogenesis in a multiple myeloma model *in vivo*. *J Pharm Pharmacol.* 2010; 62:145-151.
 16. Sugita H, Kaneki M, Furuhashi S, Hirota M, Takamori H, Baba H. Nitric oxide inhibits the proliferation and invasion of pancreatic cancer cells through degradation of insulin receptor substrate-1 protein. *Mol Cancer Res.* 2010; 8:1152-1163.
 17. Royle JS, Ross JA, Ansell I, Bollina P, Tulloch DN, Habib FK. Nitric oxide donating nonsteroidal anti-inflammatory drugs induce apoptosis in human prostate cancer cell systems and human prostatic stroma *via* caspase-3. *J Urol.* 2004; 172:338-344.
 18. Cai TB, Tang X, Nagorski J, Brauschweiger PG, Wang PG. Synthesis and cytotoxicity of 5-fluorouracil/diazoniumdiolate conjugates. *Bioorg Med Chem.* 2003; 11:4971-4975.
 19. Moharram S, Zhou A, Wiebe LI, Knaus EE. Design and synthesis of 3'- and 5'-O-(3-benzenesulfonylfuroxan-4-yl)-2'-deoxyuridines: Biological evaluation as hybrid nitric oxide donor-nucleoside anticancer agents. *J Med Chem.* 2004; 47:1840-1846.
 20. Lai Y, Shen L, Zhang Z, Liu W, Zhang Y, Ji H, Tian J. Synthesis and biological evaluation of furoxan-based nitric oxide-releasing derivatives of glycyrrhetic acid as anti-hepatocellular carcinoma agents. *Bioorg Med Chem Lett.* 2010; 20:6416-6420.
 21. Ling Y, Ye X, Zhang Z, Zhang Y, Lai Y, Ji H, Peng S, Tian J. Novel Nitric Oxide-releasing derivatives of farnesylthiosalicylic acid: Synthesis and evaluation of antihepatocellular carcinoma activity. *J Med Chem.* 2011; 54:3251-3259.
 22. Rosenberg B, Vancamp L, Krigas T. Inhibition of cell division in *Escherichia coli* by electrolysis products from a platinum electrode. *Nature.* 1965; 205:968-969.
 23. Zhao J, Gou S, Sun Y, Fang L, Wang Z. Antitumor platinum(II) complexes containing platinum-based moieties of present platinum drugs and furoxan groups as nitric oxide donors: Synthesis, DNA interaction, and cytotoxicity. *Inorg Chem.* 2012; 51:10317-10324.
 24. Zhao J, Gou S, Sun Y, Yin R, Wang Z. Nitric oxide donor-based platinum complexes as potential anticancer agents. *Chemistry.* 2012; 18:14276-14281.
 25. Abuo-Rahma Gel-D, Abdel-Aziz M, Mourad MA, Farag HH. Synthesis, anti-inflammatory activity and ulcerogenic liability of novel nitric oxide donating/chalcone hybrids. *Bioorg Med Chem.* 2012; 20:195-206.
 26. Mourad MAE, Abdel-Aziz M, Farag HH. ChemInform abstract: Design, synthesis and anticancer activity of nitric oxide donating/chalcone hybrids. *Eur J Med Chem.* 2012; 43:907-913.
 27. Ning K, Zhang JH, Feng Q, Sheng C, Tashiro S, Onodera S, Ikejima T. Induction of G2/M phase arrest and apoptosis by oridonin in human laryngeal carcinoma cells. *J Nat Prod.* 2010; 73:1058-1063.
 28. Li D, Wang L, Cai H, Zhang Y, Xu J. Synthesis and biological evaluation of novel furozan-based nitric oxide-releasing derivatives of oridonin as potential anti-tumor agents. *Molecules.* 2012; 17:7556-7568.
 29. Li DH, Wang L, Cai H, Jiang BW, Zhang YH, Sun YJ, Xu JY. Synthesis of novel furozan-based nitric oxide-releasing derivatives of 1-oxo-oridonin with anti-proliferative activity. *Chin J Nat Med.* 2012; 10:471-476.
 30. Xu S, Wang G, Lin Y, Zhang Y, Pei L, Yao H, Hu M, Qiu Y, Huang Z, Zhang Y, Xu J. Novel anticancer oridonin derivatives possessing a diazen-1-ium-1,2-diolate nitric oxide donor moiety: Design, synthesis, biological evaluation and nitric oxide release studies. *Bioorg Med Chem Lett.* 2016; 26:2795-2800.
 31. Fu J, Liu L, Huang Z, Lai Y, Ji H, Peng S, Tian J, Zhang Y. Hybrid molecule from O2-(2,4-dinitrophenyl) diazeniumdiolate and oleanolic acid: A glutathione S-transferase π -activated nitric oxide prodrug with selective anti-human hepatocellular carcinoma activity and improved stability. *J Med Chem.* 2013; 56:4641-4655.
 32. Kogias E, Osterberg N, Baumer B, Psarras N, Koentges C, Papazoglou A, Saavedra JE, Keefer LK, Weyerbrock A. Growth-inhibitory and chemosensitizing effects of the glutathione-S-transferase- π -activated nitric oxide donor PABA/NO in malignant gliomas. *Int J Cancer.* 2012; 130:1184-1194.
 33. Venugopal B, Evans TR. Developing histone deacetylase inhibitors as anti-cancer therapeutics. *Curr Med Chem.* 2011; 18:1658-1671.
 34. Müller S, Krämer OH. Inhibitors of HDACs – effective drugs against cancer? *Curr Cancer Drug Targets.* 2010; 10:210-228.
 35. Duan W, Li J, Inks ES, Chou CJ, Jia Y, Chu X, Li X, Xu W, Zhang Y. Design, synthesis, and antitumor evaluation of novel histone deacetylase inhibitors equipped with a phenylsulfonylfuroxan module as a nitric oxide donor. *J Med Chem.* 2015; 58:4325-4338.
 36. Duan W, Hou J, Chu X, Li X, Jian Z, Jin L, Xu W, Zhang Y. Synthesis and biological evaluation of novel histone deacetylases inhibitors with nitric oxide releasing activity. *Bioorg Med Chem.* 2015; 23:4481-4488.
 37. Bian H, Feng J, Li M, Xu W. Novel antileukemic agents derived from tamibarotene and nitric oxide donors. *Bioorg Med Chem Lett.* 2011; 21:7025-7029.
 38. Martínez C, Hermosilla G, León R, Pincheira G, Cifuentes V. Aspirin inhibits colon cancer cell and tumor growth and downregulates specificity protein (Sp) transcription factors. *PLoS one.* 2012; 7:e48208-e48208.
 39. Chang SY, Howden CW. Is no NSAID a good NSAID? Approaches to NSAID-associated upper gastrointestinal disease. *Curr Gastroenterol Rep.* 2004; 6:447-453.
 40. Williams JL, Borgo S, Hasan I, Castillo E, Traganos F, Rigas B. Nitric oxide-releasing nonsteroidal anti-inflammatory drugs (NSAIDs) alter the kinetics of human colon cancer cell lines more effectively than traditional NSAIDs: Implications for colon cancer chemoprevention. *Cancer Res.* 2001; 61:3285-3289.
 41. Chattopadhyay M, Kodela R, Olson KR, Kashfi K. NOSH-aspirin (NBS-1120), a novel nitric oxide- and hydrogen sulfide-releasing hybrid is a potent inhibitor of colon cancer cell growth *in vitro* and in a xenograft mouse model. *Biochem Biophys Res Commun.* 2012; 419:523-528.
 42. Kodela R, Chattopadhyay M, Velázquez-Martínez CA, Kashfi K. NOSH-aspirin (NBS-1120), a novel nitric oxide- and hydrogen sulfide-releasing hybrid has enhanced chemo-preventive properties compared to aspirin, is gastrointestinal safe with all the classic therapeutic indications. *Biochem Pharmacol.* 2015;

- 98:564-572.
43. Hagos GK, Carroll RE, Kouznetsova T, Li Q, Toader V, Fernandez PA, Swanson SM, Thatcher GR. Colon cancer chemoprevention by a novel NO chimera that shows anti-inflammatory and antiproliferative activity *in vitro* and *in vivo*. *Mol Cancer Ther.* 2007; 6:2230-2239.
44. Pathi SS, Jutooru I, Chadalapaka G, Sreevalsan S, Anand S, Thatcher GR, Safe S, Pathi SS, Jutooru I, Chadalapaka G. GT-094, a NO-NSAID, inhibits colon cancer cell growth by activation of a reactive oxygen species-microRNA-27a: ZBTB10-specificity protein pathway. *Mol Cancer Res.* 2011; 9:195-202.

(Received October 10, 2016; Revised November 1, 2016; Re-revised December 4, 2016; Accepted December 4, 2016)

The role of growth factors in nerve regeneration

Mehmet Emin Önger*, Burcu Delibaş, Aysin Pınar Türkmen, Erkan Erener, Berrin Zuhul Altunkaynak, Süleyman Kaplan

Department of Histology and Embryology, Faculty of Medicine, Ondokuz Mayıs University, Samsun, Turkey.

Summary

Nerve injuries result in functional loss in the innervated organ or body parts, and recovery is difficult unless surgical treatment has been done. Different surgical treatments have been suggested for nerve repair. Tissue engineering related to growth factors has arisen as an alternative approach for triggering and improving nerve regeneration. Therefore, the aim of this review is to provide a comprehensive analysis related to growth factors as tools for optimizing the regeneration process. Studies and reviews on the use of growth factors for nerve regeneration were compiled over the course of the review. According to literature review, it may be concluded that growth factors from different sources present promising treatment related to nerve regeneration involved in neuronal differentiation, greater myelination and axonal growth and proliferation of specific cells for nerve repair.

Keywords: Nerve regeneration, growth factors, neurotrophins, glial cell-lined derived neurotrophic factors, neuropoietic cytokines

1. Introduction

The main logic is that molecules can stimulate and assure neurons to act in new approaches, which lead to recovery of nerve fibers. Trophic factors are molecules, which behave on specific cell receptors to trigger some pathways such as protein synthesis and outgrowth. Nerve growth factor (NGF) is the main molecule of the growth factors family known as "neurotrophins". Neurotrophin is a protein molecule which provides essential functions to neurons including survival, growth, and morphologic plasticity of them (1). NGF was discovered in 1951 by Rita Levi-Montalcini and since then many neurotrophic factors have been described which have effects on the outgrowth of nerve fibers. The explanation about the neurotrophic factors especially functions and roles of them in the nervous system has still been increasing including embryonic and postnatal development after injury. There are many studies mention main aims of neurotrophic factor

researches involved in developmental roles, plasticity in the central nervous system, and mechanisms of injury and signal transduction (1-8). The objective of this review is to give an overview of neurotrophic factors and emphasize importance of what we know about the functional mechanisms by which neurotrophic factors reveal their effects from an injury response window, including axonal growth and regeneration.

2. Growth factors

The neurotrophic growth factors family is a classical growth factors family of peptides. These peptides contribute surviving and differentiating of nerve fibers in both central and peripheral nervous system by having structural and functional relation to each other (9,10). NGF was purified and identified as a diffusible factor that enhances the axonal sprouting and neurite outgrowth of neurons both *in vitro* and *in vivo* by Viktor Hamburger and Rita Levi-Montalcini, as a member of the neurotrophin family in the twentieth century (1,9). After that, brain-derived neurotrophic factor (BDNF) was purified and cloned from mammalian brain as a second member of neurotrophin family. As a result of investigations in molecular biology, we know that NGF, BDNF, neurotrophin-3 (NT-3), and neurotrophin-4/5 (NT-4/5) constitute the neurotrophin family in mammals (11) (Figure 1).

Released online in J-STAGE as advance publication October 17, 2016.

*Address correspondence to:

Dr. Mehmet Emin Önger, Department of Histology and Embryology, Faculty of Medicine, Ondokuz Mayıs University, Samsun, Turkey.

E-mail: mehmetemin.onger@gmail.com

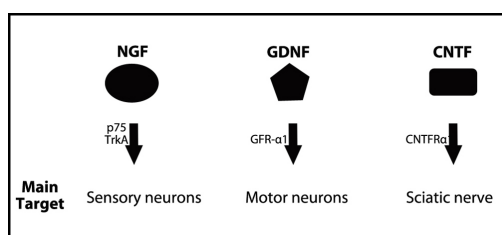


Figure 1. Main neurotrophic factors and their receptors used in nerve repair. Schematic illustration of 3 neurotrophic factor families. NGF: Neurotrophin family, GDNF: GDNF family, CNTF: Neuropoietic cytokines.

2.1. Neurotrophin family

Neurotrophins are biological molecules that are composed of noncovalent homodimers containing cysteine and their cysteine parts play a very important role in the interaction of homodimer molecules with each other (9,12). Homodimers are basically composed of two pairs of beta chains. Beta chains are bound to each other with extremely flexible 3 short bonds and these binding sites are the places where amino acid difference, which separates neurotrophins from each other, occurs (9). Neurotrophins have a very important place among neurotrophic factors. In general, they show their effect by interacting with two different receptor families. These are p75, member of the tumor necrosis factor alpha family, and tropomyosin receptor kinase (trk), a member of the tyrosine kinase receptor family (13). P75 receptors bind to all neurotrophins with similar affinity and members of tyrosine kinase receptor family are more selective in binding. For example, BDNF binds to trkb receptor while NGF binds to trka (14). Two different extracellular domain sites have been identified for neurotrophins in these interactions. One of these domains, immunoglobulin (Ig)-like domain, has been reported to have an active role in both maintaining specificity between neurotrophin ligands and in regulating the binding and activation of neurotrophins (15).

Neurotrophins are very important among neurotrophic factors in terms of their ability to guide the axons in growth cone during regeneration. The role of neurotrophins in the chemotaxis of the growth cone has recently been revealed. NT-3, NT-4/5, NGF and BDNF have been reported to be capable of inducing chemotaxis in sensory neurons. In addition, responses are inhibited in both motor and sensory neurons when antibodies that functionally block neurotrophins are used (9,10).

2.2. Glial cell-lined derived neurotrophic factor (GDNF) family

The GDNF, persephin (PSP), neurturin (NTN) and artemin (ART) constitute the GDNF family of neurotrophic factors. GDNF has been defined by the effect of increasing the survival of motor neurons,

while NTN has been defined by the effect of increasing the survival of sympathetic neurons. Similarly, PSP and ART's beneficial effects of neuronal survival have been shown *in vitro*. Although there are some differences in their biochemical structure, neurotrophic factors of GDNF family are structurally like neurotrophins (10,16-18).

The members of GDNF family show their effects through receptor complexes formed by high affinity ligand binding subunits (GFR-alpha). These subunits provide specificity at the same time. For example, while GDNF interacts with GFR alpha 1, NTN interacts with GFR alpha 2. In general, GFR alpha-receptors bind to cell membrane *via* glycosyl-phosphatidylinositol (GPI) (12,16).

2.3. Neuropoietic cytokine family

Neuropoietic cytokine family generally known as interleukin 6 (IL-6) family and it has functions, which contain different neural responses such as neural survival and differentiation (19,20). This cytokine family generally has a long chain alpha helix structure. Unlike both neurotrophins and the GDNF family, neuropoietic cytokines are not biologically active homodimers, they are secretory proteins in the form of alpha helix (19,21).

3. Interactions between neurotrophic factors

Due to the general similarity between receptor activation and adaptor proteins related with signal mechanisms, it has been suggested that there may be significant interactions and similarities between biological responses caused by the members of aforementioned three neurotrophic factor families in the related cell. This state is supported by the results of studies conducted with the combinations of GDNF and neuropoietic cytokines, which argue that they either increase each other's present effects or show a synergistic effect (9,22). It has been reported that in the differentiation of embryonic motor neurons, neurotrophic factors of each of the three families improve neurite outgrowth, even if in different degrees, and that different combinations show synergistic effect (23).

Neurotrophins, members of the GDNF family and neuropoietic cytokines have many similar and different characteristics in terms of both receptor systems and related signal transduction pathways and also their biochemical components and biological responses. For example, with a biochemical approach, while neurotrophins and members of the GDNF family are homodimeric and biologically active molecules, neuropoietic cytokines are long chain α -helix bundle proteins. Although neurotrophins bind to trk and p75, which are two different receptor classes, trk-p75 interaction is also important for neurotrophins in the

formation of high affinity binding sites. In addition, it is also known that in receptor systems, which use GDNF and neurotrophic cytokines, biological effects such as neural survival, differentiation and neurite formation affect α -subunits and signal transduction and thus may cause more positive effects (24,25).

4. Postinjury effects of neurotrophic factors

Possible changes that occur in neurotrophic factors and receptors are very important in terms of regenerative evaluation. Regulation of neurotrophic factors in motor neurons and distal regions especially after damage is important in appreciating their role in regeneration.

4.1. Changes in motor neurons

Following axonal damage, BDNF, which is underexpressed in healthy neurons, is induced quickly and BDNF mRNA (messenger ribonucleic acid) significantly increases within 8 hours after axotomy (26). The increase in BDNF level returns to normal levels within the 7th day following the damage. The BDNF mRNA increases in neurons after axotomy overlaps BDNF protein expression. This protein level reaches peak within 7 days after damage and stays high until the 14th day when compared with intact neurons (26,27). Following peripheral nerve injury, neurons neither increase nor express *trkA*. Following axotomy, *trkB* mRNA has been reported to start increasing on the second day, reach the highest level on the seventh day and maintain its increased level until the 21st day. On the contrary, *trkC* mRNA has been reported to stay relatively unchanged following axotomy while it has been reported to decrease significantly after sciatic nerve damage (26,28,29). Although what we know about the regulation of neurotrophic cytokines after peripheral nerve damage is not as much as what we know about neurotrophins, it is known for example that IL-6 mRNA increases rapidly after axotomy and returns to the basal level 24 hours later. Here, the regulation of neurotrophic cytokine receptors depends on both the content and localization of the damage (21).

4.2. Changes in distal part

Cellular and molecular changes in the distal part after damage are first degenerative and they are characterized by phagocytic processes, which are initiated by Schwann cells and maintained by macrophages. In this series of process called Wallerian degeneration, myelin sheath and axonal injuries are suppressed by the aforementioned cells. The transformation of Schwann cells from stable cell form, which provide myelination into rapid proliferating cell forms, which do not cause myelination, is effective. With this transformation, a great number of growth proteins, neurotrophic factors,

cell adhesion molecules and molecules such as basal membrane components also increase. Proliferated Schwann cells form linear bands called Bungner Bands, which guide regenerating axonal sprouts to reach the distal part (30-32). Meanwhile, the changes in the temporal expressions of the members of 3 neurotrophic factor families and receptors in the distal part have been reported to be much more dynamic when compared with those in axotomized motor neurons. After damage, the expression of NGF and BDNF, which are from neurotrophin family, increase in the distal part, while the expression of NT-3 and NT-4/5 decreases. Increase in the expression of GDNF from the GDNF family and IL-6 from the neurotrophic cytokine and decrease in the expression of CNTF (ciliary neurotrophic factor) have also been reported. While NGF mRNA can hardly be detected in intact nerve normally, it has been reported to increase 10 times in the distal part within the first 12 hours following damage and to decrease to 5 times of the normal level on the 72nd hour and stay at this level for about three weeks (25,33-35). The BDNF mRNA increase, which occurs in the distal part following the damage, is quite slow when compared with NGF. However, the increase in BDNF mRNA expression reaches a detectable level on the 7th day following the damage and continues to increase until the 28th day. The maximum level of BDNF mRNA is about ten times more than that of NGF mRNA (25,35,36). The expression of NT-3, one of the members of neurotrophin family, can be easily detected in healthy nerves with NT-3 mRNA and its expression within 12 hours following the damage has been reported to decrease rapidly and return to basal level within 2 weeks. Similarly, NT-4/5 mRNA expression has also been reported to decrease within 6-12 hours following nerve transection (29,33). GDNF, one of the members of GDNF family, has been detected in healthy nerve and it has been reported to peak in distal part on the seventh day following the damage and maintain its high level at least for two weeks. While the expression of IL-6, one of the members of neurotrophic cytokine family, is not in sufficient levels for detection, the expression of CTNF is in very high levels. However, after damage, the level of CTNF mRNA begins to drop within 24 hours, and goes about 5 times below the levels detected in healthy nerves. Unlike CTNF, the expression of IL-6 mRNA increases 35 times in the distal part after damage and it returns to basal level again 24 hours later (35,37).

A great number of experimental studies have shown that neurotrophic factors increase the survival rates of axotomized or injured nerves. Methods, which provide long-term neurotrophic factor release to increase survival, include many different strategies ranging from exogenous neurotrophic factor to adenoviral transfer. In the following sections, we will review the basic effects of neurotrophic factors one by one.

4.3. Basic effects of neurotrophins

It is well acknowledged that BDNF plays a role as a survival factor for damaged neurons (38). This survival increasing effect of exogenous BDNF is temporary and dependent on functional trkB receptors (39,40). For example, within 4-5 weeks following the damage, 95% of the neurons had died although the treatment continues. The neural survival effect of BDNF after axotomy is dose-dependent (41,42). The survival increasing effect of NT-3 and NT-4/5 in damaged neurons is still disputed and controversial. Some studies claim NT-3 and NT-4/5 are as effective as BDNF in increasing neural survival whereas other studies have reported NT-3 and NT-4/5 to increase survival in axotomized neurons, but this effect was less than the effect of BDNF. In addition, it has been reported that NT-3 does not increase survival in damaged neurons when compared with the control group (9).

4.4. Basic effects of GDNF family

The survival enhancing effect of GDNF in motor neurons following damage has been reported. In adult animals, exogenous GDNF application has been reported to save axotomized motor neurons and in addition to injured nerves. However, similar to BDNF, one dose GDNF has been reported to have a temporary effect (17,18,34,35). Thus, different methods have been examined for long-term survival increasing effect. Although there are *in vitro* studies about the motoneuronal survival increasing effect of NTN and PSP, it has not been completely found out whether the other members of the GDNF family prevent cell death induced by axotomy (43,44).

4.5. Basic effects of neurotrophic cytokines

The beneficial effects of CTNF, and IL-6 in nerve regeneration have been presented (20,45,46). Similar to the members of neurotrophic factor family such as BDNF and GDNF, neural survival effect of CTNF is also transient. In response to nerve damage, the changes in neuronal form have been expressed as the transformation of phenotype from "transmitter" to "regenerative" (47). *In vitro* studies show that, apart from the supporting effect of survival for both peripheral and central nervous system neurons, CNTF also initiates axonal sprouting and rescues the neurons from axotomy-induced cell death (48).

5. Regenerative events following damage

In addition to the survival increasing effects of three neurotrophic factor families on injured nerves, the similarity of their signal transduction mechanisms shows that they have similar abilities to reverse the

effects of axotomy.

It has been reported that neurotrophic factors provide neural survival following damage and that there is a direct association between exogenous neurotrophic factor application and axonal regeneration (22,49). In the evaluation of peripheral nerve regeneration, total number of axons in the distal part of nerve and functional tests are used (50-52). However, axonal assessment only in the distal part means ignoring the axon outgrowths, which originate from the proximal part. Thus, axon outgrowths, which develop as a response to exogenous neurotrophic factor treatment, are insufficient to estimate direct information about the accurate number of axotomized neurons (51,53,54). Briefly, combined quantitative evaluations will give more precise information about regeneration.

5.1. Neurotrophins

In axonal regeneration, BDNF can improve axonal sprouting. It has been shown that, following nerve injury, BDNF does not increase functional recovery in tests such as sciatic function index, however, it has triggering effects. Although exogenous BDNF has inefficiencies in postinjury functional recovering, endogenous BDNF is known to play an important role in peripheral nerve regeneration (38,55). Anti BDNF antibody application after damage has been reported both to diminish axonal elongation and to decrease the axonal density and number (56). One of the most important factors of poor recovery in motor functions following peripheral nerve injury is the decrease in the axonal regeneration abilities of motor neurons. During regeneration, a time-dependent decrease is seen in the total number of regenerated axons and reinnervation of muscle fibers (25,47). However, it is suggested that low dose and long term BDNF application increases both axonal regeneration and neural cell repair and thus it is very effective in reversing the negative effects caused by chronic axotomy (38). Moreover, similarly, low dose BDNF application has been shown to increase the number of reinnervated muscle fibers significantly (9). The use of BDNF by axotomized neurons can be suitable for the start of axonal growth following damage; however, temporary expression is not sufficient in the long-term support of axonal regeneration. During the first week after damage, NGF upregulation occurs in distal nerve root. NGF plays an important role of support in increasing Schwann cell organization. This support is realized through Bungner band. In addition, this temporary upregulation of NGF starts the slow developing regeneration after damage. Although the axonal regeneration initiating effect of exogenous BDNF is limited, the same is not true for NT-3. Especially in injury models, which are formed through sciatic nerve resection, NT-3 has been shown to increase both the number of regenerated axons and

myelination significantly (10,29,38).

5.2. GDNF family

Overexpression of GDNF in muscle fibers may result in hyperinnervation at the neuromuscular junctions. Thus, it is argued that GDNF eases synapse formation during regeneration or acts as "synaptotrophin" for developing neuromuscular connections. Since a similar hyperinnervation does not occur in the overexpression of NT-3 or NT-4/5, this effect of GDNF has been reported to be specific (9). Similarly, GDNF application has been shown to increase regenerated axonal outgrowth significantly in spinal cord and peripheral nerve injury (57,58). In addition, there are studies, which show that GDNF not only advances the formation of neuromuscular connections, but also induces muscle innervation plasticity and/or remodeling (59). It is argued that it plays a facilitative role in triggering axonal regeneration of axotomized motor neurons. The role of other members of the GDNF family in axonal regeneration has not been specified yet.

5.3. Neurotrophic cytokines

CNTF and neurotrophins are known to play an important role separately or in combination in axonal outgrowth and functional survival after damage (25). Studies have reported that the combinations of CNTF / BDNF treatment has neuroprotective role in the retina (60). IL-6 has been shown to be significant in axonal regeneration. Antibody application, which prevents IL-6 from binding with its receptor, has been shown to decrease axonal regeneration significantly (9). The role of neurotrophic cytokines in peripheral nerve regeneration has been examined in adult rat sensory neurons and spinal cord injury models. It has been shown that neurotrophic cytokines promote axonal regeneration and functional recovery (20,61). However, it is not known whether neurotrophic cytokines affect by increasing the rate of axonal regeneration or by increasing regenerative or terminal outgrowth in axons.

6. Conclusion

Although it is clear that neurotrophic factors support neural survival after damage and intracellular pathways are clearly determined, quantitative assessments in especially axonal regeneration are very recent. The literature shows that regeneration and functional recovery depend on the positive and negative signal balance between growth factors. Further studies of *in vitro* and *in vivo* nerve injury and repair models are required to make our information about neurotrophic factors more comprehensible. Results can cause the design of more specific treatment methods in the treatment of low functional recovery, which develops after damage.

References

1. Zochodne DW. Neurobiology of peripheral nerve regeneration. Cambridge University Press; Cambridge, UK, 2008.
2. Rask CA. Biological actions of nerve growth factor in the peripheral nervous system. *Eur Neurol.* 1999; 41 (Suppl 1):14-19.
3. Thoenen H. Neurotrophins and activity-dependent plasticity. *Prog Brain Res.* 2000; 128:183-191.
4. Costales J, Kolevzon A. The therapeutic potential of insulin-like growth factor-1 in central nervous system disorders. *Neurosci Biobehav Rev.* 2016; 63:207-222.
5. Keskin I, Kaplan S, Kalkan S, Sutcu M, Ulkay MB, Esener OB. Evaluation of neuroprotection by melatonin against adverse effects of prenatal exposure to a nonsteroidal anti-inflammatory drug during peripheral nerve development. *Int J Dev Neurosci.* 2015; 41:1-7.
6. Geuna S, Raimondo S, Fregnan F, Haastert-Talini K, Grothe C. *In vitro* models for peripheral nerve regeneration. *Eur J Neurosci.* 2016; 43:287-296.
7. Geuna S. The sciatic nerve injury model in pre-clinical research. *J Neurosci Methods.* 2015; 243:39-46.
8. Turgut M, Kaplan S. Effects of melatonin on peripheral nerve regeneration. *Recent Pat Endocr Metab Immune Drug Discov.* 2011; 5:100-108.
9. Boyd JG, Gordon T. Neurotrophic factors and their receptors in axonal regeneration and functional recovery after peripheral nerve injury. *Mol Neurobiol.* 2003; 27:277-324.
10. Sebben AD, Lichtenfels M, da Silva JLB. Peripheral nerve regeneration: Cell therapy and neurotrophic factors. *Revista Brasileira de Ortopedia (English Edition).* 2011; 46:643-649.
11. Barde YA, Edgar D, Thoenen H. Purification of a new neurotrophic factor from mammalian brain. *EMBO J.* 1982; 1:549-553.
12. Yan H, Zhang F, Chen MB, Lineaweaver WC. Chapter 10: Conduit luminal additives for peripheral nerve repair. *Int Rev Neurobiol.* 2009; 87:199-225.
13. Yano H, Chao MV. Neurotrophin receptor structure and interactions. *Pharm Acta Helv.* 2000; 74:253-260.
14. Barbacid M. The Trk family of neurotrophin receptors. *J Neurobiol.* 1994; 25:1386-1403.
15. Schneider R, Schweiger M. A novel modular mosaic of cell adhesion motifs in the extracellular domains of the neurogenic trk and trkB tyrosine kinase receptors. *Oncogene.* 1991; 6:1807-1811.
16. Saarna M, Sariola H. Other neurotrophic factors: glial cell line-derived neurotrophic factor (GDNF). *Microsc Res Tech.* 1999; 45:292-302.
17. Henderson CE, Phillips HS, Pollock RA, *et al.* GDNF: A potent survival factor for motoneurons present in peripheral nerve and muscle. *Science.* 1994; 266:1062-1064.
18. Patel M, Mao L, Wu B, VandeVord P. GDNF blended chitosan nerve guides: An *in vivo* study. *J Biomed Mater Res A.* 2009; 90:154-165.
19. Heinrich PC, Behrmann I, Muller-Newen G, Schaper F, Graeve L. Interleukin-6-type cytokine signalling through the gp130/Jak/STAT pathway. *Biochem J.* 1998; 334:297-314.
20. Yang P, Wen H, Ou S, Cui J, Fan D. IL-6 promotes regeneration and functional recovery after cortical spinal

- tract injury by reactivating intrinsic growth program of neurons and enhancing synapse formation. *Exp Neurol.* 2012; 236:19-27.
21. Stolp HB. Neuropoietic cytokines in normal brain development and neurodevelopmental disorders. *Mol Cell Neurosci.* 2013; 53:63-68.
 22. Harvey AR, Lovett SJ, Majda BT, Yoon JH, Wheeler LPG, Hodgetts SI. Neurotrophic factors for spinal cord repair: Which, where, how and when to apply, and for what period of time? *Brain Res.* 2015; 1619:36-71.
 23. Zurn AD, Winkel L, Menoud A, Djabali K, Aebischer P. Combined effects of GDNF, BDNF, and CNTF on motoneuron differentiation *in vitro*. *J Neurosci Res.* 1996; 44:133-141.
 24. Priestley JV, Ramer MS, King VR, McMahon SB, Brown RA. Stimulating regeneration in the damaged spinal cord. *J Physiol Paris.* 2002; 96:123-133.
 25. Hoyng SA, De Winter F, Gnavi S, de Boer R, Boon LI, Korvers LM, Tannemaat MR, Malessy MJ, Verhaagen J. A comparative morphological, electrophysiological and functional analysis of axon regeneration through peripheral nerve autografts genetically modified to overexpress BDNF, CNTF, GDNF, NGF, NT3 or VEGF. *Exp Neurol.* 2014; 261:578-593.
 26. Kobayashi NR, Bedard AM, Hincke MT, Tetzlaff W. Increased expression of BDNF and *trkB* mRNA in rat facial motoneurons after axotomy. *Eur J Neurosci.* 1996; 8:1018-1029.
 27. Vögelin E, Baker JM, Gates J, Dixit V, Constantinescu MA, Jones NF. Effects of local continuous release of brain derived neurotrophic factor (BDNF) on peripheral nerve regeneration in a rat model. *Exp Neurol.* 2006; 199:348-353.
 28. Tchetchelnitski V, van den Eijnden M, Schmidt F, Stoker AW. Developmental co-expression and functional redundancy of tyrosine phosphatases with neurotrophin receptors in developing sensory neurons. *Int J Dev Neurosci.* 2014; 34:48-59.
 29. Gibbons AS, Bailey KA. BDNF and NT-3 regulation of *trkB* and *trkC* mRNA levels in the developing chick spinal cord. *Neurosci Lett.* 2005; 385:41-45.
 30. Kaplan S, Odaci E, Unal B, Sahin B, Fornaro M. Chapter 2: Development of the peripheral nerve. *Int Rev Neurobiol.* 2009; 87:9-26.
 31. Onger ME, Türkmen AP, Elibol E, *et al.* Chapter 3 – Embryology of the peripheral nerves A2 – Nerves and nerve injuries. Academic Press, San Diego, USA, 2015; pp. 37-40.
 32. Türkmen AP, Altunkaynak BZ, Onger ME, *et al.* Chapter 4 – Development of the cranial nerves A2 – Nerves and nerve injuries. Academic Press, San Diego, USA, 2015; pp. 41-53.
 33. Funakoshi H, Frisén J, Barbany G, Timmusk T, Zachrisson O, Verge VM, Persson H. Differential expression of mRNAs for neurotrophins and their receptors after axotomy of the sciatic nerve. *J Cell Biol.* 1993; 123:455-465.
 34. Naveilhan P, ElShamy WM, Ernfors P. Differential regulation of mRNAs for GDNF and its receptors *Ret* and *GDNFR alpha* after sciatic nerve lesion in the mouse. *Eur J Neurosci.* 1997; 9:1450-1460.
 35. Allen SJ, Watson JJ, Shoemark DK, Barua NU, Patel NK. GDNF, NGF and BDNF as therapeutic options for neurodegeneration. *Pharmacol Ther.* 2013; 138:155-175.
 36. Meyer M, Matsuoka I, Wetmore C, Olson L, Thoenen H. Enhanced synthesis of brain-derived neurotrophic factor in the lesioned peripheral nerve: Different mechanisms are responsible for the regulation of BDNF and NGF mRNA. *J Cell Biol.* 1992; 119:45-54.
 37. Ito Y, Yamamoto M, Li M, Doyu M, Tanaka F, Mutch T, Mitsuma T, Sobue G. Differential temporal expression of mRNAs for ciliary neurotrophic factor (CNTF), leukemia inhibitory factor (LIF), interleukin-6 (IL-6), and their receptors (CNTFR alpha, LIFR beta, IL-6R alpha and gp130) in injured peripheral nerves. *Brain Res.* 1998; 793:321-327.
 38. Santos D, Giudetti G, Micera S, Navarro X, del Valle J. Focal release of neurotrophic factors by biodegradable microspheres enhance motor and sensory axonal regeneration *in vitro* and *in vivo*. *Brain Res.* 2016; 1636:93-106.
 39. Yang JW, Ru J, Ma W, Gao Y, Liang Z, Liu J, Guo JH, Li LY. BDNF promotes the growth of human neurons through crosstalk with the Wnt/ β -catenin signaling pathway *via* GSK-3 β . *Neuropeptides.* 2015; 54:35-46.
 40. Vermehren-Schmaedick A, Khanjian RA, Balkowiec A. Cellular mechanisms of activity-dependent BDNF expression in primary sensory neurons. *Neuroscience.* 2015; 310:665-673.
 41. Andero R, Choi DC, Ressler KJ. Chapter Six – BDNF-*TrkB* receptor regulation of distributed adult neural plasticity, memory formation, and psychiatric disorders. In: *Progress in Molecular Biology and Translational Science* (Zafar UK, Muly EC, eds.). Academic Press, 2014; pp. 169-192.
 42. Wei Z, Liao J, Qi F, Meng Z, Pan S. Evidence for the contribution of BDNF-*TrkB* signal strength in neurogenesis: An organotypic study. *Neurosci Lett.* 2015; 606:48-52.
 43. Milbrandt J, de Sauvage FJ, Fahrner TJ, *et al.* Persephin, a novel neurotrophic factor related to GDNF and neurturin. *Neuron.* 1998; 20:245-253.
 44. Quartu M, Serra MP, Boi M, Sestu N, Lai ML, Del Fiacco M. Tissue distribution of neurturin, persephin and artemin in the human brainstem at fetal, neonatal and adult age. *Brain Res.* 2007; 1143:102-115.
 45. Pasquin S, Sharma M, Gauchat JF. Ciliary neurotrophic factor (CNTF): New facets of an old molecule for treating neurodegenerative and metabolic syndrome pathologies. *Cytokine Growth Factor Rev.* 2015; 26:507-515.
 46. Villacampa N, Almolda B, Campbell IL, González B, Castellano B. CNS-targeted IL-6 production leads to higher recruitment of pro-inflammatory T-helper cells after facial nerve axotomy. *J Neuroimmunol.* 2014; 275:177.
 47. Geuna S, Raimondo S, Ronchi G, Di Scipio F, Tos P, Czaja K, Fornaro M. Chapter 3: Histology of the peripheral nerve and changes occurring during nerve regeneration. *Int Rev Neurobiol.* 2009; 87:27-46.
 48. Richardson PM. Ciliary neurotrophic factor: A review. *Pharmacol Ther.* 1994; 63:187-198.
 49. Audisio C, Mantovani C, Raimondo S, Geuna S, Perroteau I, Terenghi G. Neuregulin1 administration increases axonal elongation in dissociated primary sensory neuron cultures. *Exp Cell Res.* 2012; 318:570-577.
 50. Kaplan S, Eşrefoglu M, Aktaş A, Gül M, Onger ME, Altunkaynak ME, Ulkay MB, Ragbetli MÇ. The effect of prenatal exposure of a non-steroidal anti-inflammatory drug on the optic nerve of female rats: A stereological, histological, and electron microscopic study. *J Matern Fetal Neonatal Med.* 2013; 26:1860-1864.

51. Çolakoğlu S, Aktaş A, Raimondo S, Türkmen AP, Altunkaynak BZ, Odacı E, Geuna S, Kaplan S. Effects of prenatal exposure to diclofenac sodium and saline on the optic nerve of 4- and 20-week-old male rats: a stereological and histological study. *Biotech Histochem.* 2014; 89:136-144.
52. Onger ME, Altun G, Aydın I, Kivrak EG, Yurt KK, Altunkaynak BZ, Kaplan S. A Stereological Investigation Technique for Peripheral Nerve. *Türkiye Klinikleri J Neurol-Special Topics.* 2014;7:56-60.
53. Kaplan S, Geuna S, Ronchi G, Ulkay MB, von Bartheld CS. Calibration of the stereological estimation of the number of myelinated axons in the rat sciatic nerve: A multicenter study. *J Neurosci Methods.* 2010; 187:90-99.
54. Piskin A, Kaplan S, Aktaş A, Ayyıldız M, Raimondo S, Aliç T, Bozkurt HH, Geuna S. Platelet gel does not improve peripheral nerve regeneration: An electrophysiological, stereological, and electron microscopic study. *Microsurgery.* 2009; 29:144-153.
55. Kishino A, Ishige Y, Tatsuno T, Nakayama C, Noguchi H. BDNF prevents and reverses adult rat motor neuron degeneration and induces axonal outgrowth. *Exp Neurol.* 1997; 144:273-286.
56. Zhang JY, Luo XG, Xian CJ, Liu ZH, Zhou XF. Endogenous BDNF is required for myelination and regeneration of injured sciatic nerve in rodents. *Eur J Neurosci.* 2000; 12:4171-4180.
57. Deng LX, Hu J, Liu N, Wang X, Smith GM, Wen X, Xu XM. GDNF modifies reactive astrogliosis allowing robust axonal regeneration through Schwann cell-seeded guidance channels after spinal cord injury. *Exp Neurol.* 2011; 229:238-250.
58. Shakhbazau A, Mohanty C, Shcharbin D, Bryszewska M, Caminade AM, Majoral JP, Alant J, Midha R. Doxycycline-regulated GDNF expression promotes axonal regeneration and functional recovery in transected peripheral nerve. *J Control Release.* 2013; 172:841-851.
59. Gyorkos AM, McCullough MJ, Spitsbergen JM. Glial cell line-derived neurotrophic factor (GDNF) expression and NMJ plasticity in skeletal muscle following endurance exercise. *Neuroscience.* 2014; 257:111-118.
60. Azadi S, Johnson LE, Paquet-Durand F, Perez MT, Zhang Y, Ekström PA, van Veen T. CNTF + BDNF treatment and neuroprotective pathways in the rd1 mouse retina. *Brain Res.* 2007; 1129:116-129.
61. Thompson SWN, Priestley JV, Southall A. GP130 cytokines, leukemia inhibitory factor and interleukin-6, induce neuropeptide expression in intact adult rat sensory neurons *in vivo*: Time-course, specificity and comparison with sciatic nerve axotomy. *Neuroscience.* 1998; 84:1247-1255.

(Received September 7, 2016; Revised October 5, 2016; Accepted October 6, 2016)

A review of complementary therapies for chemotherapy induced gastrointestinal mucositis

Raja A.H Kuchay*

School of Biosciences & Biotechnology, CBS, BGSB University, J&K, India.

Summary Administration of chemotherapy often leads to gastrointestinal mucositis (GIM). GIM manifests as nausea, abdominal pain and diarrhoea in recipients of chemotherapy. GIM is a major complication occurring in approximately 80% of patients receiving 5-fluorouracil treatment. These side-effects may become so severe that significant dose reductions are required, ultimately affecting treatment efficacy and patient survival. Complementary and alternative medicine (CAM) is a growing area of public interest. This review will provide an overview of current knowledge of complementary medicinal therapies for chemotherapy induced GIM. An understanding of this evolving literature is useful in discussing these therapies with patients who are considering using them.

Keywords: Mucositis, intestine, complementary medicine

1. Introduction

The fast-renewing intestinal epithelium is vulnerable to the cytotoxicity of chemotherapy. Cytotoxic agents used during chemotherapy are effective at killing cancerous cells however they also indiscriminately target certain healthy tissue. Chemotherapy-induced gastrointestinal mucositis (GIM) is a dose-limiting side effect of many chemoagents. It has been pathologically described as an intestinal inflammation characterized by an early event of epithelia apoptosis (1-3). GIM is a major oncological problem, caused by the treatment of malignant disease with chemotherapeutic agents. It affects the entire gastrointestinal tract and causes pain and ulceration in the mouth as well as abdominal bloating, vomiting and diarrhoea in the small and large intestines (4,5). After treatment with standard dose chemotherapy, approximately 40% of all patients and up to 100% of patients undergoing high-dose chemotherapy with bone marrow or stem cell transplantation reportedly develop GIM (4-6). GIM and its associated complications lead to a dose reduction of chemotherapy and compromises overall survival in cancer patients. GIM adds substantial

burden on the medical care required for cancer patients, increases healthcare costs and reduces patient quality of life (7). Current therapies for treatment of GIM are suboptimal and potentially toxic. There is an acute need for the development of more effective treatment strategies for chemotherapy-induced GIM. Emerging evidence suggests that complementary and alternative medicine (CAM) based therapeutic modalities are highly effective in modulating the immune system, disrupting the proinflammatory cascade and restoring digestive health while improving patient's quality of life. In this context we will review some of the complementary medicine based therapeutics for treatment of GIM. However, before going into these details, it is necessary to understand the architecture of small intestine and current molecular model for pathobiology of GIM.

2. Small intestinal architecture

GIM has been attributed to the high proliferation rate in the intestine that is interrupted and reduced by chemotherapy drugs, and also to direct killing of crypt cells (4-6). The intestinal epithelium is the largest of the body's mucosal surfaces, covering ~400 m² of surface area with a single layer of cells organized into crypts and villi. This surface is continually renewed by pluripotent intestinal epithelial stem cells that reside in the base of crypts, where the pro-liferation, differentiation and functional potential of epithelial cell

Released online in J-STAGE as advance publication October 17, 2016.

*Address correspondence to:

Dr. Raja A.H Kuchay, School of Biosciences & Biotechnology, CBS, BGSB University, J&K, 185234, India.

E-mail: kuchay_bgsbu@yahoo.com

progenitors is regulated by the local stem cell niche (8-10). The epithelial layer of the GI tract is a rapidly renewing tissue with a high cell turnover rate. Stem cells in the lower half of the crypts give rise to daughter cells, thereby producing all the cells of the epithelium. Newly produced cells migrate out of the crypts up to the villus or migrate downward into the base of the crypts and reside under or between the stem cells. During migration up to the villus, most cells differentiate into functional enterocytes (11). It is generally accepted that once epithelial cells complete their migration along the crypt-villous axis they are sloughed off into the lumen. This rapid turnover of cells explains why the GI tract is particularly susceptible to the effects of cytotoxic agents (12). Despite the different sites of action of various chemoagents, the end result is intestinal crypt hyperplasia (4,5). The epithelial stem cells in the small intestine become damaged and no longer divide or differentiate into specific cell lineages following chemotherapy leading to a rapid loss of structure and function (13).

3. Pathobiology of GIM

In the last decade, significant progress has been made in understanding the pathobiology of GIM. It has been postulated that GIM occurs in five overlapping phases: initiation, up-regulation and message generation, signalling and amplification, ulceration and healing (14-16). Upon anti-cancer treatment, both DNA and non-DNA damages occur. DNA strand breaks cause direct injury in cells of the basal epithelium. At the same time, reactive oxygen species (ROS) are formed, starting downstream biological events. Nuclear factor kappa B (NF κ B), cyclooxygenase-2 (COX-2) as well as pro-inflammatory cytokines like interleukin-6 (IL-6), interleukin-1 β (IL-1 β) and tumour-necrosis factor (TNF) have been suggested to play a key role in the development of GIM (17-20). These overlapping steps are thought to be largely driven by the activation of NF κ B, subsequently promoting key pro-inflammatory cytokines. Furthermore, apoptosis, pathogenic bacteria, inflammation, matrix metalloproteinases (MMPs), loss of mucosal barrier integrity and toll like receptors (TLRs) have also been reported to play an important role in GIM (21-28).

There is evidence that chemotherapy can induce GIM through various pathways. The timing of histological lesions, peak tissue levels of NF κ B and pro-inflammatory cytokines are different according to the chemotherapy agents like irinotecan, methotrexate (MTX) or 5-fluorouracil (5-FU) (29). Commensal bacteria play an important role in intestinal homeostasis, and have some protective effect on the intestinal integrity. Their interactions with TLRs and subsequent activation of NF κ B signalling pathway contributes to intestinal homeostasis, maintaining

the barrier function and promoting wound repair and tissue regeneration (30,31). TLRs initiate the innate immune response and the production of pro-inflammatory mediators including IL-1 β , nitric oxide and IL-18, whose role in intestinal GIM is well known (32-34). Recently, TLR/MyD88/NF- κ B pathway has been implicated in the mechanisms of damage involved in chemotherapy-related GIM (27). It has also been reported that TLR-2 acts as a central regulator of xenobiotic defense and targeting TLR2 may represent a novel therapeutic approach in chemotherapy-induced GIM (26).

Role of platelet-activating factor (PAF) in chemotherapy-induced GIM has also been reported (35). NADPH oxidase 1 (NOX1) has also been suggested to be involved in pathogenesis of GIM (36). Furthermore, role of NOX-2 mediated inflammasome activation and inflammasome-dependent production of IL-1 β and IL-18 has also been verified (37). The mucin layer is an integral component of barrier function in the intestine and chemotherapy agents significantly decreased epithelial mucin levels in the jejunum of rats (38). Findings strongly suggest chemotherapy causes tight junction defects which lead to mucosal barrier dysfunction and the development of GIM (23). Thus, it is quite clear that pathobiology of GIM involves many signalling pathways and diverse range of molecules.

Given the literature summarised above, it is clear that some kind of preventative therapy is required for GIM in patients receiving cancer chemotherapy treatment. In many cases of cancer chemotherapy the treatment needs to be discontinued due to high incidence of GIM, risking the life of patients. CAM is widely used, particularly for chronic medical conditions that are difficult to treat. Because only a limited number of treatments are available for GIM, many patients can opt for CAM. Two of the most important CAM therapeutic modalities for chemotherapy induced GIM are based on plants and probiotics.

4. Plant based complementary therapies

Aged garlic extract (AGE) administration has been reported to decrease the severity of jejunal damage against MTX-induced GIM in the small intestine of rats (39,40). MTX induced apoptosis of IEC-6 cells was shown to be depressed by AGE (41). The MTX-induced loss of viable IEC-6 cells was almost completely prevented by the presence of more than 0.1% AGE (41). Grape seed extract (GSE) represent a new therapeutic option to decrease the symptoms of GIM. Compared with 5-FU controls, GSE significantly decreased the histological damage score, increased jejunal crypt depth, attenuated the chemotherapy-induced reduction of mucosal thickness and decreased myeloperoxidase activity in rat models of GIM (42,43). GSE has also been reported to improves epithelial

structure, intestinal epithelial differentiation and suppress inflammation in ileum of IL-10-deficient mice (44,45). Grapes are rich in polyphenols that vary in their distribution inside the grapes with less than 10% in the pulp, 60-70% deposited in seeds, and 20-35% in the skin (46). Proanthocyanidins are believed to be the key bioactive constituents in GSE (47). Administration of proanthocyanidin decreased the jejunal damage and malondialdehyde level, which were caused by MTX treatment and increased superoxide dismutase and glutathione peroxidase levels in rats (48,49).

It has been reported that apricot and beta-carotene treatment may protect the impairment of oxidative stress and ameliorate MTX-induced intestine damage at biochemical and histological levels (50). Single or combined application of apricot and beta-carotene ameliorated the effects like fusion and shortening in the villus, epithelial desquamation, crypt loss, inflammatory cell infiltration in the lamina propria, goblet cell depletion and microvillar damage in the small intestine of rats treated with MTX (50). Administration of Vitamin A is also known to decrease the MTX-induced damage to the small intestine (51). Ellagic acid (EA) and pumpkin seed oil (PSO) have been suggest to protect the small intestine of rats from MTX-induced damage through their antioxidant and anti-inflammatory effects (52). Administration of EA and PSO decreased the intestinal damage, prostaglandin E2 and nitric oxide level (52). Hesperidin, a flavanone glycoside mainly found in citrus fruits has been reported to prevent intestinal epithelial injury resulting from chemotherapy treatment (53). The small intestinal damage score, inducible nitric oxide synthase and interleukin-8 levels were lower MTX plus hesperidin group (53).

Aqueous extract of *Chimonanthus nitens* var. *salicifolius* (CS), a traditional Chinese herb has been found to be beneficial against 5-FU induced GIM in mice (54). CS attenuated the subsequent body weight loss, diarrhea, and faecal blood, reducing the hepatic injury, and maintaining both intestinal length and villus structure (54). Downregulation of apoptotic gene caspase3 in CS group compared with mice treated with 5-FU only was reported (54). CS aqueous extract treatments suppressed the elevation of TNF- α induced by 5-FU challenge. Furthermore, other cytokines, including IL-1 β and IL-12b, were also inhibited by CS treatment, suggesting an anti-inflammatory effect of CS (54). Three flavonoids rutin, quercetin, and kaempferol were identified by HPLC to be abundant in the aqueous extract of CS (54). Rutin is considered as a powerful antioxidant with pharmacological benefits including antitumor, anti-inflammatory, and anti-diarrhoeal effects (55,56).

Curcumin has been reported to significantly reverse chemotherapy-induced weight-loss and damage to intestinal mucosa (57). Curcumin also reduced the expression of pro-apoptotic Bax but stimulated anti-apoptotic Bcl-2 to attenuate 5-FU-induced apoptosis

of intestinal epithelial cells (57). Curcumin decreased the levels of ICAM-1, IL-1 β and TNF- α , but increased the levels of IL-10 and SOD in rat models of GIM (58). Furthermore, mitogen-activated protein kinase phosphatase-1 (MKP-1) was activated but phospho-p38 was inhibited by curcumin (58). Curcumin also repressed I- κ B and interfered with the translocation of NF- κ B into nucleus (58). These findings suggest that curcumin, with anti-inflammatory and anti-oxidant activities may be used as an effective reagent for protecting intestinal mucosa barrier during chemotherapy-induced GIM (58). Administration of beta-glucan following MTX has been reported to attenuate the tissue damage (59). Stimulation index, an indicator of oxidative burst in the neutrophils, was decreased by MTX, while beta-glucan abolished this effect (59). Furthermore, increased leukocyte apoptosis and cell death in MTX-treated animals were inhibited by beta-glucan. These findings suggest that beta-glucan, through its antioxidant and immunoregulatory effects, may be of therapeutic value in alleviating the leukocyte apoptosis, oxidative tissue injury and thereby the intestinal and hepato-renal side effects of MTX treatment (59).

Saireito, a traditional Japanese herbal medicine and a combined formulation of two herbal medicines (shosaikoto and goreisan) reduced 5-FU-induced GIM through reduction of apoptosis in the intestinal crypt *via* suppression of the up-regulation of inflammatory cytokines (60). Administration of saireito significantly suppressed the activation of caspase-3 and reduced 5-FU-increased apoptotic cells, with an inhibition rate of 67.8% (60). Furthermore, it significantly attenuated the up-regulation of both TNF- α and IL-1 β mRNA induced by 5-FU. The inhibition rate was 72.5 and 77.6% for TNF- α and IL-1 β , respectively (60). Iberogast, a mixture of extracts from bitter candytuft (*Iberis amara*), angelica root (*Angelicae radix*), milk thistle fruit (*Silybi mariani fructus*), celandine herb (*Chelidonii herba*), caraway fruit (*Carvi fructus*), liquorice root (*Liquiritiae radix*), peppermint herb (*Menthae piperitae folium*), balm leaf (*Melissae folium*) and chamomile flower (*Matricariae flos*) partially improved the histopathological features of 5-FU induced GIM in rats (61,62). Acteoside, a phenylpropanoid glycoside derived from plant species in the *Scrophularia* genus alleviated MTX-induced small intestinal mucositis possibly by preventing inflammation (63,64). Mucoadhesive formulation of *Bidens pilosa* L. (Asteraceae) has recently been reported to reduce intestinal injury from 5-FU induced GIM in mice (65). Plant based complementary medicine therapeutics useful for treatment of chemotherapy induced GIM are summarized in Table 1.

5. Probiotics

Previous studies have indicated that gastrointestinal microflora may be involved in the development

Table 1. Plant based complementary therapies for GIM

Complementary Therapy	Effect	Reference
Aged garlic extract	Apoptosis (Decrease)	39,40,41
Grape seed extract	Inflammation (Decrease), Myeloperoxidase activity (Decrease)	42,43,44,45
Apricot and β -carotene	Inflammatory cell infiltration (Decrease)	50,51
Ellagic acid & pumpkin seed oil	Prostaglandin E2 (Decrease), Nitric oxide (Decrease)	52
Hesperidin	Inducible nitric oxide synthase, Interleukin-8 (Decrease)	53
Aqueous extract of <i>Chimonanthus nitens</i>	Caspase3, TNF- α (Decrease)	54
Curcumin	Bax, IL-1 β , TNF- α , I- κ B (Decrease)	57,58
β -glucan	Leukocyte apoptosis (Decrease)	59
Saireito	Apoptosis, IL-1 β , TNF- α (Decrease)	60
Iberogast	Histopathological features (Improve)	61,62
Acteoside	Inflammation (Decrease)	63, 64
Mucoadhesive formulation of <i>Bidens pilosa</i>	Bax (Decrease), Myeloperoxidase activity (Decrease)	65

of chemotherapy-induced mucositis and diarrhoea (66,67). It has been suggested that intestinal bacteria can attenuate or aggravate GIM by influencing the intestinal inflammatory process, influencing intestinal permeability, influencing the composition of the mucus layer, influencing resistance to harmful stimuli and enhancing epithelial repair, and the activation and release of immune effector molecules (67). Mucins play an important role in maintaining the integrity of the normal intestinal flora by providing attachment sites for intestinal flora and pathogenic bacteria (68). Therefore, maintaining a healthy microbiota and mucin layer during chemotherapy treatment could minimise the complications associated with GIM. In this context, probiotic microorganisms represent a promising therapeutic option in treatment of GIM (69,70). Probiotics are defined as living microorganisms which when administered in adequate amounts, exert desirable health benefits on the host (71). Probiotics are known to exert beneficial effects to the host when ingested, and therefore could be useful in controlling the intestinal microflora during chemotherapy (72,73). Most commonly used probiotic bacteria include genera of *Lactobacillus* and *Bifidobacterium*. However, few strains of *Enterococcus*, *Streptococcus*, *Lactococcus* and certain species of non-pathogenic *Escherichia* strains have also been classified as probiotics (73).

Lactobacillus acidophilus administration concomitantly with 5-FU and alone for two additional days has been reported to significantly reverse the side effects of GIM (74). These include improvement in villus height-crypt depth ratio and decrease in TNF- α and IL-1 β levels after 5-FU treatment (74). Probiotic mixture VSL#3 reduced weight loss, prevented diarrhea and inhibited apoptosis in small and large intestine after treatment with irinotecan (75). *Saccharomyces boulardii* significantly reversed histopathological changes, reduced neutrophil infiltration and reduced concentrations of TNF- α and IL-1 β after 5-FU treatment (76). Cow's milk yoghurt fermented with *Lactobacillus johnsonii* and Sheep's milk yoghurt containing *Lactobacillus bulgaricus* and *Streptococcus thermophilus* improved small intestinal barrier functions as determined by

lactulose/mannitol ratio in MTX-induced rat models of GIM (77).

Orally ingested *Streptococcus thermophilus* attenuated MTX-induced small bowel damage in rats as indicated by non-invasive sucrose breath test (78). Probiotic derived supernatant from *Escherichia coli* Nissle 1971 (EcN) partially protected the intestine of dark agouti rats from 5-FU induced GIM and significantly decreased cell death induced in IEC-6 cell lines after treatment with 5-FU (79,80). *Lactobacillus fermentum* BR11 reduced jejunal inflammation as evident from reduced myeloperoxidase activity in 5-FU induced rat models of GIM (81). Pre-treatment EcN and LGG (*Lactobacillus rhamnosus*) supernatants lowered caspase activity, inhibited enterocyte apoptosis and loss of intestinal barrier function induced by 5-FU treatment of IEC-6 cells (82). Oral administration of probiotics *Lactobacillus casei* variety *rhamnosus* (Lcr35) or *Lactobacillus acidophilus* and *Bifidobacterium bifidum* (LaBi) appeared to ameliorate the intestinal mucositis severity by inhibition the expressions of proinflammatory cytokines (83). Various microorganisms used as probiotics for treatment of chemotherapy induced GIM are summarized in Table 2.

6. Miscellaneous complementary therapies

Administration of Emu oil daily via orogastric gavage after intraperitoneally injected single dose of 5-FU improved rate of recovery from GIM (84). Significant decrease in activated neutrophil infiltration, improvement in crypt depth and villus height, decrease in acute inflammation and overall improvement in mucosal architecture in the intestine have been reported after Emu oil supplementation (84,85). Lyprinol, a lipid extract derived from mussels and rich in omega-3 polyunsaturated fatty acids partially improved 5-FU induced GIM in rat models (86). Mice that received dietary supplementation with omega-3 fatty acid were associated with mucosal integrity and a reduced number of apoptotic cells in the ileum mucosa compared to the mice that received the control diet and 5-FU injection (87).

Table 2. Probiotic based complementary therapies for GIM

Complementary Therapy	Effect	Reference
<i>Lactobacillus acidophilus</i>	TNF- α , IL-1 β (Decrease)	74
Probiotic mixture VSL#3	Diarrhea, Apoptosis (Decrease)	75
<i>Saccharomyces boulardii</i>	Neutrophil infiltration (Decrease)	76
<i>Lactobacillus johnsonii</i>	Intestinal barrier functions (Improve)	77
<i>Lactobacillus bulgaricus</i>	Intestinal barrier functions (Improve)	77
<i>Streptococcus thermophilus</i>	Intestinal barrier functions(Improve)	77,78
<i>Escherichia coli</i> Nissle 1971	Apoptosis (Decrease)	79,80
<i>Lactobacillus fermentum</i> BR11	Myeloperoxidase activity (Decrease)	81
<i>Lactobacillus rhamnosus</i> & <i>Escherichia coli</i> Nissle 1971	Caspase activity (Decrease)	82
<i>Lactobacillus acidophilus</i> & <i>Bifidobacterium bifidum</i>	Proinflammatory cytokines (Decrease)	83
<i>Lactobacillus casei</i> variety <i>rhamnosus</i>	Proinflammatory cytokines (Decrease)	83

Table 3. Miscellaneous complementary therapies for GIM

Complementary Therapy	Effect	Reference
Emu oil	Neutrophil infiltration (Decrease)	84,85
Lyprinol	Crypt cell proliferation (Decrease)	86
Omega-3 fatty acid	Mucosal integrity (Improve)	87
L-arginine supplementation	Enterocyte apoptosis (Decrease)	88,89
β -Hydroxy- β -Methylbutyrate, L-Glutamine and L-Arginine	Enterocyte apoptosis (Decrease)	90
Insulin-like growth factor-I	Histopathological parameters (Improve)	91

Dietary L-arginine supplementation decreased enterocyte apoptosis accompanied by decrease in Bax mRNA and protein expression and increased Bcl-2 protein levels in rat model of MTX-induced GIM (88). L-arginine attenuated the histopathological score and myeloperoxidase activity promoting partial mucosal recovery, reducing inflammation and improving intestinal permeability in 5-FU induced GIM (89). Diet containing β -hydroxy- β -methylbutyrate, L-glutamine and L-arginine significantly decreased apoptosis in rats after administration of 5-FU (90). Pre-treatment with insulin-like growth factor-I in rats improved various intestinal parameters and partially attenuated features of intestinal mucositis when assessed 48 h after 5-FU chemotherapy (91). Table 3 summarizes these therapies.

7. Conclusions

Treatment options for patients with GIM are limited, and prevention requires an understanding of the pathophysiological mechanisms underlying GIM development. Despite the debilitating symptoms of chemotherapy-induced GIM, there remains no truly effective treatment strategy capable of preventing the associated intestinal damage. In this context, the role of CAM in treatment of GIM is very critical. Therapies based on CAM have been reported to improve the symptoms of GIM. Enthusiasm for CAM use and research is clearly growing. Medline citations for alternative medicine have steadily increased from 69 citations in the 1970s to 423 citations since 2000 (92). GIM with its varied pathobiology presents many molecular steps that can be targeted with CAM. However, the absence of rigorous scientific testing has

delayed the use of CAM in mainstream medicine. In this review, many studies related to use of CAM in treating GIM have been reported. Further studies are required to optimize the use of these novel agents to alleviate the distressing symptoms of intestinal mucositis. We have much still to learn about CAM treatments in terms of efficacy, safety and cost-effectiveness. For safe treatment of chemotherapy induced GIM, a truly collaborative effort between CAM practitioners, conventional physicians and research scientists is needed.

Acknowledgements

The author is thankful to Dr. Safrun Mahmood (PGIMER, Chandigarh), Prof. Akhtar Mahmood (Panjab University, Chandigarh), Dr. Mumtaz Anwar (University of Chicago, Illinois), and Dr. Showkat Ganie (Department of Clinical Biochemistry, University of Kashmir) for their support and suggestions.

References

- Daniele B, Secondulfo M, De Vivo R, Pignata S, De Magistris L, Delrio P, Palaia R, Barletta E, Tambaro R, Carratù R. Effect of chemotherapy with 5-fluorouracil on intestinal permeability and absorption in patients with advanced colorectal cancer. *J Clin Gastroenterol.* 2001; 32:228-230.
- Duncan M, Grant G. Oral and intestinal mucositis-causes and possible treatments. *Aliment Pharmacol Ther.* 2003; 18:853-874.
- Bowen JM, Gibson RJ, Cummins AG, Keefe DM. Intestinal mucositis: The role of the Bcl-2 family, p53 and caspases in chemotherapy-induced damage. *Support Care Cancer.* 2006; 14:713-731.

4. Keefe DM, Brealey J, Goland GJ, Cummins AG. Chemotherapy for cancer causes apoptosis that precedes hypoplasia in crypts of the small intestine in humans. *Gut*. 2000; 47:632-637.
5. Keefe DM, Gibson RJ, Hauer-Jensen M. Gastrointestinal mucositis. *Semin Oncol Nurs*. 2004; 20:38-47.
6. Keefe DM, Cummins AG, Dale BM, Kotasek D, Robb TA, Sage RE. Effect of high-dose chemotherapy on intestinal permeability in humans. *Clin Sci (Lond)*. 1997; 92:385-389.
7. Elting LS, Cooksley CD, Chambers MS, Garden AS. Risk, outcomes, and costs of radiation-induced oral mucositis among patients with head-and-neck malignancies. *Int J Radiat Oncol Biol Phys*. 2007; 68:1110-1120.
8. Peterson LW, Artis D. Intestinal epithelial cells: Regulators of barrier function and immune homeostasis. *Nat Rev Immunol*. 2014; 14:141-153.
9. Crosnier C, Stamataki D, Lewis J. Organizing cell renewal in the intestine: Stem cells, signals and combinatorial control. *Nat Rev Genet*. 2006; 7:349-359.
10. Van der Flier LG, Clevers H. Stem cells, self renewal, and differentiation in the intestinal epithelium. *Annu Rev Physiol*. 2009; 71:241-260.
11. Potten CS, Booth C, Hargreaves D. The small intestine as a model for evaluating adult tissue stem cell drug targets. *Cell Prolif*. 2003; 36:115-129.
12. Booth C, Potten CS. Gut instincts: Thoughts on intestinal epithelial stem cells. *J Clin Invest*. 2000; 105:1493-1499.
13. Gibson RJ, Bowen JM, Inglis MR, Cummins AG, Keefe DM. Irinotecan causes severe small intestinal damage, as well as colonic damage, in the rat with implanted breast cancer. *J Gastroenterol Hepatol*. 2003; 18:1095-1100.
14. Sonis ST. The pathobiology of mucositis. *Nat Rev Cancer*. 2004; 4:277-284.
15. Logan RM, Stringer AM, Bowen JM, Yeoh AS, Gibson RJ, Sonis ST, Keefe DM. The role of pro-inflammatory cytokines in cancer treatment-induced alimentary tract mucositis: Pathobiology, animal models and cytotoxic drugs. *Cancer Treat Rev*. 2007; 33:448-460.
16. Bowen JM, Gibson RJ, Cummins AG, Tyskin A, Keefe DM. Irinotecan changes gene expression in the small intestine of the rat with breast cancer. *Cancer Chemother Pharmacol*. 2007; 59:337-348.
17. Bowen JM, Gibson RJ, Tyskin A, Stringer AM, Logan RM, Keefe DM. Gene expression analysis of multiple gastrointestinal regions reveals activation of common cell regulatory pathways following cytotoxic chemotherapy. *Int J Cancer*. 2007; 121:1847-1856.
18. Chang CT, Ho TY, Lin H, Liang JA, Huang HC, Li CC, Lo HY, Wu SL, Huang YF, Hsiang CY. 5-Fluorouracil induced intestinal mucositis via nuclear factor- κ B activation by transcriptomic analysis and *in vivo* bioluminescence imaging. *PLoS One*. 2012; 7:e31808.
19. Ong ZY, Gibson RJ, Bowen JM, Stringer AM, Darby JM, Logan RM, Yeoh AS, Keefe DM. Pro-inflammatory cytokines play a key role in the development of radiotherapy-induced gastrointestinal mucositis. *Radiat Oncol*. 2010; 5:22.
20. Logan RM, Gibson RJ, Bowen JM, Stringer AM, Sonis ST, Keefe DM. Characterisation of mucosal changes in the alimentary tract following administration of irinotecan: Implications for the pathobiology of mucositis. *Cancer Chemother Pharmacol*. 2008; 62:33-41.
21. Bowen JM, Gibson RJ, Keefe DM. Cytotoxic chemotherapy up-regulates pro-apoptotic Bax and Bak in the small intestine of rats and humans. *Pathology*. 2005; 37:56-62.
22. Stringer AM, Gibson RJ, Logan RM, Bowen JM, Yeoh AS, Laurence J, Keefe DM. Irinotecan induced mucositis is associated with changes in intestinal mucins. *Cancer Chemother Pharmacol*. 2009; 64:123-132.
23. Wardill HR, Bowen JM, Al-Dasooqi N, Sultani M, Bateman E, Stansborough R, Shirren J, Gibson RJ. Irinotecan disrupts tight junction proteins within the gut: Implications for chemotherapy-induced gut toxicity. *Cancer Biol Ther*. 2014; 15:236-244.
24. Al-Dasooqi N, Wardill HR, Gibson RJ. Gastrointestinal mucositis: The role of MMP-tight junction interactions in tissue injury. *Pathol Oncol Res*. 2014; 3:485-491.
25. Kaczmarek A, Brinkman BM, Heyndrickx L, Vandenabeele P, Krysko DV. Severity of doxorubicin-induced small intestinal mucositis is regulated by the TLR-2 and TLR-9 pathways. *J Pathol*. 2012; 226:598-608.
26. Frank M, Hennenberg EM, Eyking A, Rünzi M, Gerken G, Scott P, Parkhill J, Walker AW, Cario E. TLR signaling modulates side effects of anticancer therapy in the small intestine. *J Immunol*. 2015; 194:1983-1995.
27. Wong DV, Lima-Júnior RC, Carvalho CB, Borges VF, Wanderley CW, Bem AX, Leite CA, Teixeira MA, Batista GL, Silva RL, Cunha TM, Brito GA, Almeida PR, Cunha FQ, Ribeiro RA. The adaptor protein Myd88 is a key signaling molecule in the pathogenesis of irinotecan-induced intestinal mucositis. *PLoS One*. 2015; 10:e0139985.
28. Wardill HR, Gibson RJ, Logan RM, Bowen JM. TLR4/ PKC-mediated tight junction modulation: A clinical marker of chemotherapy-induced gut toxicity? *Int J Cancer*. 2014; 135:2483-2492.
29. Logan RM, Stringer AM, Bowen JM, Gibson RJ, Sonis ST, Keefe DM. Is the pathobiology of chemotherapy-induced alimentary tract mucositis influenced by the type of mucotoxic drug administered? *Cancer Chemother Pharmacol*. 2009; 63:239-251.
30. Stringer AM. Interaction between host cells and microbes in chemotherapy induced mucositis. *Nutrients*. 2013; 5:1488-1499.
31. Cario E. Innate immune signalling at intestinal mucosal surfaces: A fine line between host protection and destruction. *Curr Opin Gastroenterol*. 2008; 24:725-732.
32. Carvalho FA, Aitken JD, Vijay-Kumar M, Gewirtz AT. Toll-like receptor-gut microbiota interactions: Perturb at your own risk! *Annu Rev Physiol*. 2012; 74:177-198.
33. Shi D, Das J, Das G. Inflammatory bowel disease requires the interplay between innate and adaptive immune signals. *Cell Res*. 2006; 16:70-74.
34. Fernandes-Alnemri T, Kang S, Anderson C, Fitzgerald KA, Alnemri ES. Cutting edge: TLR signaling licenses IRAK1 for rapid activation of the NLRP3 inflammasome. *J Immunol*. 2013; 191:3995-3999.
35. Soares PM, Lima-Junior RC, Mota JM, Justino PF, Brito GA, Ribeiro RA, Cunha FQ, Souza MH. Role of platelet-activating factor in the pathogenesis of 5-fluorouracil-induced intestinal mucositis in mice. *Cancer Chemother Pharmacol*. 2011; 68:713-720.
36. Yasuda M, Kato S, Yamanaka N, Iimori M, Utsumi D, Kitahara Y, Iwata K, Matsuno K, Amagase K, Yabe-Nishimura C, Takeuchi K. Potential role of the NADPH oxidase NOX1 in the pathogenesis of 5-fluorouracil-induced intestinal mucositis in mice. *Am J Physiol Gastrointest Liver Physiol*. 2012; 302:1133-1142.

37. Arifa RD, Madeira MF, de Paula TP, Lima RL, Tavares LD, Menezes-Garcia Z, Fagundes CT, Rachid MA, Ryffel B, Zamboni DS, Teixeira MM, Souza DG. Inflammasome activation is reactive oxygen species dependent and mediates irinotecan-induced mucositis through IL-1 β and IL-18 in mice. *Am J Pathol.* 2014; 184:2023-2034.
38. Stringer AM, Gibson RJ, Logan RM, Bowen JM, Yeoh AS, Hamilton J, Keefe DM. Gastrointestinal microflora and mucins may play a critical role in the development of 5-fluorouracil-induced gastrointestinal mucositis. *Exp Biol Med (Maywood).* 2009; 234:430-441.
39. Horie T, Matsumoto H, Kasagi M, Sugiyama A, Kikuchi M, Karasawa C, Awazu S, Itakura Y, Fuwa T. Protective effect of aged garlic extract on the small intestinal damage of rats induced by methotrexate treatment. *Planta Med.* 1999; 65:545-548.
40. Yuncu M, Eralp A, Celik A. Effect of aged garlic extract against methotrexate-induced damage to the small intestine in rats. *Phytother Res.* 2006; 20:504-510.
41. Li T, Ito K, Sumi S, Fuwa T, Horie T. Protective effect of aged garlic extract (AGE) on the apoptosis of intestinal epithelial cells caused by methotrexate. *Cancer Chemother Pharmacol.* 2009; 63:873-880.
42. Cheah KY, Howarth GS, Bastian SE. Grape seed extract dose-responsively decreases disease severity in a rat model of mucositis; concomitantly enhancing chemotherapeutic effectiveness in colon cancer cells. *PLoS One.* 2014; 9:e85184.
43. Cheah KY, Howarth GS, Yazbeck R, Wright TH, Whitford EJ, Payne C, Butler RN, Bastian SE. Grape seed extract protects IEC-6 cells from chemotherapy-induced cytotoxicity and improves parameters of small intestinal mucositis in rats with experimentally-induced mucositis. *Cancer Biol Ther.* 2009; 8:382-390.
44. Yang G, Wangm H, Kang Y, Zhu MJ. Grape seed extract improves epithelial structure and suppresses inflammation in ileum of IL-10-deficient mice. *Food Funct.* 2014; 5:2558-2563.
45. Yang G, Xue Y, Zhang H, Du M, Zhu MJ. Favourable effects of grape seed extract on intestinal epithelial differentiation and barrier function in IL10-deficient mice. *Br J Nutr.* 2015; 114:15-23.
46. Shi J, Yu J, Pohorly JE, Kakuda Y. Polyphenolics in grape seeds-biochemistry and functionality. *J Med Food.* 2003; 6:291-299.
47. Gu L, Kelm MA, Hammerstone JF, Beecher G, Holden J, Haytowitz D, Gebhardt S, Prior RL. Concentrations of proanthocyanidins in common foods and estimations of normal consumption. *J Nutr.* 2004; 134:613-617.
48. Gulgun M, Erdem O, Oztas E, Kesik V, Balamtekin N, Vurucu S, Kul M, Kismet E, Koseoglu V. Proanthocyanidin prevents methotrexate-induced intestinal damage and oxidative stress. *Exptl Toxicol Path.* 2010; 62:109-115.
49. Gulgun M, Karaoglu A, Kesik V, Kurt B, Erdem O, Tok D, Kismet E, Koseoglu V, Ozcan O. Effect of proanthocyanidin, arginine and glutamine supplementation on methotrexate-induced gastrointestinal toxicity in rats. *Methods Find Exp Clin Pharmacol.* 2010; 32:657-661.
50. Vardi N, Parlakpınar H, Ozturk F, Ates B, Gul M, Cetin A, Erdogan A, Otlu A. Potent protective effect of apricot and beta-carotene on methotrexate-induced intestinal oxidative damage in rats. *Food Chem Toxicol.* 2008; 46:3015-3022.
51. Yuncu M, Eralp A, Koruk M, Sari I, Bağcı C, Inalöz S. Effect of vitamin A against methotrexate-induced damage to the small intestine in rats. *Med Princ Pract.* 2004; 13:346-352.
52. El-Boghdady NA. Protective effect of ellagic acid and pumpkin seed oil against methotrexate-induced small intestine damage in rats. *Indian J Biochem Biophys.* 2011; 48:380-387.
53. Acipayam C, Bayram I, Daglioglu K, Doran F, Yilmaz S, Sezgin G, Totan Ateş B, Ozkan A, Tanyeli A. The protective effect of hesperidin on methotrexate-induced intestinal epithelial damage in rats: An experimental study. *Med Princ Pract.* 2014; 23:45-52.
54. Liu Z, Xi J, Schröder S, Wang W, Xie T, Wang Z, Bao S, Fei J. *Chimonanthus nitens* var. *salicifolius* aqueous extract protects against 5-fluorouracil induced gastrointerstitial mucositis in a mouse model. *Evid Based Complement Alternat Med.* 2013; 2013:789263.
55. Arjumand W, Seth A, Sultana S. Rutin attenuates cisplatin induced renal inflammation and apoptosis by reducing NF κ B, TNF- α and caspase-3 expression in Wistar rats. *Food Chem Toxicol.* 2011; 49:2013-2021.
56. Gong G, Qin Y, Huang W, Zhou S, Yang X, Li D. Rutin inhibits hydrogen peroxide-induced apoptosis through regulating reactive oxygen species mediated mitochondrial dysfunction pathway in human umbilical vein endothelial cells. *Eur J Pharmacol.* 2010; 628:27-35.
57. Yao Q, Ye X, Wang L, Gu J, Fu T, Wang Y, Lai Y, Wang Y, Wang X, Jin H, Guo Y. Protective effect of curcumin on chemotherapy-induced intestinal dysfunction. *Int J Clin Exp Pathol.* 2013; 6:2342-2349.
58. Song WB, Wang YY, Meng FS, Zhang QH, Zeng JY, Xiao LP, Yu XP, Peng DD, Su L, Xiao B, Zhang ZS. Curcumin protects intestinal mucosal barrier function of rat enteritis via activation of MKP-1 and attenuation of p38 and NF-kappaB activation. *PloS One.* 2010; 5:e12969.
59. Sener G, Ekşioğlu-Demiralp E, Cetiner M, Ercan F, Yeğen BC. Beta-glucan ameliorates methotrexate induced oxidative organ injury via its antioxidant and immunomodulatory effects. *Eur J Pharmacol.* 2006; 542:170-178.
60. Kato S, Hayashi S, Kitahara Y, Nagasawa K, Aono H, Shibata J, Utsumi D, Amagase K, Kadowaki M. Saireito (TJ-114), a Japanese traditional herbal medicine, reduces 5-fluorouracil-induced intestinal mucositis in mice by inhibiting cytokine-mediated apoptosis in intestinal crypt cells. *PLoS One.* 2015; 10:e0116213.
61. Germann I, Hagelauer D, Kelber O, Vinson B, Laufer S, Weiser D, Heinle H. Antioxidative properties of the gastrointestinal phytopharmaceutical remedy STW 5 (Iberogast). *Phytomedicine.* 2006; 13:45-50.
62. Wright TH, Yazbeck R, Lynn KA, Whitford EJ, Cheah KY, Butler RN, Feinle-Bisset C, Pilichiewicz AN, Mashtoub S, Howarth GS. The herbal extract, Iberogast, improves jejunal integrity in rats with 5-fluorouracil (5-FU)-induced mucositis. *Cancer Biol Ther.* 2009; 8:923-929.
63. Díaz AM, Abad MJ, Fernández L, Silván AM, De Santos J, Bermejo P. Phenylpropanoid glycosides from *Scrophularia scorodonia*: *In vitro* anti-inflammatory activity. *Life Sci.* 2004; 74:2515-2526.
64. Reinke D, Kritas S, Polychronopoulos P, Skaltsounis AL, Aligiannis N, Tran CD. Herbal substance, acteoside, alleviates intestinal mucositis in mice. *Gastroenterol Res Pract.* 2015; 2015:327872.
65. Ávila PH, Ávila RI, Filho EX, Bastos CC, Batista AC, Mendonça EF, Serpa RC, Marreto RN, Cruz AF, Lima

- EM, Valadares MC. Mucoadhesive formulation of *Bidens pilosa* L. (Asteraceae) reduces intestinal injury from 5-fluorouracil-induced mucositis in mice. *Toxicol Rep*. 2015; 2:563-573.
66. Stringer AM, Gibson RJ, Logan RM, Bowen JM, Yeoh AS, Burns J, Keefe DM. Chemotherapy-induced diarrhea is associated with changes in the luminal environment in the DA rat. *Exp Biol Med* (Maywood). 2007; 232:96-106.
 67. Van Vliet MJ, Harmsen HJ, de Bont ES, Tissing WJ. The role of intestinal microbiota in the development and severity of chemotherapy-induced mucositis. *PLoS Pathog*. 2010; 6:e1000879.
 68. Robbe C, Capon C, Coddeville B, Michalski JC. Structural diversity and specific distribution of O-glycans in normal human mucins along the intestinal tract. *Biochem J*. 2004; 384:307-316.
 69. Wang H, Geier MS, Howarth GS. Prebiotics: A potential treatment strategy for the chemotherapy-damaged gut? *Crit Rev Food Sci Nutr*. 2016; 56:946-956.
 70. Prisciandaro LD, Geier MS, Butler RN, Cummins AG, Howarth GS. Evidence supporting the use of probiotics for the prevention and treatment of chemotherapy-induced intestinal mucositis. *Crit Rev Food Sci Nutr*. 2011; 51:239-247.
 71. Reid G. The importance of guidelines in the development and application of probiotics. *Curr Pharm Des*. 2005; 11:11-16.
 72. Quigley EM. Probiotics in the management of colonic disorders. *Curr Gastroenterol Rep*. 2007; 9:434-440.
 73. Borchers AT, Selmi C, Meyers FJ, Keen CL, Gershwin ME. Probiotics and immunity. *J Gastroenterol*. 2009; 44:26-46.
 74. Justino PF, Melo LF, Nogueira AF, Morais CM, Mendes WO, Franco AX, Souza EP, Ribeiro RA, Souza MH, Soares PM. Regulatory role of *Lactobacillus acidophilus* on inflammation and gastric dysmotility in intestinal mucositis induced by 5-fluorouracil in mice. *Cancer Chemother Pharmacol*. 2015; 75:559-567.
 75. Bowen JM, Stringer AM, Gibson RJ, Yeoh AS, Hannam S, Keefe DM. VSL#3 probiotic treatment reduces chemotherapy-induced diarrhoea and weight loss. *Cancer Biol Ther*. 2007; 6:1449-1454.
 76. Justino PF, Melo LF, Nogueira AF, Costa JV, Silva LM, Santos CM, Mendes WO, Costa MR, Franco AX, Lima AA, Ribeiro RA, Souza MH, Soares PM. Treatment with *Saccharomyces boulardii* reduces the inflammation and dysfunction of the gastrointestinal tract in 5-fluorouracil-induced intestinal mucositis in mice. *Br J Nutr*. 2014; 111:1611-1621.
 77. Southcott E, Tooley KL, Howarth GS, Davidson GP, Butler RN. Yoghurts containing probiotics reduce disruption of the small intestinal barrier in methotrexate-treated rats. *Dig Dis Sci*. 2008; 53:1837-1841.
 78. Tooley K, Howarth G, Lymn K, Lawrence A, Butler RN. Oral ingestion of *Streptococcus thermophilus* diminishes severity of small intestinal mucositis in methotrexate treated rats. *Cancer Biol Ther*. 2006; 5:593-600.
 79. Prisciandaro LD, Geier MS, Butler RN, Cummins AG, Howarth GS. Probiotic factors partially improve parameters of 5-fluorouracil-induced intestinal mucositis in rats. *Cancer Biol Ther*. 2011; 11:671-677.
 80. Wang H, Bastian SE, Cheah KY, Lawrence A, Howarth GS. *Escherichia coli* Nissle 1917-derived factors reduce cell death and late apoptosis and increase transepithelial electrical resistance in a model of 5-fluorouracil induced intestinal epithelial cell damage. *Cancer Biol Ther*. 2014; 15:560-569.
 81. Smith CL, Geier MS, Yazbeck R, Torres DM, Butler RN, Howarth GS. *Lactobacillus fermentum* BR11 and fructo oligosaccharide partially reduce jejunal inflammation in a model of intestinal mucositis in rats. *Nutr Cancer*. 2008; 60:757-767.
 82. Prisciandaro LD, Geier MS, Chua AE, Butler RN, Cummins AG, Sander GR, Howarth GS. Probiotic factors partially prevent changes to caspases 3 and 7 activation and transepithelial electrical resistance in a model of 5-fluorouracil-induced epithelial cell damage. *Support Care Cancer*. 2012; 20:3205-3210.
 83. Yeung CY, Chan WT, Jiang CB, Cheng ML, Liu CY, Chang SW, Chiang Chiau JS, Lee HC. Amelioration of chemotherapy-induced intestinal mucositis by orally administered probiotics in a mouse model. *PLoS One*. 2015; 10:e0138746.
 84. Lindsay RJ, Geier MS, Yazbeck R, Butler RN, Howarth GS. Orally administered emu oil decreases acute inflammation and alters selected small intestinal parameters in a rat model of mucositis. *Br J Nutr*. 2010; 104:513-519.
 85. Mashtoub S, Tran CD, Howarth GS. Emu oil expedites small intestinal repair following 5-fluorouracil-induced mucositis in rats. *Exp Biol Med* (Maywood). 2013; 238:1305-1317.
 86. Torres DM, Tooley KL, Butler RN, Smith CL, Geier MS, Howarth GS. Lyprinol only partially improves indicators of small intestinal integrity in a rat model of 5-fluorouracil-induced mucositis. *Cancer Biol Ther*. 2008; 7:295-302.
 87. Generoso Sde V, Rodrigues NM, Trindade LM, Paiva NC, Cardoso VN, Carneiro CM, Ferreira AV, Faria AM, Maioli TU. Dietary supplementation with omega-3 fatty acid attenuates 5 fluorouracil induced mucositis in mice. *Lipids Health Dis*. 2015; 14:54.
 88. Koppelman T, Pollak Y, Mogilner J, Bejar J, Coran AG, Sukhotnik I. Dietary L-arginine supplementation reduces methotrexate-induced intestinal mucosal injury in rat. *BMC Gastroenterol*. 2012; 12:41.
 89. Leocádio PC, Antunes MM, Teixeira LG, Leonel AJ, Alvarez-Leite JI, Machado DC, Generoso SV, Cardoso VN, Correia MI. L-arginine pretreatment reduces intestinal mucositis as induced by 5-FU in mice. *Nutr Cancer*. 2015; 67:486-493.
 90. Alsan Cetin I, Atasoy BM, Cilaker S, Alicikus LZ, Karaman M, Ersoy N, Demiral AN, Yilmaz O. A diet containing beta-hydroxy-beta methylbutyrate, L glutamine and L-arginine ameliorates chemo-radiation induced gastrointestinal injury in rats. *Radiat Res*. 2015; 184:411-421.
 91. Cool JC, Dyer JL, Xian CJ, Butler RN, Geier MS, Howarth GS. Pre-treatment with insulin-like growth factor-I partially ameliorates 5-fluorouracil induced intestinal mucositis in rats. *Growth Horm IGF Res*. 2005; 15:72-82.
 92. Tillisch K. Complementary and alternative medicine for functional gastrointestinal disorders. *Gut*. 2006; 55:593-596.

(Received September 8, 2016; Revised September 30, 2016; Accepted October 6, 2016)

Generic selection criteria for safety and patient benefit [VI]: Comparing the physicochemical and pharmaceutical properties of brand-name, generic, and OTC felbinac tapes

Yuko Wada¹, Yukie Takaoka¹, Mitsuru Nozawa², Miho Goto², Ken-ichi Shimokawa¹, Fumiyoshi Ishii^{1,*}

¹Department of Pharmaceutical Sciences, Meiji Pharmaceutical University, Tokyo, Japan;

²Triad Japan Co., Ltd., Kanagawa, Japan.

Summary

We measured the pH, water-vapor permeability, adhesive force, peeling-force, elongation rate, support flexibility, and peeling time of medicinal and over-the-counter (OTC) tape preparations containing felbinac. When measuring the pH of each preparation, Felnabion (pH 4.5) was weakly acidic, and EMEC and Tokuon (pH 7.0) were neutral. When measuring the water-vapor permeability of each preparation, that of a generic product, EMEC (380 g/m²/24 h), was twice as high as that of a brand-name product, Seltouch (189 g/m²/24 h). The adhesive force was measured using the ball tack test. The adhesive forces of OTC drugs, Salomethyl, Homepass, and Tokuhon (1.04 g), were higher than that of Seltouch (0.06 g). Concerning peeling-force measurement, the peeling-forces of a generic product, Falzy (4.15 N), and an OTC drug, Omuneed (4.89 N), were higher than that of Seltouch (0.91 N). The elongation rates of a generic product, Sumilu (319%), and OTC drugs, Nabolin (298%) and Homepass (299%), were higher than that of Seltouch (251%), but that of Tokuhon (72%) was lower. The support flexibilities of EMEC (150 degrees) and Tokuhon (131 degrees) were higher than that of Seltouch (96 degrees). In addition, the peeling time of Seltouch was 120 min or more, whereas those of EMEC and Nabolin were 1.4 and 0.2 min, respectively. These results suggest that the differences in pharmaceutical properties, such as the pH, water-vapor permeability, adhesive force, peeling-force, elongation rate, support flexibility, and peeling time, among the preparations markedly influence patients' subjective comfortableness. The results of this study facilitated individuals' comfortableness-matched drug selection.

Keywords: Brand-name products, generic products, OTC, tape preparation, felbinac

1. Introduction

A topical preparation containing a nonsteroidal anti-inflammatory drug, felbinac-containing tape preparation, is selected for many patients to relieve muscular or articular pain (1). Concerning this drug, a brand-name medicinal product, Seltouch, and many generic products

are commercially available, and a large number of switched OTC drugs are also commercially available. The active component contents of these switched OTC drugs are equivalent to those of medicinal products; similar effects may be obtained. As for merit, the former can be purchased at a drug store without prescription. As anyone can purchase the switched OTC drugs without consulting a hospital, these drugs may reduce expanded health expenditures as an important social problem. However, the effects are not sufficient (2,3).

In the future, to promote the widespread use of proprietary drugs, including switched OTC drugs, it is necessary to appeal to their wide usefulness. To provide adequate drug information to patients, pharmacists must understand the pharmaceutical properties of both

Released online in J-STAGE as advance publication October 4, 2016.

*Address correspondence to:

Dr. Fumiyoshi Ishii, Department of Pharmaceutical Sciences, Meiji Pharmaceutical University, 2-522-1, Noshio, Kiyose, Tokyo 204-8588, Japan.
E-mail: fishii@my-pharm.ac.jp

Table 1. Products used in this experiment

Product name	Abbreviated name	Class	Company	Size (cm)	Serial number
Seltouch [®] tape 70	Seltouch	brand-name	Teikoku Seiyaku Co., Ltd.	10 × 14	12K06A
Felbinac [®] tape 70 mg "EMEC"	EMEC	generic	Kyukyu Pharmaceutical Co., Ltd.	10 × 14	2W21P
Sumilu [®] tape 70 mg	Sumilu	generic	Mikasa Seiyaku Co., Ltd.	10 × 14	301222
Flex [®] tape 70 mg	Flex	generic	Hisamitsu Pharmaceutical Co., Inc.	10 × 14	N301U
Felnabion [®] tape 70 mg	Felnabion	generic	Okayama Taiho Pharmaceutical Co., Ltd.	10 × 14	2I89
Falzy [®] tape 70 mg	Falzy	generic	Nipro Patch Co., Ltd.	10 × 14	FJ001
Nabolin [®] Felbinac 70	Nabolin	OTC	Kyukyu Pharmaceutical Co., Ltd.	10 × 14	2T11W
Patecs [®] Felbinastar VL	Patecs	OTC	Daiichi Sankyo Healthcare Co., Ltd.	10 × 14	GK002
Faitus [®] 3.5 αL	Faitus	OTC	Hisamitsu Pharmaceutical Co., Inc.	10 × 14	N221U
Salomethyl [®] FB Patch 35	Salomethyl	OTC	Toko Pharmaceutical Industrial Co., Ltd.	7 × 10	LXBK
Omuneed [®] FB Plaster	Omuneed	OTC	Teikoku Seiyaku Co., Ltd.	7 × 10	6205
Homepass [®] FR	Homepass	OTC	Oishi Koseido Co., Ltd.	7 × 10	241212
Tokuhon [®] Felbina Plaster	Tokuhon	OTC	Tokuhon Co., Ltd.	5.6 × 6.5	2E02
Menfla [®] Felbinac Onkan	Menfla	OTC	Kyoritsu Pharmaceutical Industres Co., Ltd.	7 × 10	13E02

OTC: over-the-counter drug.

medicinal and proprietary drugs. However, information on these drugs is not sufficient (4).

We have compared the pharmaceutical properties of various medicinal drugs between brand-name and generic products (5-9). In this study, with respect to felbinac-containing tape preparations, which are used in many patients, we compared the pharmaceutical properties of 6 medicinal drugs (1 brand-name and 5 generic products) and 8 OTC drugs.

2. Materials and Methods

2.1. Materials

As felbinac tape, a brand-name product, Seltouch[®] tape 70 (Teikoku Seiyaku Co., Ltd., Kagawa, Japan), generic products, Felbinac[®] tape 70 mg "EMEC" (Kyukyu Pharmaceutical Co., Ltd., Tokyo, Japan), Sumilu[®] tape 70 mg (Mikasa Seiyaku Co., Ltd., Tokyo, Japan), Flex[®] tape 70 mg (Hisamitsu Pharmaceutical Co., Inc., Osaka, Japan), Felnabion[®] tape 70 mg (Okayama Taiho Pharmaceutical Co., Ltd., Okayama, Japan), Falzy[®] tape 70 mg (Nipro Patch Co., Ltd., Saitama, Japan), and OTC products, Nabolin[®] Felbinac 70 (Kyukyu Pharmaceutical Co., Ltd., Tokyo, Japan), Patecs[®] Felbinastar VL (Daiichi Sankyo Healthcare Co., Ltd., Tokyo, Japan), Faitus[®] 3.5αL (Hisamitsu Pharmaceutical Co., Inc., Osaka, Japan), Salomethyl[®] FB Patch 35 (Toko Pharmaceutical Industrial Co., Ltd., Tokyo, Japan), Omuneed[®] FB Plaster (Teikoku Seiyaku Co., Ltd., Kagawa, Japan), Homepass[®] FR (Oishi Koseido Co., Ltd., Saga, Japan), Tokuhon[®] Felbina Plaster (Tokuhon Co., Ltd., Tokyo, Japan), Menfla[®] Felbinac Onkan (Kyoritsu Pharmaceutical Industres Co., Ltd., Tokyo, Japan), were purchased and used in this experiment (Table 1). All the other reagents were of analytical grade.

2.2. Measurement of pH

We measured pH values, as described by Wada *et al.*

(8). Briefly, each preparation was cut into sections measuring 70 × 50 mm, placed in sample bottles containing 20 mL of purified water, and agitated for 24 h. Subsequently, the pH of the solution was measured using a Benchtop pH meter F-74 (HORIBA, Ltd., Kyoto, Japan). For each product, measurement was conducted 3 times, and the mean was adopted as its pH value.

2.3. Measurement of the water-vapor permeability

The water-vapor permeability test was performed, as described by Hiyoshi *et al.* (10). Briefly, 10 mL of purified water was placed in a glass container, and its opening was covered with a round section of each product measuring 40 mm in diameter. After the periphery was fixed with a piece of elastic paraffin film (Parafilm[®]: Bemis Flexible Packaging, IL, USA), the weight was measured. Subsequently, each sample was allowed to stand for 24 h in an environment chamber KCL-2000W (Tokyo Rikakikai Co., Ltd., Tokyo, Japan) under the following conditions: temperature, 40°C; relative humidity, 50%. Additionally, the weight was measured. The water-vapor permeability was calculated from the rate of change in the weight using the following formula: water-vapor permeability (g/m²/24 h) = (W₀ - W₁) × 10,000/A [W₀: weight before testing (g), W₁: weight after testing (g), A: area of the glass container's opening (cm²)]. With respect to each product, a measurement was conducted 3 times, and the mean was regarded as the water-vapor permeability.

2.4. Measurement of the adhesive force

The adhesive force was measured according to the inclined ball tack test method established in the Japanese Industrial Standards (JIS) (11). A section of each product measuring 10 × 200 mm was longitudinally attached on the inclined ball tack examination device TransTack[®] Ball-Tack Meter (CosMED Pharmaceutical

Co. Ltd., Kyoto, Japan) under the following conditions: temperature, 25°C; relative humidity, 50%. The weight of the maximum ball number was measured by the inclined ball tuck examination device. With respect to each product, a measurement was conducted 3 times, and the mean was regarded as the adhesive force.

2.5. Measurement of the peeling-force

The peeling-force was measured according to the adhesive tape/sheet test method described by Miura *et al.* (12). Briefly, a slide table P90-200N (Imada Co., Ltd., Aichi, Japan) for 90 degrees peeling test was fixed on an MX2-500N (Imada Co., Ltd., Aichi, Japan) stand for measurements, and controlled caliper ethylene vinyl acetate (EVA) membrane (3M CoTran™ 9702, 3M Japan Ltd., Tokyo Japan) as a type of artificial skin was fixed on the slide table. On its surface, a section of each product measuring 30 × 52 mm was longitudinally attached. In addition, a cylindrical weight (4 kg) was rolled over each product. Subsequently, the peeling-force was measured by pinching a 2-mm area of the upper margin with a film clip FC-40 (Imada Co., Ltd., Aichi, Japan) and pulling it at a constant rate (1 mm/sec) so that the adhesive surface was vertical to a digital force gauge, ZP-50N (Imada Co., Ltd., Aichi, Japan), until the tape had been completely exfoliated from the EVA membrane. With respect to each product, a measurement was conducted 3 times, and the mean was regarded as the peeling-force.

2.6. Measurement of the elongatedness

An elongatedness test was performed, as described by Terada *et al.* (13). The end (20 mm) of a section of each product measuring 20 × 100 mm was fixed on an experimental table with the adhesive surface. The maximum extension distance (cm) was measured by pulling the other side. The elongatedness (%) was calculated from the values before and after. For each product, a measurement was conducted 3 times, and the mean was regarded as the elongatedness.

2.7. Measurement of the support flexibility

Each preparation was cut into a square (50 × 50mm) and half areas (25 × 50mm) were stuck on the edge of the test table, and the bending angle of the remaining half was measured. The flexibility of the support was evaluated. For each product, a measurement was conducted 3 times, and the mean was regarded as the flexibility.

2.8. Measurement of time before exfoliating from skin when the preparation was wet with water

Each preparation was cut by into a square (50 × 50 mm) and affixed by constant pressure on artificial skin (bioskin

No.10A; Beulax Co., Ltd., Saitama, Japan), and stirred in purified water on a magnetic stirrer (1,000 rpm). The peeling time for each preparation was measured. For each product, a measurement was conducted 3 times, and the mean was regarded as the peeling time.

2.9. Statistical analysis

The values were compared using *Dunnnett's* test. A *p*-value of 0.05 or 0.01 was regarded as significant.

3. Results

3.1. Measurement of pH

The pH is an important factor reflecting the stability of the active component in each preparation or skin irritability. The results of pH measurements for each product are shown in Figure 1. There were marked differences in pH among the brand-name, generic, and OTC products. The pH values of generic products, Sumilu (pH 4.7), Flex (pH 4.7), Felnabion (pH 4.5), and Falzy (pH 4.6), were similar to that of a brand-name product, Seltouch (pH 4.6). Those of OTC products, Patecs (pH 4.8), Faitus (pH 4.9), Salomethyl (pH 4.7), Omuneed (pH 4.6), and Menfla (pH 4.7), were also similar to that of Seltouch. On the other hand, the pH values of a generic product, EMEC (pH 7.0), and OTC products, Nabolin (pH 5.6), Homepass (pH 5.1), and Tokuhon (pH 7.0), were higher. Significance tests of these products were conducted. There were significant differences between EMEC/Nabolin/Homepass/Tokuhon and Seltouch (*p* < 0.01) (Figure 1).

3.2. Measurement of the water-vapor permeability

The water-vapor permeability of each preparation may induce maceration stimuli when the skin water permeability is low on attachment. We measured the water-vapor permeability of each product. The results are shown in Figure 2. There were marked differences

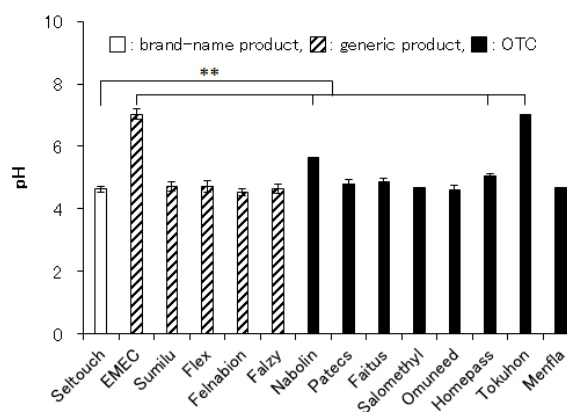


Figure 1. pH comparison of various products (n = 3). ***p* < 0.01 (brand-name vs. generics, *Dunnnett's* test).

in the water-vapor permeability among the products; the water-vapor permeabilities of EMEC (380 g/m²/24 h), Sumilu (318 g/m²/24 h), and Nabolin (269 g/m²/24 h) were higher than that of Seltouch (189 g/m²/24 h). In addition, the results showed significant differences between EMEC, Sumilu, Nabolin and Seltouch ($p < 0.01$, $p < 0.01$, and $p < 0.05$, respectively) (Figure 2).

3.3. Measurement of the adhesive force

Preparations with a strong adhesive force may not peel off when attached to the skin, whereas those with a weak adhesive force tend to peel off. We measured the adhesive force of each product. The results are shown in Figure 3. There were marked differences in the adhesive force among the products; the adhesive forces of OTC products, Salomethyl, Homepass, and Tokuhon (1.04 g), were higher than that of Seltouch (0.06 g). In addition, the results showed significant differences between all generic/OTC products and Seltouch ($p < 0.01$) (Figure 3).

3.4. Measurement of the peeling-force

The peeling-force refers to a force required to peel off the

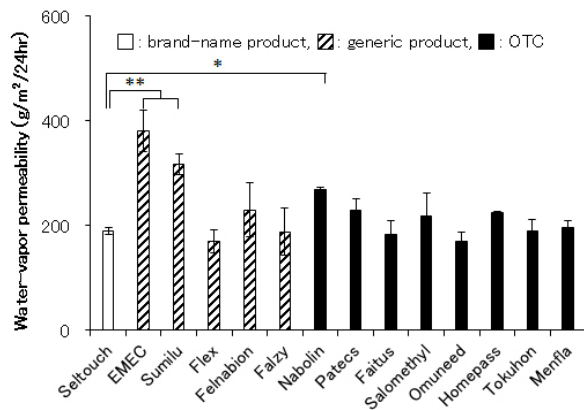


Figure 2. Comparison of water-vapor permeability of the various products ($n = 3$). $*p < 0.05$, $p < 0.01$ (brand-name vs. generics, Dunnett's test).**

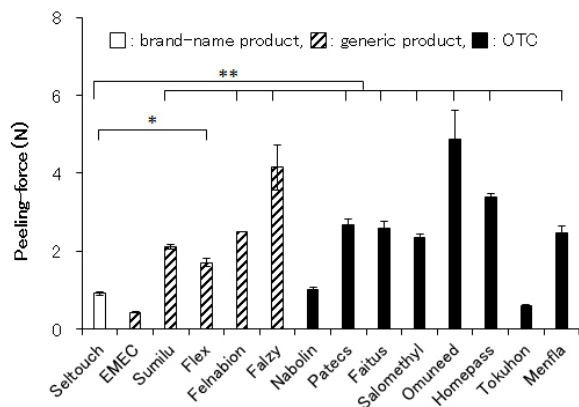


Figure 4. Comparison of peeling-force of the various products ($n = 3$). $*p < 0.05$, $p < 0.01$ (brand-name vs. generics, Dunnett's test).**

preparation after attachment. We measured the peeling-force of each product. The results are shown in Figure 4. The peeling-forces of Falzy (4.15 N), Omuneed (4.89 N), and Homepass (3.39 N) were higher than that of Seltouch (0.91 N), whereas those of EMEC (0.42 N) and Tokuhon (0.58 N) were lower than that of Seltouch. In addition, significance tests of various preparations were conducted. Generic products, Sumilu, Felhabion, and Falzy, and OTC products, Patecs, Faitus, Salomethyl, Omuneed, Homepass, and Menfla, showed significant differences in comparison with Seltouch ($p < 0.01$). There was also a significant difference between Flex and Seltouch ($p < 0.05$) (Figure 4).

3.5. Measurement of the elongation rate

In many products, a stretchy material is used for the support layer to prevent turning-up or peeling after attachment to articular regions such as the knees and elbows. The results of elongation-rate measurement are shown in Figure 5. The elongation rates of Sumilu (319%), Flex (282%), Nabolin (298%), Faitus (287%), and Homepass (299%) were higher than that of Seltouch (251%). On the other hand, the elongation rate of

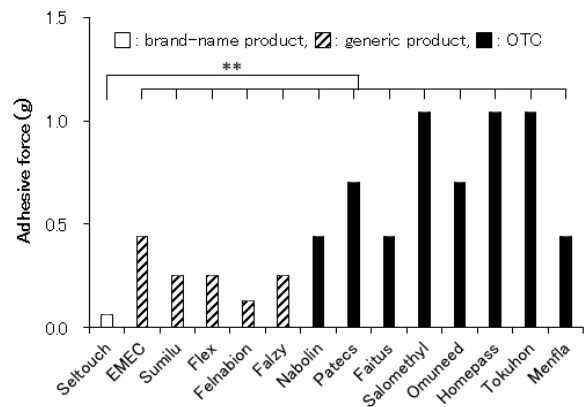


Figure 3. Comparison of adhesive force of the various products ($n = 3$). $p < 0.01$ (brand-name vs. generics, Dunnett's test).**

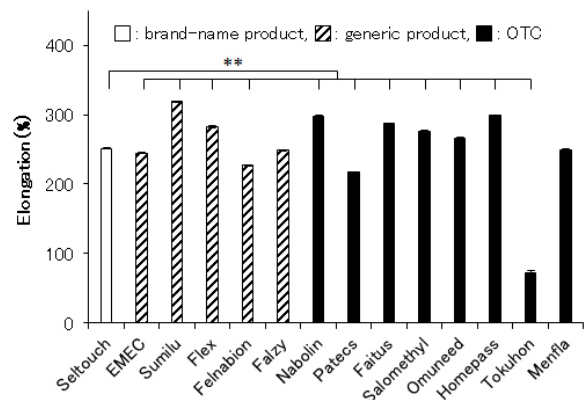


Figure 5. Comparison of elongation of the various products ($n = 3$). $p < 0.01$ (brand-name vs. generics, Dunnett's test).**

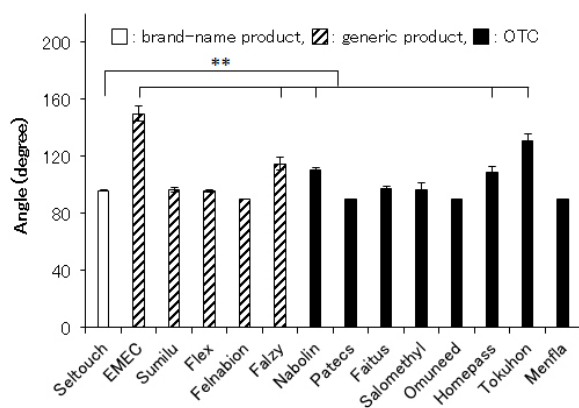


Figure 6. Comparison of flexibility of the support of the various products ($n = 3$). $p < 0.01$ (brand-name vs. generics, *Dunnnett's test*).**

Tokuhon (72%) was lower than that of Seltouch. In addition, significance tests of various products were conducted. There were significant differences between Falzy/OTC products other than Menfla and Seltouch ($p < 0.01$) (Figure 5).

3.6. Measurement of the flexibility of the support layer

When the support layer of each preparation is highly flexible, a portion of the preparation often adheres to another portion on removing a liner. However, this can be prevented if the rigidity of the support layer is adequate. The results of support-layer flexibility measurement are shown in Figure 6. The flexibilities of EMEC (150 degrees), Falzy (115 degrees), Nabolin (110 degrees), Homepass (108 degrees), and Tokuhon (131 degrees) were higher than that of Seltouch (96 degrees). In addition, significance tests of these products were conducted. EMEC, Falzy, Nabolin, Homepass, and Tokuhon showed significant differences in comparison with Seltouch ($p < 0.01$) (Figure 6).

3.7. Measurement of the interval until exfoliation from artificial skin in a wet state

Some tape preparations attached to the skin may easily peel off in a wet state. We examined the interval until various preparations peel from artificial skin in a wet state, as shown in Figure 7. The intervals of EMEC (1.4 min), Flex (30.5 min), Falzy (24.1 min), Nabolin (0.2 min), Patecs (26.3 min), and Homepass (15.6 min) were shorter than that of Seltouch (120 min). In addition, significance tests of these products were conducted. EMEC, Flex, Falzy, Nabolin, Patecs, and Homepass showed significant differences in comparison with Seltouch ($p < 0.01$) (Figure 7).

4. Discussion

The pH of each preparation may influence its stability

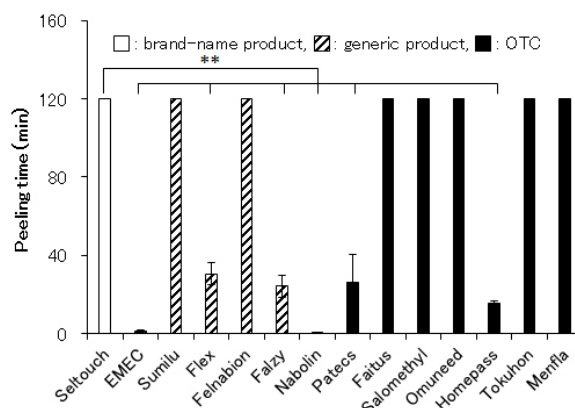


Figure 7. Comparison of the peeling time of the various products ($n = 3$). $p < 0.01$ (brand-name vs. generics, *Dunnnett's test*).**

and comfortableness, such as stimulation at the time of use. The skin surface pH is 4 to 5.5 (weakly acidic) in healthy adults (14). However, according to a study, the skin may be readily influenced by external stimuli when the pH of a preparation is lower than that of the skin surface, or when it is alkaline; the skin may become more sensitive (15). We measured the pH of each preparation. The pH values of most preparations used in this study were approximately 5, being within the skin pH range of healthy adults (Figure 1). On the other hand, the pH values of EMEC and Tokuhon were 7.0, being higher than that of the skin surface in healthy adults (pH 4. to 6.0). However, the pH values of these preparations were within the weakly acidic to neutral range; and therefore, there may be no harmful effects on the skin.

Skin stimuli related to patch preparations are primarily classified into 3 types: physical stimuli associated with strong adhesive force related corneal layer exfoliation/injury or support layer stress-related dermal stress, chemical stimuli related to the transfer of an active ingredient from the skin surface to the inner area, and maceration stimuli associated with the absence of water-vapor permeability on sweating (10). Felbinac-containing tape preparations are anti-inflammatory analgesic drugs, and may be used at the affected site for a long period, suggesting the marked influence of maceration stimuli. We examined the presence or absence of maceration stimuli by measuring the water evaporation (water-vapor permeability) from each preparation (Figure 2). The water-vapor permeabilities of the tape preparations used in this study ranged from 169 to 380 $\text{g/m}^2/24 \text{ h}$. In particular, EMEC showed the highest value (380 $\text{g/m}^2/24 \text{ h}$). This suggests that EMEC with a high water-vapor permeability does not frequently induce maceration stimuli. However, an increase in the water-vapor permeability reduces the sealing property of a patch preparation, decreasing the skin transfer of the drug; and therefore caution is needed. Therefore, it may be necessary to select drugs

in accordance with patients' wishes (16).

Preparations with a strong adhesive force may not peel off when attached to the skin, whereas those with a weak adhesive force tend to peel off. In particular, preparations with a weak adhesive force may be turned off or peel off due to clothes-related friction after attachment or attachment to mobile areas, such as the elbows and knees, directly influencing patients' comfortableness (4,8). Using the inclined ball tack test, we measured the adhesive forces of various preparations based on the ball weight (Figure 3). The adhesive forces of Salomethyl, Homepass, and Tokuhon (1.04 g, highest) were higher than that of Seltouch (0.06 g). These results showed that the adhesive forces of all other preparations were higher than that of Seltouch, suggesting that they do not peel off.

The peeling-force refers to the force required to peel off the preparation. Tape preparations with a strong adhesive force are attachable to the skin even in mobile areas, such as the elbows and knees, facilitating attachment for a long period. However, the strong adhesive force may cause physical stimuli, such as corneal-layer exfoliation on peeling, inducing symptoms, such as flare (16). We evaluated the peeling-forces of various preparations by measuring the force required to peel off the preparation (N) (Figure 4). The values ranged from 0.4 to 4.9 N. The peeling-force of Omuneed was the highest (4.9 N), followed by that of Falzy (4.1 N). These results show that a peeling-force 4 to 5 times higher than that of Seltouch (0.9 N) was required to peel off these preparations, suggesting that it induces physical stimuli, such as corneal-layer exfoliation, after peeling.

Many tape preparations containing felbinac are available for articular areas, such as the knees and elbows, due to their support flexibility. Non-flexible preparations may not resist affected-site motions when attached to a mobile region, leading to turning-up or peeling. Therefore, it is important to adopt a support layer consisting of a flexible material. Furthermore, flexible preparations are more closely adhered to the skin, increasing the permeability of an active ingredient; and they may be more effective (13). We measured the elongation rate (%) in comparison with the baseline length by elongating various preparations at a specific force (Figure 5). The elongation rates of most preparations ranged from 217 to 319%. That of Sumilu was the highest (319%), followed by those of Homepass (299%) and Nabolin (298%). On the other hand, the elongation rate of Tokuhon was low (72%). These results suggest that the preparations, excluding Tokuhon, are extensible (elongation rate: $\geq 200\%$).

When attaching a preparation to the skin, it is possible to effectively permeate an active ingredient by removing the liner, as indicated in the package inserts, and attaching the preparation to the affected site, although methods differ among various preparations.

However, concerning attachment to the back, lumbar, and gluteal region, a portion of the preparation often adheres to another portion on removing the liner. This may occur when the support layer of a preparation is flexible. When the support layer is adequately hard, this can be prevented. We measured the angle of each preparation's flexion to investigate the flexibility of the support layers of various preparations, and considered that preparations with a greater angle were more flexible (Figure 6). Most tape preparations containing felbinac used in this study, including Seltouch (96 degrees), showed an angle of 90 to 115 degrees. However, EMEC and Tokuhon showed higher values (150 and 131 degrees, respectively). This suggests that the support layers of these products are more flexible than those of the other products, leading to adhesion between a portion and another portion or wrinkles on attachment. On the other hand, hard preparations with a less flexible support layer are not attachable to mobile areas, such as joints, which may result in patients' discomfort (13). Therefore, the flexibility of the support layer must be considered for drug selection.

A patch preparation can be readily peeled from the affected site by getting it wet with water or warm water. However, a patch preparation that does not readily peel off is more appropriate for some sites to become wet, such as the wrists. We examined the interval until exfoliation from artificial skin in a wet state. The values of EMEC and Nabolin were 1.4 and 0.2 min, respectively. Furthermore, those of Flex and Homepass were 30.5 and 15.6 min, respectively (Figure 7). On the other hand, 8 products (Sumilu, Felnabion, Faitus, Salomethyl, Omuneed, Tokuhon, Menfla, and Seltouch) did not peel off even after 120 min, suggesting their water resistance.

The results of this study showed that there were differences in pharmaceutical properties among the tape preparations containing the same component. These properties may influence patients' comfortableness. If the properties of various preparations are understood, their requests may be met. For example, when patients attach one of the felbinac-containing tape preparations used in this study complain of stuffiness, a product with a higher water-vapor permeability can be recommended. When patients complain of pain on exfoliation, a product with a smaller peeling-force can be recommended. When patients complain of a short interval until exfoliation, a product with a stronger adhesive force should be selected. For patients attaching a product to an articular site, a product with a higher elongation rate, that is, a stretchable product, can be recommended. For patients with impaired hands or those living alone, a product that can be attached by themselves (a product with a hard support layer preventing adhesion to fingers or portion-to-portion adhesion) should be selected. In addition, a waterproof product should be selected for housewives, and a low-adhesiveness product should

be recommended for patients who wish to attach a tape preparation that can be readily peeled off in a wet state. Thus, pharmacists can understand these properties based on the results of this study, and select preparations appropriate for individual patients, leading to more favorable drug adherence.

References

1. Seltouch® Tape 70, Pharmaceutical products interview form, Pfizer Japan Inc. October, 2014 (ten revision). (in Japanese)
2. Ministry of Health, Labour and Welfare. Trend of recent medical expenses, [approximate medical expenses], February, 2015 issue. <http://www.mhlw.go.jp/topics/medias/month/15/02.html> (accessed September 18, 2016). (in Japanese)
3. Ohtanti M, Matsumoto M, Namiki M, Yamamura Y, Sugiura M, Uchino K. Evaluation of pharmaceutical equivalency between genuine and generic ketoprofen tape. *J Pharm Sci Tech Jpn.* 2011; 71:120-125. (in Japanese)
4. Takuya Uematsu, Atsushi Kobayashi, Kenichi Serizawa, Fumikazu Kinoshita, Toru Matsuura, Akihito Nagumo, Tomoyuki Kakinuma, Takahiro Sugao. Comparison of adhesive force between brand-name and generic ketoprofen tapes with tack rolling ball test. *J Jpn Soc Hosp Pharm.* 2015; 52:513-517. (in Japanese)
5. Wada Y, Nozawa M, Goto M, Shimokawa K, Ishii F. Generic selection criteria for safety and patient benefit [I]: Comparing the original drugs and generic ones in pharmaceutical properties. *J Community Pharm Pharm Sci.* 2014; 6:97-105. (in Japanese)
6. Nozawa M, Wada Y, Yamazaki N, Shimokawa K, Ishii F. Generic selection criteria for safety and patient benefit [II]: Physicochemical characteristics of original versus generic drugs for different difluprednate-containing products (ointment, cream, and lotion). *Jpn Soc Community Pharm Pharm.* 2014; 2:37-48. (in Japanese)
7. Wada Y, Nozawa M, Goto M, Shimokawa K, Ishii F. Generic selection criteria for safety and patient benefit [III]: Comparing the pharmaceutical properties and patient usability of original and generic ophthalmic solutions containing Timolol maleate. *Jpn Soc Pharm Health Care Sci.* 2015; 41:394-403. (in Japanese)
8. Wada Y, Kihara M, Nozawa M, Shimokawa K, Ishii F. Generic selection criteria for safety and patient benefit [IV]: Physicochemical and pharmaceutical properties of brand-name and generic ketoprofen tapes. *Drug Discov Ther.* 2015; 9:229-233.
9. Wada Y, Ami S, Nozawa M, Goto M, Shimokawa K, Ishii F. Generic selection criteria for safety and patient benefit [V]: Comparing the pharmaceutical properties and patient usability of original and generic nasal spray containing ketotifen fumarate. *Drug Discov Ther.* 2016; 10:88-92.
10. Hiyoshi M. Pharmaceutical assessment of Romal® tape 20/40 in ketoprofen tape. *Prog Med.* 2009; 29:193-196. (In Japanese)
11. JIS Z 0237: 2009 Testing methods of pressure-sensitive adhesive tapes and sheets. <http://kikakurui.com/z0/Z0237-2009-01.html> (accessed September 18, 2016). (in Japanese)
12. Miura T, Matsuzaki H, Nouno H. Questions from patients: Adhesiveness of percutaneous bronchodilator delivery system tulobuterol. *J Ambul Gen Ped.* 2008; 11:14-19. (in Japanese)
13. Terada H. Pharmaceutical characteristics and pharmacologic effect of NSAID pap. *Jpn J Med Pharm Sci.* 2007; 58:49-54. (in Japanese)
14. Kuriyama S, Tomonari H, Hayashi F, Numata M, Kimura H, Kanome K, Ebihara T, Kawaguchi Y, Hosoya T. The role of the skin pH-acid mantle in exit-site infection in CARD patients. *Nihon Toseki Igakkai Zasshi.* 1998; 31:997-1000. (in Japanese)
15. Ueno M, Kanda K, Kasagi N. Effect of tape stripping and skin cleansing repeatedly on skin barrier. *J Yonago Med Ass.* 2006; 57:103-112. (in Japanese)
16. Shinkai N, Okumura Y, Saito H, Kusunoki A, Yamauchi H. Drug properties and skin irritation of anti-inflammatory analgesic agent. *Pharma Medica.* 2007; 25:113-117. (in Japanese)

(Received August 23, 2016; Revised September 19, 2016; Accepted September 20, 2016)

Fabrication of Janus particles composed of poly (lactic-co-glycolic) acid and hard fat using a solvent evaporation method

Akihiro Matsumoto^{1,2,*}, Satoshi Murao¹, Michiko Matsumoto¹, Chie Watanabe¹, Masahiro Murakami^{1,*}

¹Laboratory of Pharmaceutics, Faculty of Pharmacy, Osaka Ohtani University, Osaka, Japan;

²Hanshin Yakkyoku Co.,Ltd., Osaka, Japan.

Summary

The feasibility of fabricating Janus particles based on phase separation between a hard fat and a biocompatible polymer was investigated. The solvent evaporation method used involved preparing an oil-in-water (o/w) emulsion with a mixture of poly (lactic-co-glycolic) acid (PLGA), hard fat, and an organic solvent as the oil phase and a polyvinyl alcohol aqueous solution as the water phase. The Janus particles were formed when the solvent was evaporated to obtain certain concentrations of PLGA and hard fat in the oil phase, at which phase separation was estimated to occur based on the phase diagram analysis. The hard fat hemisphere was proven to be the oil phase using a lipophilic dye Oil Red O. When the solvent evaporation process was performed maintaining a specific volume during the emulsification process; Janus particles were formed within 1.5 h. However, the formed Janus particles were destroyed by stirring for over 6 h. In contrast, a few Janus particles were formed when enough water to dissolve the oil phase solvent was added to the emulsion immediately after the emulsification process. The optimized volume of the solvent evaporation medium dominantly formed Janus particles and maintained the conformation for over 6 h with stirring. These results indicate that the formation and stability of Janus particles depend on the rate of solvent evaporation. Therefore, optimization of the solvent evaporation rate is critical to obtaining stable PLGA and hard fat Janus particles.

Keywords: Janus particle, PLGA, hard fat, phase separation, solvent evaporation

1. Introduction

Microparticles have been widely used in pharmaceutical formulations including as carriers for oral (1-5) and pulmonary drug delivery (6) or injectable formulations for long-term drug release (7). Developing microparticles as oral drug carriers to improve drug absorption in the gastrointestinal (GI) tract is an attractive challenge in the pharmaceutical field and a current focus. Strategies for improving intestinal drug absorption have been investigated in numerous research

studies, especially for drugs with low stability and permeability such as peptides, proteins, and nucleotides, and are an attractive research focus. Several methods such as using absorption enhancers (8,9), enzyme inhibitors (10), and mucoadhesive polymers (11) have been proposed to improve intestinal drug absorption. Microparticles used for improving drug absorption should ideally possess the desired characteristic of protecting the loaded drug against enzymatic attack until it reaches the absorption window to ensure intact drug delivery. In contrast, drug release from conventional microparticles lacks directional specificity and, so, drugs released on the opposite side of the mucosa or toward the luminal side are easily degraded by enzymes in the lumen.

To overcome this problem, Takada (12,13) proposed the hemispherical patch system as a new formulation for improving intestinal drug absorption, which releases drug only from the flat and not the spherical surface, thereby limiting the release direction. The flat surface

*Address correspondence to:

Dr. Akihiro Matsumoto, Laboratory of Pharmaceutics, Faculty of Pharmacy, Osaka Ohtani University, 3-11-1 Nishikori-kita, Tondabayashi, Osaka 584-0854, Japan.
E-mail: matumoaki@osaka-ohtani.ac.jp

Dr. Masahiro Murakami, Laboratory of Pharmaceutics, Faculty of Pharmacy, Osaka Ohtani University, 3-11-1 Nishikori-kita, Tondabayashi, Osaka 584-0854, Japan.
E-mail: murakam@osaka-ohtani.ac.jp

also plays a role in attaching the system to the mucosal surface to maintain the drug concentration near the site of absorption. In contrast, the spherical surface prevents drug release toward the lumen, which is the opposite side of the mucosa and acts as a barrier against enzymatic degradation. They demonstrated that the system enables the intestinal delivery of peptide drugs such as granulocyte-colony stimulating factor (14) and interferon (15). Thus, the hemisphere formulation appears to be a promising intestinal delivery system. However, there are some technical challenges in fabricating micro- or nano-sized hemispherical preparations. The hemispheric delivery system can be produced using several fabrication processes that may require entirely different manufacturing systems from those used for any conventional preparation. In addition, it should be costly effective.

The Janus particle is a heterogeneous particle consisting of two distinct hemispheres of different materials that impart different characters or functions to each hemisphere. Janus particles have been reported to show unique properties that conventional homogeneous particles do not possess, and have been proposed for use in various applications including as amphiphilic surfactants (16), elementary particles of the display in an electric field (17), and particles for magnetolytic therapy (18). Recently, the pulmonary delivery of hydrophilic and hydrophobic anticancer drugs has been reported (19). In this study, we hypothesized that Janus particles could be used to enhance drug absorption, and the concept is illustrated in Figure 1. Janus particles consist of biocompatible polymeric and thermosensitive lipid hemispheres and can reach the epithelium while blocking the leakage of the loaded drug and the attack by enzymes. Then, the lipid hemisphere attaches to the surface of the epithelium before melting to produce the micro-hemisphere of the polymer. The drug incorporated in the lipid hemisphere is subsequently released in a selective direction, and the polymeric hemisphere acts as a barrier against the leakage of encapsulated drug to the luminal side and enzymatic attack from the luminal side (20).

Here, we report the results of the designed preliminary step for proving the concept. Specifically, the feasibility of fabricating polymer-lipid Janus particles was investigated using poly (lactic-co-glycolic) acid (PLGA) and hard fat as the materials for the polymeric and lipid hemispheres, respectively. The solvent evaporation method was used to fabricate the Janus particles.

2. Materials and Methods

2.1. Materials

PLGA (molecular weight [MW] 20,000, lactic:glycolic, 50:50) was purchased from Wako Pure Chemicals Co.,

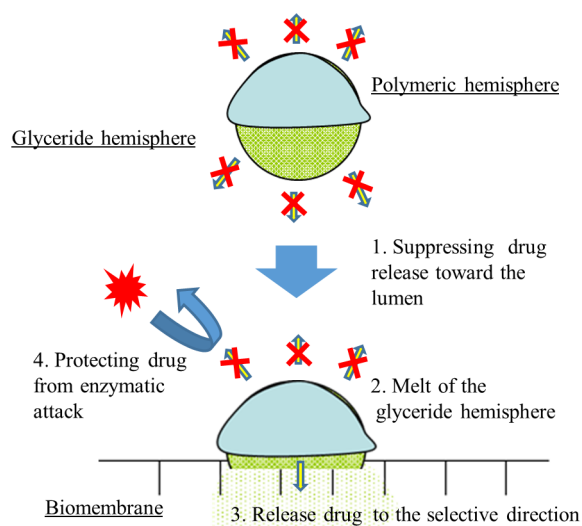


Figure 1. Janus particle-mediated drug absorption through biomembrane (concept). (1) Janus particles consist of polymeric and lipid hemispheres. (2) Slight luminal drug release. (3) Lipid hemispheres melt, and Janus particles change to micro-hemispheres. (4) Drug encapsulated in lipid hemispheres would be released to selective directions. Polymeric micro-hemispheres attach to biomembrane as a barrier against leakage of encapsulated drug to luminal side and enzymatic attack from luminal side.

Ltd. (Japan). Suppocire[®] AM pellets were a kind gift from Gattefossé, s.a., (France) and were used as the hard fat. Polyvinyl alcohol (PVA, POVAL[®] 220C) was obtained from KURARAY Co., Ltd. (Japan). All the other chemicals used were of reagent grade.

2.2. Analysis of phase diagram and identification of each phase

The mixture of PLGA and Suppocire[®] AM with various ratios was dissolved in methylene chloride or ethyl acetate. The solvent was slowly evaporated at 20-23°C until phase separation was observed, and the solution was weighed at that time. The concentrations of polymer and lipid were calculated. In addition, we identified each phase in the separated solution. A mixture of 200 mg each of PLGA and Suppocire[®] AM was dissolved in 0.3 mL methylene chloride and Oil Red O was added to the resultant separating solution, which was then centrifuged. The state of the solution was visually observed.

2.3. Fabrication of Janus particles

The Janus particles were fabricated using an oil-in-water (o/w) emulsion solvent evaporation method (Figure 2). PLGA and Suppocire[®] AM were dissolved in methylene chloride or ethyl acetate to prepare the oil phase. Then, Oil Red O (1 mg) was added to the oil phase as needed, and this was emulsified into a 0.5% PVA aqueous solution using a homogenizer (ULTRA-TURRAX[®] T18, IKA[®], Germany) for 5 min at 20-23°C. The resultant emulsion was added to the water all at once as needed

and stirred at 20–23°C to remove the solvent, which constitutes the solvent evaporation process. For Ex.4, the emulsion was weighed during the solvent evaporation process at predetermined times to evaluate the residual solvent or the PLGA- Suppocire® AM concentration in oil phase. The details of the amount of each component and conditions are summarized in Table 1. The obtained hardened particles were sieved through 149- μ m sieves to remove any aggregates.

2.4. Microscopic observations

During the solvent evaporation process, the emulsion and fabricated Janus particles were observed using an optical microscope system (Motic PA300, Shimadzu Co., Ltd., Kyoto, Japan).

2.5. Determination of Janus particle size

The sizes of the fabricated Janus particles were determined using a laser diffraction particle size analyzer (SALD-2200, Shimadzu Co., Ltd., Kyoto, Japan).

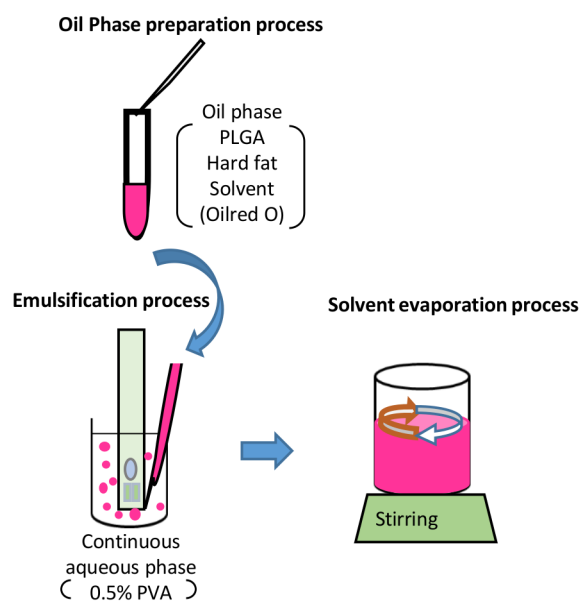


Figure 2. Illustration on fabrication process of Janus particles. Fabrication process is based on oil-in-water (o/w) emulsion solvent evaporation method.

3. Results

3.1. Phase diagram of PLGA-hard fat solution

The phase diagram of PLGA-hard fat in methylene chloride or ethyl acetate is shown in Figure 3. PLGA and the hard fat dissolved in common solvents such as methylene chloride and ethyl acetate. However, phase separation occurred above a certain concentration. The critical concentrations at which a phase separation was observed differed between the methylene chloride and ethyl acetate solutions. Phase separation occurred at a higher concentration in methylene chloride than it did in ethyl acetate.

3.2. Conformation of Janus particles

The optical micrograph of the obtained particles is shown in Figure 4, and phase separation was observed in the particles fabricated using both methylene chloride and ethyl acetate solutions. The Janus particles consisted of two clearly observed hemispheres. The Janus particles fabricated using the Oil Red O-containing oil phase were only stained on one side of the hemispheres. Figure 5 shows the state of the oil phase following the addition of Oil Red O, which exhibited phase separation. The bottom layer showed high viscosity and was slightly stained by

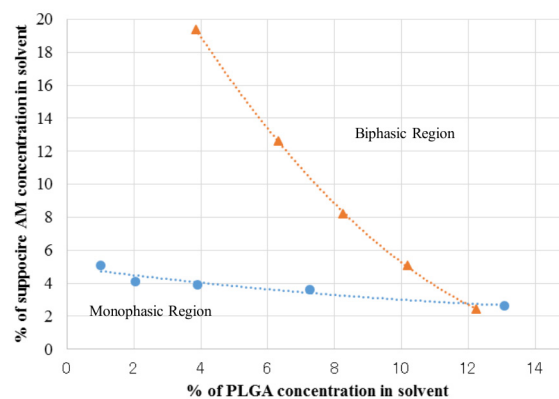


Figure 3. Phase diagram of poly (lactic-co-glycolic) acid (PLGA)-Suppocire® AM-organic solvent. Critical line between monophasic and biphasic region, using (▲) methylene chloride and (●) ethyl acetate as organic solvents.

Table 1. Fabrication condition

Number	A	B	C	D	E
Ex.1	MC 2 g	5 mL	5,000 rpm 3 min	5 mL	3 h
Ex.2	EA 3 mL	5 mL	5,000 rpm 3 min	5 mL	3 h
Ex.3	MC 2 g + Oil Red O	5 mL	5,000 rpm 3 min	5 mL	3 h
Ex.4	MC 2 g + Oil Red O	3 mL	3,000 rpm 5 min	3mL	4 h
Ex.5	MC 2 g + Oil Red O	3 mL	5,000 rpm 3 min	3mL	6 h
Ex.6	MC 2 g + Oil Red O	3 mL	5,000 rpm 3 min	100 mL	6 h
Ex.7	MC 2 g + Oil Red O	3 mL	5,000 rpm 3 min	200 mL	6 h

A: solvent of oil phase, B: volume of water phase at emulsification process, C: strength and duration of emulsification, D: volume of solvent evaporation medium, E: duration of solvent evaporation process, MC: methylene chloride, and EA: ethylacetate.

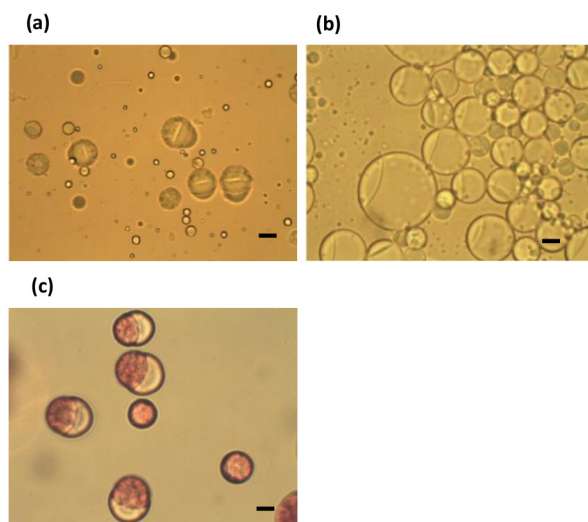


Figure 4. Optical micrograph of Janus particles. Janus particles fabricated using (a) methylene chloride; Ex.1 and (b) ethyl acetate; Ex.2 as oil phase solvents. (c) Janus particles fabricated using methylene chloride adding Oil Red O to oil phase solvent; Ex.3. Scale bar, 20 μm .



Figure 5. Partition in phase separated solution of poly (lactic-co-glycolic) acid (PLGA)-Suppcire[®] AM-methylene chloride. Poly (lactic-co-glycolic) acid (PLGA) and Suppcire AM (200 mg each) were dissolved in 0.3 g 0.02% Oil Red O-methylene chloride, and resultant solution was centrifuged.

the hydrophobic dye. In contrast, the upper layer had low viscosity and was strongly stained with the dye.

3.3. Relationship between residual solvent profiles and Janus formation

The PLGA-Suppcire[®] AM concentration monitored during the solvent evaporation process and the emulsion state are shown in Figure 6. The dispersed phase was solidified as the residual solvent decreased. Phase separation occurred at 90 min when the estimated concentration in the dispersed oil phase corresponded to the critical concentration in Figure 3. The Janus particles were obtained at over 90 min.

3.4. Effect of volume of solvent evaporation medium

After the oil phase containing 2 g methylene chloride was emulsified with 0.5% PVA solution, the resultant

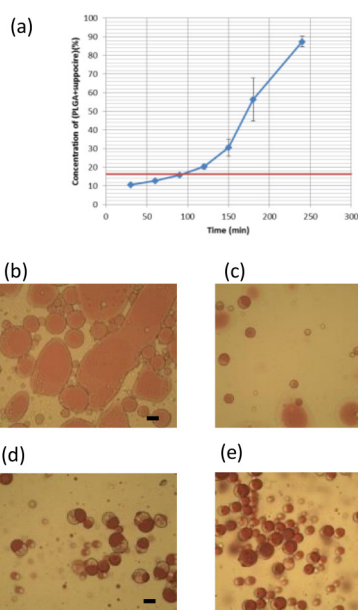


Figure 6. PLGA-Suppcire[®] AM concentration profile and state of emulsion during solvent evaporation process. (a) Residual solvent profile during solvent evaporation process. Red line indicates critical concentration of phase separation. The state of emulsion was (b) 60, (c) 90, (d) 150, and (e) 240 min of solvent evaporation time; Ex. 4. Scale bar, 20 μm .

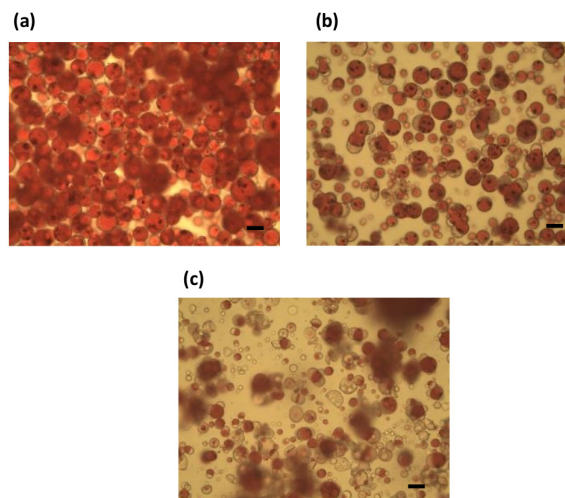


Figure 7. Effect of addition of aqueous phase after emulsification process on formation of Janus particles. Optical micrograph of emulsion after 360 min of solvent evaporation process. Addition of (a) 200 mL water (condition A); Ex.7, (b) 100 mL water (condition B); Ex.6, and (c) no water (condition C); Ex.5. Scale bar, 20 μm .

emulsion was added to varying volumes of water and solvent evaporation was performed. The particles obtained after 360 min of the solvent evaporation process are shown in Figure 7. Monolithic particles and a few Janus particles were observed in condition A (200 mL solvent evaporation medium). We observed that most of the particles in condition B were Janus particles (100 mL solvent evaporation medium). Furthermore, stained and unstained particles were observed in condition C (3 mL solvent evaporation medium).

4. Discussion

Research on Janus particles has drawn increasing attention over the last decade. Janus particles with an anisotropic structure likely possess numerous unknown functions and have not been utilized as much as conventional microparticles with homogeneous properties have been. In the pharmaceutical field, anisotropic formulations such as bilayer tablets have been available on the market. In a bilayer tablet, two active ingredients are loaded into distinct layers to avoid a chemical interaction between them, or the drug release from the tablet is controlled by the different release profiles of the two layers. However, even in the pharmaceutical field, few investigations on anisotropic microparticles have been performed, and so their functional applicability remains unknown. As mentioned in the introduction section, we hypothesized that Janus particles can attach and form hemispheres on the biomembrane to localize intact drug at its site of absorption and thereby enhance drug absorption (Figure 1). We performed these investigations to prove our hypothesis using PLGA and hard fat.

Several fabrication methods for Janus particles have been reported, such as the selective surface modification of isotropic particles (21) using a microfluidic device (22) and seed polymerization (23). Among these methods, we selected phase separation using a solvent evaporation method (24) because it is simple and does not require the use of synthetic organic chemistry. Moreover, the solvent evaporation method is a proven fabrication method for the commercial production of prolonged release injection formulations such as Lupron depot[®]. When phase separation is adopted as the fabrication method of Janus particles, it is necessary to induce phase separation between two components. First, we monitored the phase separation process between PLGA and Suppocire[®] AM. In the common solvent used, phase separation occurred above a certain concentration, which differed between methylene chloride and ethyl acetate. The critical concentration that induced phase separation in methylene chloride was higher than that in ethyl acetate (Figure 3). In addition to this result, the effect of the PLGA/ Suppocire[®] AM ratio on the critical concentration differed between the two solvents. In ethyl acetate, phase separation was less independent of PLGA concentration and occurred near 3-5% of Suppocire[®] AM. This phenomenon is similar to the precipitation of polymer by adding poor solvents. In contrast, in methylene chloride, the phase separation occurred when the total concentration of two components exceed a critical concentration, more independent of the mixing ratio of two components. This phenomenon is similar to the phase separation that occurs between polymers such as polylactic acid and PLGA in solvents (25). Dobry and Boyerkawenoki (26) reported the spontaneous combination of various

polymers in an organic solvent. Polymers generally have higher mixing entropy than low molecular weight substances, so phase separation tends to occur between two polymers. The phase separation of PLGA and Suppocire[®] AM in methylene chloride may be related to the high mixing entropy.

Next, we investigated the formation of Janus particles from methylene chloride or ethyl acetate using the solvent evaporation method, and particle formation was confirmed in both solvents (Figure 4). This indicates that phase separation occurred even in the oil droplets of the o/w emulsion similar to the results shown in Figure 3. When Oil Red O, a non-polar dye used for staining triglycerides in cells in cytology, was added to the oil phase of methylene chloride, only one side of the hemispheres was stained. To identify the hemispheres stained, we analyzed the properties of each phase in the oil phase. Because the density of Suppocire[®] AM is lower than that of PLGA, the PLGA and Suppocire[®] AM layer are considered as the bottom and upper layers, respectively. Based on the results showing that the less stained bottom layer had a high viscosity, the unstained hemisphere in the Janus particle was estimated to be PLGA. The strongly stained upper layer had a low viscosity and, therefore, the stained hemisphere in the Janus particle was estimated to be Suppocire[®] AM.

Next, the relationship between the PLGA-Suppocire[®] AM concentration in the emulsion and Janus formation were investigated. Methylene chloride has 1.3% w/w solubility in water at 20°C, so approximately 40 mg methylene chloride can be dissolved in 3 mL of the continuous aqueous phase. Therefore, this amount was considered negligible compared to the 2 g of methylene chloride in the dispersed oil phase. Hence, the residual solvent in the emulsion corresponded to the approximate residual solvent in the oil phase. The formation of Janus particles was observed at a concentration over the critical concentration for phase separation (Red line in Figure 6a). The result also indicates that the phase separation occurred even in the oil droplets of the emulsion similar to the results shown in Figure 3.

Finally, we examined the effect of the medium volume used in the solvent evaporation process on the formation of Janus particles. The medium volume is related to the extraction rate of the solvent from the dispersed oil phase to the continuous aqueous phase. If the volume of the solvent evaporation medium is enough to dissolve the oil phase solvent, the solvent in the dispersed oil phase is rapidly extracted into the continuous aqueous phase. In contrast, if the volume of solvent evaporation medium is not sufficient to dissolve the oil phase solvent, the solvent rapidly reaches at the saturation point and the solvent remains in the oil phase. Furthermore, the solvent is extracted slowly as it evaporates from the saturated aqueous phase. Condition A consisted

of 200 mL solvent evaporation medium, which was sufficient to dissolve the solvent of oil phase solvent, produced a few Janus particles (Figure 7a). To form Janus particles, the droplets produced by phase separation in the dispersed oil phase need to aggregate and coalesce before the coalescing droplets migrate to form two layers. When the rate of solvent extraction from the dispersed oil phase is rapid, the viscosity of the dispersed oil phase increases so rapidly that the droplets produced by phase separation do not have time to coalesce and migrate. Contrastingly, in condition C with 3 mL solvent evaporation medium (Figure 7c), a small amount of solvent was extracted into the continuous aqueous phase from the dispersed oil phase, and there is enough time for the separated phases to coalesce and migrate near the point of phase separation. However, the low viscosity lasts long so that the separated phases can completely migrate. The complete migration reduces the cohesion of both hemispheres, which may be too weak to maintain the Janus conformation and both hemispheres completely separated ultimately. In this study, condition B with 100 mL solvent evaporation medium (Figure 7b) was the optimum condition required to produce stable Janus particles. Approximate 65% (1.3 g) of solvent in the dispersed oil phase is estimated to be extracted into the continuous aqueous phase at the beginning of the solvent evaporation process in condition B in the view of the solubility of methylene chloride in water. However, phase separation occurred in the dispersed oil phase when approximate 1.1 g of solvent was extracted in the continuous aqueous phase, which is close to the saturation point of methylene chloride in water. The dissolution rate near the saturation point reduces in comparison with that in a sink condition. Hence, the dissolution rate of methylene chloride in condition B is slower than that in condition A and is faster than that in condition C. The optimum dissolution rate is considered to provide the optimum balance among the coalescing and migration of the separated phases and the cohesion of both hemispheres.

In conclusion, we demonstrated that Janus particles composed of PLGA and hard fat could be fabricated using the solvent evaporation method from an o/w emulsion formation. Furthermore, this study revealed that the formation of Janus particles was affected by the extraction rate from the dispersed phase. In addition to the extraction rate, there may be other factors that affect the formation of Janus particles including the balance of interfacial tension. The conformation of particles composed of two materials has been reported to be affected by the interfacial tension between the phases of both materials in the dispersed oil phase and between the continuous aqueous phase and each phase in dispersed oil phase (27). The investigation of the effect of the balance in the interfacial tension will be the focus of our next investigation. In addition to demonstrating

the feasibility of the formation of Janus particles, the localization of Oil Red O in one side of the particle hemispheres is another notable finding of this study. These observations indicate that the distribution of materials in Janus particles may be controllable, which is also another potential focus of future investigations.

Acknowledgements

We would like to thank Ms. Kayoko Murakami for her technical assistance and CBC Co., Ltd., for financially supporting this study. We are also grateful to Editage (www.editage.jp) for English language editing.

References

- Vaghani S, Vasanti S, Chaturvedi K, Satish CS, Jivani NP. Stomach-specific drug delivery of 5-fluorouracil using ethylcellulose floating microspheres. *Pharm Dev Technol.* 2010; 15:154-161.
- Tozuka Y, Sugiyama E, Takeuchi H. Release profile of insulin entrapped on mesoporous materials by freeze-thaw method. *Int J Pharm.* 2010; 386:172-177.
- Zhang Y, Zhi Z, Jiang T, Zhang J, Wang Z, Wang S. Spherical mesoporous silica nanoparticles for loading and release of the poorly water-soluble drug telmisartan. *J Control Release.* 2010; 145:257-263.
- Bhise SB, More AB, Malayandi R. Formulation and in vitro evaluation of rifampicin loaded porous microspheres. *Sci Pharm.* 2010; 78:291-302.
- Kapoor S, Hegde R, Bhattacharyya AJ. Influence of surface chemistry of mesoporous alumina with wide pore distribution on controlled drug release. *J Control Release.* 2009; 140:34-39.
- Arnold MM, Gorman EM, Schieber LJ, Munson EJ, Berkland C. NanoCipro encapsulation in monodisperse large porous PLGA microparticles. *J Control Release.* 2007; 121:100-109.
- Ogawa Y, Yamamoto M, Takada S, Okada H, Shimamoto T. Controlled-release of leuprolide acetate from polylactic acid or copoly(lactic/glycolic) acid microcapsules: influence of molecular weight and copolymer ratio of polymer. *Chem Pharm Bull (Tokyo).* 1988; 36:1502-1507.
- Maher S, Leonard TW, Jacobsen J, Brayden DJ. Safety and efficacy of sodium caprate in promoting oral drug absorption: from in vitro to the clinic. *Adv Drug Deliv Rev.* 2009; 61:1427-1449.
- Muranishi S. Absorption enhancers. *Crit Rev Ther Drug Carrier Syst.* 1990; 7:1-33.
- Yamamoto A, Taniguchi T, Rikyuu K, Tsuji T, Fujita T, Murakami M, Muranishi S. Effects of various protease inhibitors on the intestinal absorption and degradation of insulin in rats. *Pharm Res.* 1994; 11:1496-1500.
- Luessen HL, de Leeuw BJ, Langemeyer MW, de Boer AB, Verhoef JC, Junginger HE. Mucoadhesive polymers in peroral peptide drug delivery. VI. Carbomer and chitosan improve the intestinal absorption of the peptide drug busserelin in vivo. *Pharm Res.* 1996; 13:1668-1672.
- Eaimtrakarn S, Prasad YV, Puthli SP, Yoshikawa Y, Shibata N, Takada K. Evaluation of gastrointestinal transit characteristics of oral patch preparation using

- caffeine as a model drug in human volunteers. *Drug Metab Pharmacokinet.* 2002; 17:284-291.
13. Venkatesan N, Uchino K, Amagase K, Ito Y, Shibata N, Takada K. Gastro-intestinal patch system for the delivery of erythropoietin. *J Control Release.* 2006; 111:19-26.
 14. Eiamtrakarn S, Itoh Y, Kishimoto J, Yoshikawa Y, Shibata N, Murakami M, Takada K. Gastrointestinal mucoadhesive patch system (GI-MAPS) for oral administration of G-CSF, a model protein. *Biomaterials.* 2002; 23:145-152.
 15. Ito Y, Tosh B, Togashi Y, Amagase K, Kishida T, Kishida T, Sugioka N, Shibata N, Takada K. Absorption of interferon alpha from patches in rats. *J Drug Target.* 2005; 13:383-390.
 16. Ruhland TM, Groschel AH, Walther A, Muller AH. Janus cylinders at liquid-liquid interfaces. *Langmuir.* 2011; 27:9807-9814.
 17. Yin SN, Wang CF, Yu ZY, Wang J, Liu SS, Chen S. Versatile bifunctional magnetic-fluorescent responsive Janus supraballs towards the flexible bead display. *Adv Mater.* 2011; 23:2915-2919.
 18. Hu SH, Gao X. Nanocomposites with spatially separated functionalities for combined imaging and magnetolytic therapy. *J Am Chem Soc.* 2010; 132:7234-7237.
 19. Garbuzenko OB, Winkler J, Tomassone MS, Minko T. Biodegradable Janus nanoparticles for local pulmonary delivery of hydrophilic and hydrophobic molecules to the lungs. *Langmuir.* 2014; 30:12941-12949.
 20. Murakami M. PCT/JP2015/083082.
 21. Pawar AB, Kretzschmar I. Fabrication, assembly, and application of patchy particles. *Macromol Rapid Commun.* 2010; 31:150-168.
 22. Li X, Yang YT, Wu LJ, Li YC, Ye MY, Chang ZQ, Meng DQ, Serra CA. Fabrication of electro- and color-responsive CB/PTFE Janus beads in a simple microfluidic device. *Materials Letters.* 2015; 142:258-261.
 23. Kaewsaneha C, Bitar A, Tangboriboonrat P, Polpanich D, Elaissari A. Fluorescent-magnetic Janus particles prepared via seed emulsion polymerization. *J Colloid Interface Sci.* 2014; 424:98-103.
 24. Romanski FS, Winkler JS, Riccobene RC, Tomassone MS. Production and characterization of anisotropic particles from biodegradable materials. *Langmuir.* 2012; 28:3756-3765.
 25. Matsumoto A, Matsukawa Y, Suzuki T, Yoshino H, Kobayashi M. The polymer-alloys method as a new preparation method of biodegradable microspheres: principle and application to cisplatin-loaded microspheres. *J Controlled Release.* 1997; 48:19-27.
 26. Dobry A, Boyer-Kawenoki F. Phase separation in polymer solution. *J Polymer Sci.* 1947; 2:90-100.
 27. Pekarek KJ, Jacob JS, Mathiowitz E. Double-walled polymer microspheres for controlled drug release. *Nature.* 1994; 367:258-260.

(Received December 25, 2016; Accepted December 30, 2016)

The serum/PDGF-dependent "melanogenic" role of the minute level of the oncogenic kinase PAK1 in melanoma cells proven by the highly sensitive kinase assay

Pham Thi Be Tu^{1,3}, Binh Cao Quan Nguyen^{1,3}, Shinkichi Tawata¹, Cheong-Yong Yun², Eung Gook Kim², Hiroshi Maruta^{1,4,*}

¹PAK Research Center, University of the Ryukyus, Okinawa, Japan;

²College of Medicine, Chungbuk National University, Choengju, Korea;

³Department of Bioscience and Biotechnology, The United Graduate School of Agricultural Sciences, Kagoshima University, Kagoshima, Japan;

⁴PAK Research Center, Brunswick West, Melbourne, Victoria, Australia.

Summary

We previously demonstrated that the oncogenic kinase PAK4, which both melanomas and normal melanocytes express at a very high level, is essential for their melanogenesis. In the present study, using the highly sensitive "Macaroni-Western" (IP-ATP-Glo) kinase assay, we investigated the melanogenic potential of another oncogenic kinase PAK1, which melanoma (B16F10) cells express only at a very minute level. After transfecting melanoma cells with PAK1-shRNA for silencing PAK1 gene, melanin content, tyrosinase activity, and kinase activity of PAK1 were compared between the wild-type and transfectants. We found that (i) PAK1 is significantly activated by melanogenic hormones such as IBMX (3-isobutyl-1-methyl xanthine) and α -MSH (melanocyte-stimulating hormone), (ii) silencing the endogenous PAK1 gene in melanoma cells through PAK1-specific shRNA reduces both melanin content and tyrosinase activity in the presence of both serum and melanogenic hormones to the basal level, (iii) the exogenously added wild-type PAK1 in the melanoma cells boosts the α -MSH-inducible melanin level by several folds without affecting the basal, and (iv) α -MSH/IBMX-induced melanogenesis hardly takes place in the absence of either serum or PAK1, clearly indicating that PAK1 is essential mainly for serum- and α -MSH/IBMX-dependent melanogenesis, but not the basal, in melanoma cells. The outcome of this study might provide the first scientific basis for explaining why a wide variety of herbal PAK1-blockers such as CAPE (caffeic acid phenethyl ester), curcumin and shikonin in cosmetics are useful for skin-whitening.

Keywords: PAK1, melanogenesis, melanomas, tyrosinase, MITF, skin-whitening, serum

1. Introduction

The color of hairs, eye irises, and skin is controlled by a family of pigments called melanins. The intracellular source of melanin is tyrosine, and is converted to melanin through a series of enzymatic oxidation (hydroxylation) which involves tyrosinase, TRP

(tyrosinase-related protein) 1 and TRP2. Expression of genes encoding for these melanogenic enzymes requires at least two oncogenic/melanogenic transcription factors (MTFs): beta-catenin and MITF (microphthalmia-associated transcription factor). The majority of herbal compounds in skin-whitening cosmetics either inhibit directly these melanogenic enzymes or down-regulate the MTFs. Tyrosine analogues such as kojic acid belong to the first category (tyrosinase inhibitors), while the majority of remainings such as CAPE (caffeic acid phenethyl ester), curcumin and shikonin belong to the second category (MTF regulators) (1,2). Interestingly, many of these MTF regulators including CAPE, curcumin, shikonin and cucurbitacin are known

Released online in J-STAGE as advance publication October 17, 2016.

*Address correspondence to:

Dr. Hiroshi Maruta, PAK Research Center, Melbourne, Victoria, Australia.

E-mail: maruta20420@yahoo.com

to block the oncogenic/ageing kinase PAK1 (RAC/CDC42-activated kinase 1) (3-5). Thus, it is most likely that PAK1 is involved in the activation of these melanogenic/oncogenic transcription factors in hair cells, eye irises or skin melanocytes. Indeed, at least beta-catenin is among the direct substrates of PAK1 (6). PAK1 phosphorylates beta-catenin at Ser 675 for the activation, leading to malignant transformation. Furthermore, beta-catenin is essential for the activation of MITF, leading to melanogenesis or/and oncogenesis of melanocytes (7).

Interestingly, however, it was recently revealed that knocking-out PAK1 gene *per se* in pigmented mice fails to produce any albino mice (Hong He *et al.*, unpublished observation), clearly indicating that at least the basal melanogenesis in both hair cells and eye irises is independent of PAK1, although the contribution of PAK1 to skin melanogenesis still remains to be clarified.

We have previously shown that the oncogenic kinase PAK4 (CDC42-dependent kinase 4) is highly expressed in both melanoma and normal melanocyte cell lines, and responsible for their melanogenesis, activating CREB/beta-catenin-MITF-tyrosinase pathway, while PAK2 (RAC/CDC42-activated kinase 2), another highly expressed member of PAK family, plays no role in their melanogenesis (8).

In this study, we provide the first biochemical evidence for a specific role of another oncogenic kinase called PAK1 in skin melanogenesis, despite of the fact that its expression level is minute: shRNA-induced silencing of PAK1 gene in melanocytes (B16F10) derived from mouse melanoma significantly reduced the α -MSH/IBMX-inducible melanogenesis to the basal level, while over-expression of PAK1 gene boosted the α -MSH-inducible melanogenesis without affecting the basal. Furthermore, we found that the α -MSH/IBMX-inducible melanogenesis absolutely requires a serum factor which is most likely PDGF (platelet-derived growth factor). In the serum-free medium, only the basal melanogenesis takes place.

2. Materials and Methods

2.1. Materials

B16F10 melanoma cells were purchased from American Type Culture Collection (Rockville, MD, USA). PAK1-SureSilencing plasmids, attractene transfection, endofree[®] plasmid maxi kit were purchased from Qiagen (Valencia, CA 91355, USA). Primary PAK1-antibodies, biotinylated secondary antibodies, signalfire[™] ECL reagent were obtained from Cell Signalling Technology (Danver, MA, USA). Kinase Glo reagent and ATP (ATP_Glo kinase kit) were purchased from Promega (Madison, Wisconsin, USA). Lipofectamin and JM109 competent cells

were purchased from Invitrogen and Life Technology. AG1295 and AG1478 were purchased from Calbiochem (San Diego, CA, USA). All other chemicals including human PDGF-bb were purchased from Sigma-Aldrich (St. Louis, MO, USA).

2.2. Silencing of PAK1 gene in mouse melanocytes (B16F10) by stable transfection with mouse PAK1-specific shRNA

2.2.1. Cell culture

B16F10 melanoma cells were cultured in DMEM supplemented with 10% heat-activated FBS and 1% penicillin/streptomycin (10,000 U/mL and 100 μ g/mL) at 37°C in a humidified atmosphere containing 5% CO₂.

2.2.2. Stable transfection with mouse PAK1-specific shRNA

ShRNA transfection of B16F10 cell line was carried out basically through the same procedure previously described (9), but with mouse PAK1-specific shRNAs (# KM04553, Qiagen). The following four distinct clones of shRNAs were used for the transfection: clone 1 (CCAGAGAAGTTGTCAGCTATT), clone 2 (CATCAAGAGTGACAATATTCT), clone 3 (GTACACACGGTTCGAGAAGAT), and clone 4 (GTACCACCAGTGTCAGAAGAT) as well as shCONTROL nontargeting shRNA as the negative control (WT). However, in this study, clones 1 and 2 turned out to be more effective than clones 3 and 4 for silencing mouse PAK1 gene in this melanocyte line (data not shown). Stable transfectants were selected in the presence of G418 (1 mg/mL) which kills more than 99% of non-transfected cells.

2.2.3. Western-blot analysis of PAK1 protein level and in vitro assay for the kinase activity of PAK1 in transfectants

2.2.3.1. Western blot analysis

In order to quantify the extremely low level of PAK1 in both control (WT) cell line and PAK1-silenced transfectants (G418-resistant), by minimizing the "non-specific noise" levels, we conducted the western blot analysis using a rabbit polyclonal antibody against PAK1 (#2062, Cell Signaling Technology) as the primary antibody. Briefly, each clone was seeded at the concentration of 2×10^5 cells/well in a 6 well plate, pre-cultured for 48 h, and the cell lysates were boiled in 25 μ L of SDS-PAGE buffer for 5 min. Eight μ L (containing 15 μ g of total protein) of each supernatant per each slot was used for SDS-PAGE. The nitrocellulose was blotted with the anti-PAK1 IgG (1:1,000 dilution as a primary

antibody), and as secondary antibodies the HRP-linked anti-rabbit IgG and anti-biotin IgG (#7074, #7075, Cell Signaling) were used to detect both PAK1 and β -actin bands which were eventually visualized with the ECL system from Amersham. The western blot assays were representative of three independent experiments.

2.2.3.2. "Macaroni-Western" (IP- ATP_Glo) kinase assay for PAK1 in melanoma cells

The kinase activity of PAK1 in the WT melanocytes and shRNA transfectants (SHs) was measured by a substantial modification (5) of a decade old method (which we coined "Macaroni-Western") developed by an Italian group (10). Briefly, B16F10 melanoma cell lines (WT or SHs, 2×10^5 cells/mL) were pre-cultured on 6-well plate for 24 h. Then cells were treated with 100 nM α -MSH or 100 μ M IBMX for 48 h. Cells were disrupted by lysis buffer containing 50 mM Tris-HCl pH 7.5 and 150 mM NaCl and 1% Triton-X. For the immunoprecipitation (IP) of PAK1, the cleared cell lysates were incubated with anti-PAK1 IgG (1:50 dilution) and protein A-agarose beads for 1-2 h in cold room with continuous shaking by a rotary mixer (Nissin, Suginami-ku, Tokyo, Japan). The resultant IP (PAK1) from each lysate was incubated with ATP-Glo kinase assay kit (Promega) in the presence of ATP and MBP (myelin basic protein) for 1 h at 37°C, and the remaining ATP level was measured by the ATP-dependent Luciferin-Luciferase reaction which eventually generates a luminescence (10). The final suspension was centrifuged, and the supernatant was transferred to 96-well plate for reading. Luminescence was recorded by MTP-880Lab microplate reader (Corona, Hitachinaka-ku, Ibaraki, Japan) with an integration time of 0.5 s per well.

2.3. Measuring melanin content and tyrosinase activity in transfectants

2.3.1. Measurement of melanin content

Melanin content was determined as previously described (11). In brief, B16F10 cells (wild-type or PAK1-specific shRNA transfectants) were plated at a density of 2×10^4 cells/well in a 24-well plate. After 24 h of culture, 100 μ M isobutyl-1-methylxanthine (IBMX) or 100 nM α -MSH was added and incubated for an additional 72 h at 37°C. The cells were washed twice with phosphate buffer, then lysed with 500 μ L of a solution containing 1 M NaOH and 10% DMSO and incubated at 80°C for 1 h, to solubilize the melanin, and the melanin content was measured at 490 nm. To compare the melanin content in the wild-type and transfectant cells, the total amount of melanin produced by the wild-type melanocytes was considered as the control (100%), and those by the transfectants were

calculated accordingly.

2.3.2. Assay for intracellular tyrosinase activity

Tyrosinase activity was determined as previously described (12), with a slight modifications. B16F10 cells (wild-type or the transfectants) were plated at a density of 2×10^4 cells/well, and after 24 h of culture, 100 μ M IBMX or 100 nM α -MSH was added and incubated for an additional 72 h at 37°C. The cells were then washed with ice cold phosphate buffer and lysed with phosphate buffer (pH 6.8) containing 1% Triton-X (500 μ L/well). The plates were frozen at -80°C for 30 min. After thawing, 100 μ L of 1% L-DOPA was added to each well. Following incubation at 37°C for 2 h, the absorbance was measured at 490 nm.

2.4. Measuring the melanin content in the wild-type and PAK1-overexpressing melanocytes after α -MSH treatment

Using Myc vector (2 μ g), melanocytes (B16F10) were transfected transiently with either wild-type (WT) PAK1 or so-called "constitutively activated" (CA) PAK1 carrying T423E mutation. After 3 days of culture, each transfected clone was harvested for the further experiment. The effect of PAK1-overexpression on the melanin content was measured through the basically same procedures described previously (8). Briefly, melanocytes, either the wild-type or PAK1-overexpressers which express either the wild-type PAK1 or its CA mutant, were incubated with 100 nM α -MSH for 3 days. Cells were lysed with a solution containing 1 M NaOH and 20% DMSO to dissolve the melanin, and its content was determined at 405 nm.

2.5. Melanogenesis in a serum-free medium

B16F10 cells (wild-type or PAK1-specific shRNA transfectants) were plated at a density of 2×10^4 cells/well in a 24-well plate in the presence of 10% FBS. After 24 h of incubation, the culture medium is replaced with a serum-free medium, and cultured for an additional 72 h with or without 100 μ M IBMX or 100 nM α -MSH to measure the melanin content.

2.6. Effect of PDGF/EGF receptor inhibitors on serum-dependent melanogenesis

2×10^4 B16F10 cells were seeded in each well for 24 h in 10% FBS-containing medium, and then cultured for additional 72 h in the fresh medium containing 100 nM α -MSH and followings: (1) no serum, (2) 10% FBS alone, (3) 10% FBS plus 2 μ M AG1295 (PDGF receptor inhibitor), and (4) 10% FBS plus 400 nM AG1478 (EGF receptor inhibitor), to measure the melanin content.

2.7. Statistical analysis

Data are expressed as mean values with their standard errors. Statistical comparisons were performed by one-way ANOVA followed by Duncan's multiple-range test. Statistical analysis was conducted using SAS (release 9.2; SAS Institute, Cary, NC, USA) and $p \leq 0.05$ was considered significant.

3. Results

3.1. Activation of PAK1 in melanoma cell line (B16F10) by melanogenic hormones

Two melanogenic hormones, α -MSH (melanocyte-stimulating hormone) and IBMX (3-isobutyl-1-methyl xanthine), are often used to stimulate melanogenesis in melanocytes such as melanoma cell line B16F10. Thus, we first examined if these hormones can activate PAK1 in this cell line, although the protein level of PAK1 there is extremely low, compared with those of PAK2 and PAK4 (8). To monitor the changes in kinase activity of PAK1 in cells, we recently developed a highly sensitive/specific kinase assay called "Macaroni-Western" (IP-ATP-Glo) kinase assay protocol by combining the immuno-precipitation (IP) of PAK1 from cell lysates and Promega's ATP_Glo kinase kit (5). Using this kinase assay, we found that both α -MSH (100 nM) and IBMX (100 μ M) activate PAK1 in melanoma cells, with α -MSH being more potent than IBMX (see in Figure 1). However, we should remind readers that the fold activation of PAK1 shown here is only apparent, because during this time-consuming test tube IP and kinase assay (over 3 h in total) taking place without these melanogenic hormones, PAK1 would be gradually normalized over time. In other words we cannot freeze the exact kinase status of PAK1 at the end of cell culture treated with these stimulators, and the fold activation is only an under-estimated reflection of PAK1 activation taken place during cell culture by these stimulators.

3.2. Silencing of PAK1 gene by shRNAs in mouse melanoma cell line

In order to investigate further biochemically if PAK1 contributes to the melanogenesis in skin cells (melanocytes), we stably transfected the melanoma cell line B16F10 with mouse PAK1-specific shRNA to silence PAK1 gene selectively.

3.2.1. Silencing PAK1 gene in melanocytes

Our preliminary western blot analysis suggested that in two distinct PAK1-silenced clones (SH1 and 2) the PAK1 protein levels are significantly (by around 75%) reduced, but the growth rate of this melanoma cell line *per se* was not significantly affected by the PAK1 silencing (data

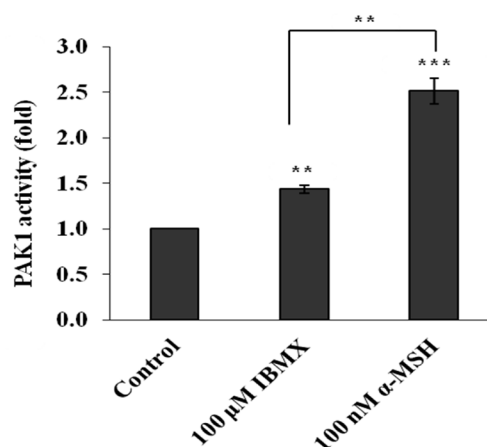


Figure 1. Activation of PAK1 by IBMX and α -MSH in melanocytes. B16F10 cells were treated with IBMX (100 μ M) and α -MSH (100 nM) for 72 h. PAK1 was immuno-precipitated from cells lysates, and PAK1 activity was measured by "Macaroni-Western" kinase assay. The results are mean \pm SE of three independent experiments. Data have significant difference by ANOVA analysis at $p \leq 0.05$. Statistically significant differences relative to control are indicated by asterisks. * $0.01 \leq p \leq 0.05$, ** $p \leq 0.01$, *** $p \leq 0.001$.

not shown). However, the accurate quantification of PAK1 protein levels by scanning this western blot was rather difficult, mainly because of the high background noise around the PAK1 band in the effort to visualize its extremely low expression levels. Instead, using the "Macaroni-Western" kinase assay (5,10), we verified that the kinase activity of PAK1 in both SH1 and 2 clones are only around 25-30% of that in the control (WT) cells (see Figure 2A).

3.2.2. Reduction in the melanogenesis by silencing PAK1 gene

Our next critical question was if such a reduction in the kinase activity of PAK1 affects the melanogenesis. Thus, the melanin content in these clones (SH1 and 2) was compared with the wild-type (WT) melanoma cells, after treating all these cells with α -MSH, a melanogenic inducer, for 72 h. As shown in Figure 2B, the melanin content in these PAK1-deficient melanocytes (SH1 and 2) is reduced by around 50% (51-55%), reaching the basal level in the WT without melanogenic hormone. To see if this reduction in melanin content is associated with the suppression of tyrosinase activity, we measured the tyrosinase activity in PAK1-deficient cells (clones SH1 and 2), compared with the WT. As shown in Figure 2C, the tyrosinase activity in PAK1-deficient cells is only around 45% (33-58%) of that in the WT, again reaching the basal (non-stimulated) level, clearly indicating that PAK1 is essential for α -MSH-induced melanin production by tyrosinase in melanocytes. Furthermore, in a very similar manner the IBMX-induced melanogenesis was also reduced by silencing PAK1 gene in this melanoma cell line (data not shown). However, taking the following two factors into account, it is most likely

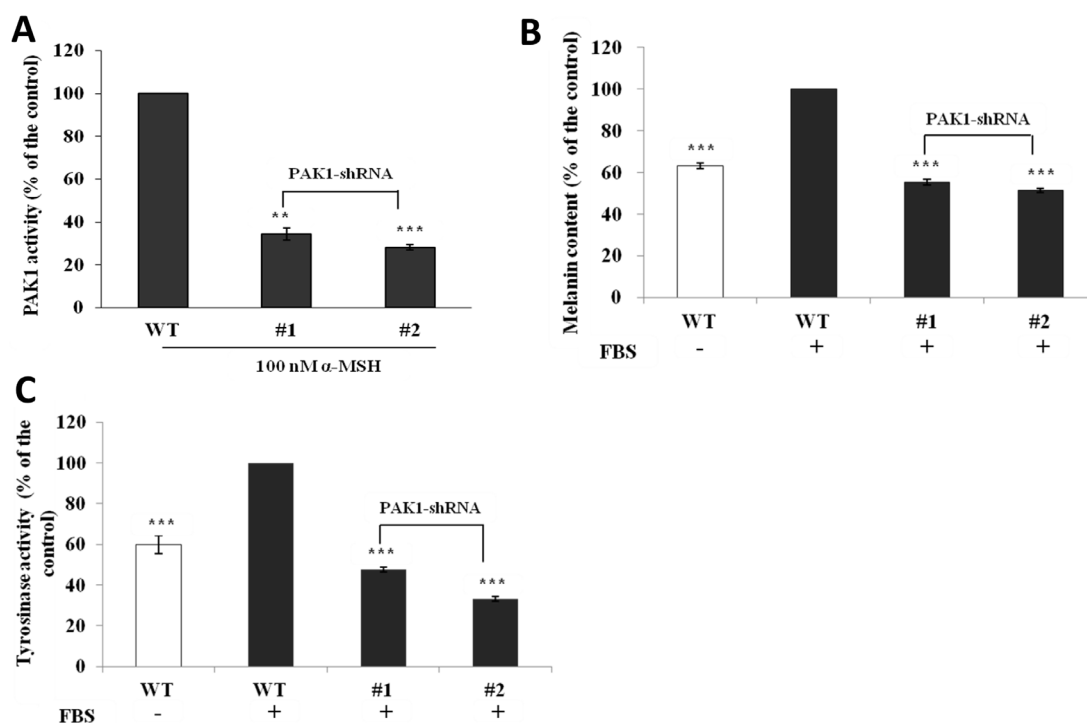


Figure 2. Reduction of melanogenesis by down-regulation of PAK1. (A) Down-regulation of PAK1 by shRNAs. Kinase activity of PAK1 in the transfectant (SH1 and SH2) with PAK1-specific shRNA, compared with the WT melanocytes. Cells were treated with α -MSH (100 nM) for 48 h. PAK1 was immuno-precipitated from cells lysates, and PAK1 activity was measured by "Macaroni-Western" kinase assay. (B) Reduction in melanin content by silencing PAK1 gene. The total α -MSH-induced melanin content is reduced around 53% in SH transfectants (1-2), respectively, reaching the basal level in the WT (compare with lane 1). (C) Reduction in tyrosinase activity by silencing PAK1 gene. The total tyrosinase activity in SH transfectants (SH1-2) is around 45% of that in the WT, reaching the basal (non-stimulated) level. Values indicate the mean \pm SE from three independent experiments. Data have significant difference by ANOVA analysis at $p \leq 0.05$. Statistically significant difference from the control (WT treated with α -MSH) are indicated by asterisks. * $0.01 \leq p \leq 0.05$, ** $p \leq 0.01$, *** $p \leq 0.001$.

that only a half of melanogenesis in melanocytes is PAK1-dependent, and the remaining (largely "basic") is PAK4-dependent: (i) PAK4 is also essential for the α -MSH-induced melanogenesis in melanocytes (8), and (ii) around 25% of PAK1 gene appears to be still expressed in these transfectants (SH1 and 2). However, it still remains to be clarified vigorously whether PAK1 is responsible for the hormone-inducible or the basal melanogenesis.

Furthermore, we have confirmed that the endogenous PAK1 is significantly activated by melanogenic inducers such as IBMX and α -MSH in this melanoma cell line (see Figure 1), but without any significant change in its auto-phosphorylation at Thr 423 as judged by the anti-pPAK1 antibody (data not shown).

3.3. Increase in α -MSH-inducible melanogenesis by over-expressed PAK1

By over-expression of the wild-type (WT) PAK1 gene in melanocytes (B16F10 cell line) by transfection, we revealed that the exogenously added PAK1 gene boosts the α -MSH-inducible melanin level by several folds (see the left of Figure 3, compare lanes 2 and 4), while it hardly affects the independent "basal" melanin level *per se* (compare lanes 1 and 3 in the left panel of Figure 3), suggesting that PAK1 contributes mainly to α -MSH/

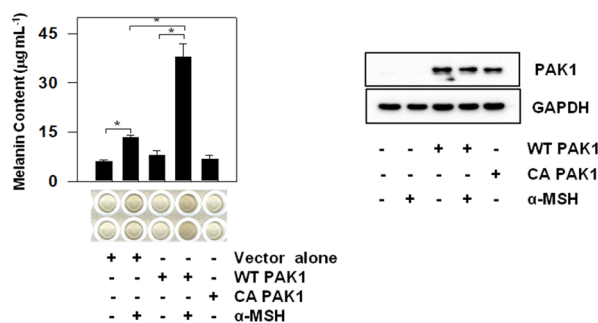


Figure 3. Increase in melanin content by over-expressing PAK1 gene. Left panel: Quantification of melanin content. Lanes 1 and 2 with the control (MYC vector alone) transfection, lanes 3 and 4 with WT PAK1 transfection, and lane 5 with CA PAK1 transfection. The transfection of WT PAK1 gene increased the melanin content more than twice in the presence of α -MSH (compare lanes 2 and 4). Right panel: western blot analysis. Lanes 3-5 show the expression of transfected PAK1 genes (WT or CA). Data were subjected to ANOVA analysis and statistical significance is indicated by asterisks. ** $p < 0.01$.

IBMX-dependent melanogenesis, and not the basal melanogenesis without exogenous stimulator(s).

3.4. Serum effect on α -MSH/IBMX-inducible melanogenesis

More interestingly, we found that the induction of

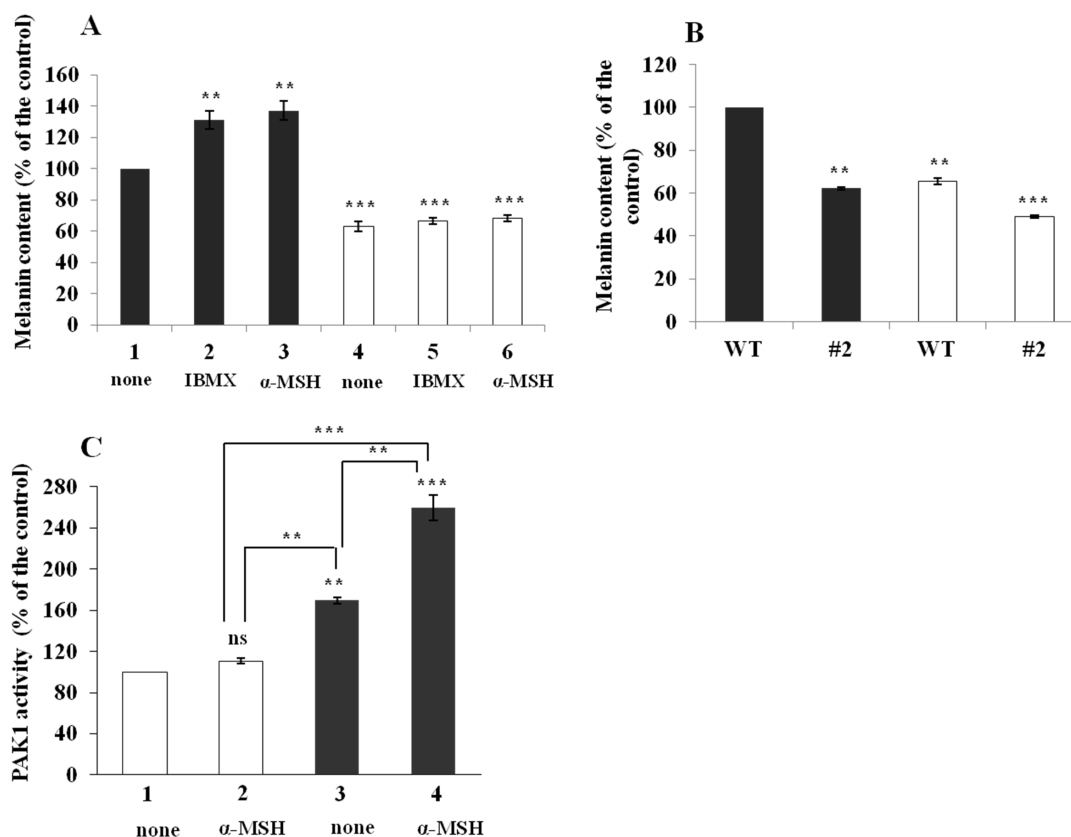


Figure 4. Serum/PAK1-dependency of melanogenesis. Open bars, the control (no serum); closed bars, 10% FBS. **(A)** α -MSH/IBMX requires FBS for their induction of melanogenesis. **(B)** PAK1 is essential for the serum-dependent melanogenesis. WT, the control wild type; #2, PAK1-deficient transfectant. **(C)** α -MSH requires FBS for its robust activation of PAK1. The results are mean \pm SE. Data have significance by ANOVA analysis at $p \leq 0.05$. Statistically significant difference in relative to control is indicated by asterisks. ** $p \leq 0.01$, *** $p \leq 0.001$, ns: no significance.

melanogenesis by α -MSH/IBMX absolutely requires 10% FBS (fetal bovine serum) in addition to PAK1. As shown in Figure 4A, in a serum-free medium, either α -MSH or IBMX hardly induced the melanogenesis in the WT cells, although the 10% FBS alone (without α -MSH/IBMX) induced the melanogenesis significantly (by around 60%). Interestingly the melanogenesis in SH transfectants (PAK1-deficient cells) in the presence or absence of serum was basically the same level as that in WT cells in the absence of serum (see Figure 4B), suggesting that the serum-dependent melanogenesis also requires PAK1. In supporting this notion, serum alone significantly activates the kinase activity of PAK1 in WT cells, but the α -MSH-dependent activation of PAK1 in WT cells absolutely requires serum (see Figure 4C).

Regarding the chemical nature of melanogenic serum factor that alone activates PAK1, we speculate that it is PDGF (platelet-derived growth factor) from the following reasons: (i) more than a decade ago we have shown that PDGF is the sole growth factor in serum that activates PAK1 through the transactivation of EGF (epidermal growth factor) receptor by PDGF receptor (13,14), and very recently others have proven that either PDGF or EGF alone indeed stimulates the melanogenesis of melanocytes (15,16).

3.5. The serum/PDGF-dependent melanogenesis requires EGF receptor

In an attempt to identify the specific chemical nature of this melanogenic serum factor, we have tested the effect of either AG1295 (inhibitor specific for PDGF receptor) or AG1478 (inhibitor specific for EGF receptor) on the serum-dependent melanogenesis in melanocytes. As shown in Figure 5, either 2 μ M AG1295 or 400 nM AG1478 strongly reduced the serum-dependent melanogenesis to the level equivalent to the basic (serum-free) melanogenesis. Since PDGF is abundantly present in serum, but not EGF, and AG1295 does not inhibit EGF receptor, while AG1478 does not inhibit PDGF receptor (13), it is most likely that PDGF in serum activates its receptor that in turn trans-activates EGF receptor that eventually activates PAK1 that is essential for serum-dependent melanogenesis (for detail, see Figure 6). Based on this assumption, we shall discuss later the most likely mechanism underlying the apparent synergy between α -MSH and serum/PDGF for the activation of PAK1, leading to the robust melanogenesis.

Lastly, it should be worth pointing out that the "basal" melanin content without α -MSH was not significantly changed by over-expressed CA (constitutively active)

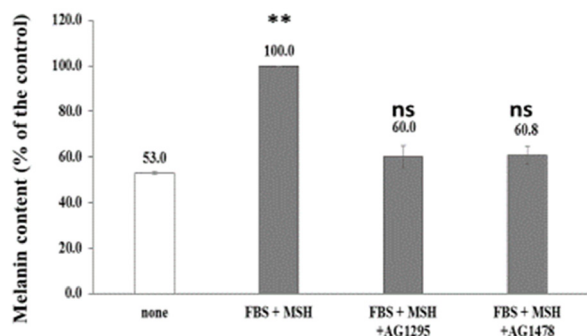


Figure 5. PAK1-dependent serum-induced melanogenesis requires both PDGF and EGF receptors. Open bar, the control (no serum); closed bars, 10% FBS plus α -MSH. The last two bars, plus either AG1295 or AG1478. Both inhibitors equally reduced the serum-induced melanogenesis to the basal (serum-free) level. The results are mean \pm SE. Data have significance by ANOVA analysis at $p \leq 0.05$. Statistically significant difference in relative to control is indicated by asterisks. ** $p \leq 0.01$, ns: no significance.

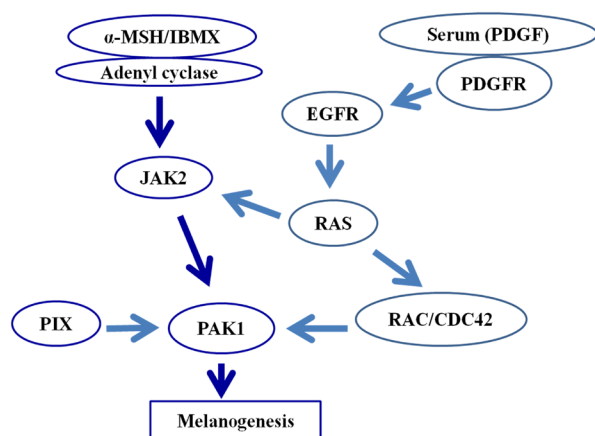


Figure 6. Most likely mechanism underlying the Serum/PAK1-dependent melanogenesis. Either α -MSH or IBMX activates PAK1 through adenyl cyclase that produces cAMP, which in turn activates PKA, and JAK2 that secures the PIX-PAK1 interaction. However, the PIX-PAK1 interaction alone is not sufficient for the full activation of PAK1. It needs RAC/CDC42 which is activated by the oncogenic RAS-PI3 kinase signalling cascade. To activate RAS, cells need either PDGFR or EGFR. Serum is the major source of PDGF, and its receptor (PDGFR) trans-activates EGF receptor. Once RAS is activated, two complementary pathways are activated: one leading to RAC/CDC42 activation, and the other heading for JAK2 activation that secures the PIX-PAK1 interaction. Thus, serum alone can induced melanogenesis through RAC/CDC42- and PIX-dependent PAK1 pathways, but α -MSH or IBMX can further boost the melanogenesis by enhancing the "rate-limiting" PIX-dependent pathway.

mutant of PAK1 carrying T423E mutation (see the left panel of Figure 3, lane 5), as if it were either a DN (dominant negative) or inactive mutant. In fact, α -MSH did not induce the phosphorylation of WT PAK1 at Thr 423 at all (data not shown). Thus, it could be concluded that the auto-phosphorylation of PAK1 at Thr 423 has nothing to do with α -MSH-induced activation of PAK1, which leads to the robust melanogenesis in melanoma cells. Since T423E mutant of PAK1 is well known to be highly oncogenic (6), perhaps the auto-phosphorylation

at Thr 423 might serve a switch from "melanogenic" to "oncogenic" signalling.

4. Discussion

From our observation on both PAK1-dependent and PAK4-dependent melanogenesis in melanocyte/melanoma cells, there rise two potentially interesting issues to be pointed out: (i) The "specific" melanogenic activity of PAK1 (only minutely expressed) must be far higher than that of PAK4 (highly expressed) in melanoma cells. (ii) It appears that PAK1 is mainly responsible for serum-induced melanogenesis, while PAK4 is mainly responsible for the intrinsic (basal) melanogenesis. In other words, although PAK4-deficiency is embryonically lethal in mice, while PAK1-deficiency alone fails to produce "albino" mice, the apparent difference in the original skin color (basic melanogenesis) between black and white people for instance could be at least partly a reflection of the difference in the expression level of PAK4, as well as difference in the level of melanogenic tyrosinases.

In vivo, using HRM-2 (pigmented but hairless) mice, we have recently shown that a cream containing 10 μ M PF3758309 (PAK1/PAK4-inhibitor) reduces the UV-induced melanogenesis in their skin to the basal level, although it still remains to be clarified whether PAK4 or PAK1 is responsible for UV-induction of melanogenesis (8). Since PAK1 is responsible for the inducible, but not the basal, melanogenesis, it would be worth testing if PAK1 significantly contributes to the UV-inducible melanogenesis (sun tanning) as well, using the rare PAK1 KO (knock out) mutant derived from C57B16 strain of mice carrying dark hairs and eyes (Hong He *et al.*, unpublished observation), in an attempt to understand if a variety of herbal PAK1 blockers in cosmetics are useful for sun-screening agents or not. Interestingly PAK1 was reported to be activated by UV irradiation and other DNA-damaging agents (17).

It has been shown that α -MSH activates the Tyrosinase JAK2 (18), which in turn activates PAK1 by the phosphorylation at Tyr 285, (instead of Thr 423), leading to the PIX-PAK1 interaction (19). This could explain why neither α -MSH-dependent activation of PAK1 nor melanogenesis involves the autophosphorylation of PAK1 at Thr 423. Thus, we recently investigated if the PAK1-dependent melanogenesis is blocked by a potent herbal JAK2-inhibitor called cucurbitacin I (CBI) from bitter melon (Goya) that inhibits directly JAK2 (20), and found that CBI inhibits the melanogenesis in the presence of melanogenic hormones by more than 70%, suggesting the possibility that CBI blocks not only PAK1 but also PAK4 (5).

In this context, it would be of great interest to note that the herbal PAK1-blockers such as CAPE, curcumin, shikonin, and FTY 720 could inhibit the α -MSH-

induced melanogenesis in mouse or human skin cells only by around 50% even at their concentrations where PAK1 is almost completely blocked (1,2), whereas the synthetic pan-PAK-blocker PF3758309, inhibiting both PAK1 and PAK4, abolishes the melanogenesis in skin cells by around 90% at 300 nM (8). In other words, the α -MSH-induced melanogenic system in melanocytes could distinguish the PAK1-specific blockers from pan-PAK-blockers. So far no herbal PAK4-specific blockers (other than PAK4-specific siRNAs) have been identified. However, a very potent quassinoid called glaucarubinone derived from bitter tree grown in Amazon jungles has recently been shown to block both PAK1 and PAK4, inhibiting the growth of pancreatic cancer cells both *in vitro* and *in vivo* (21). Thus, it would be of great interest to test if this herbal PAK-blocker suppresses the melanogenesis of skin cells almost completely as does PF3758309.

The major aim of this study was to focus on the specific melanogenic role of PAK1, and not to investigate in detail how PAK1 activates the melanogenic signalling pathway including melanogenic enzymes and MTFs. However, it is most likely that PAK1 activates directly beta-catenin by phosphorylating at Ser 675, leading to the activation of MITF which is essential for expression of genes encoding for melanogenic enzymes such as tyrosinase (Tyr).

Recently we found that PAK4 (CDC42-dependent kinase 4) is also involved in melanogenesis of the same melanoma cell line by activating two transcription factors, CREB and beta-catenin, both of which are essential for MITF activation (8). Since CREB is known to be activated by LIM kinase (22,23) which like beta-catenin, is among the common direct substrates of both PAK1 and PAK4 (6,18), it is most likely that PAK1 and PAK4 share the same CREB/beta-catenin-MITF signalling pathways to activate the melanogenic enzyme genes.

However, the detailed signal pathways leading to the α -MSH/IBMX-dependent activation of PAK1 could differ significantly from those leading to the activation of PAK4, mainly because the former clearly involve the serum factor (PDGF). The serum alone is capable of activating PAK1 (13), and boosts the α -MSH/IBMX-dependent activation of PAK1 as well. In other words, there is a clear synergy between the serum and these melanogenic hormones in both PAK1 activation and melanogenesis.

The following is our working hypothesis as to how this synergy could take place. The major signalling pathway leading to the PAK1 activation is the oncogenic EGFR (epidermal growth factor receptor)-RAS-PI 3 kinase-RAC/CDC42-PAK1 cascade. However, this cascade alone is not sufficient for the full-activation. It needs another factor called PIX, an SH3 adaptor protein that binds directly PAK1 through its Pro-rich motif of 18 amino acids called PAK18. The PIX-PAK1 interaction

needs a third protein called JAK2, a Tyr-kinase, that phosphorylates PAK1 at Tyr 285. RAS up-regulates JAK2 through prolactin. According to a few previous findings by us and others (13-16), PDGF (platelet-derived growth factor) is the major melanogenic serum factor(s) essential for the α -MSH/IBMX-induced melanogenesis, because it activates its receptor (PDGFR) Tyr-kinase that in turn trans-activates EGFR (epidermal growth factor receptor=ErbB1) Tyr-kinase, leading to the activation of PAK1 through the oncogenic RAS-PI3 kinase-RAC/CDC42 pathway (13). Thus, PDGF in serum alone can activate PAK1 and induce melanogenesis up to a half way. However, for the full activation of PAK1-dependent melanogenesis, α -MSH/IBMX is needed to activate the JAK2 through a cAMP-dependent pathway (which might involve PKA) that eventually secures the PIX-PAK1 interaction (for detail, see Figure 6).

In conclusion, here we present the very first biochemical evidences which might explain how a variety of herbal PAK1-blockers such as CAPE, curcumin and shikonin in cosmetic creams could contribute to the "skin-whitening" effects. A series of analogous studies with human melanocytes are awaited for the further proof or confirmation.

Acknowledgements

We are very grateful to Dr. Jon Chernoff of Fox Chase Cancer Center for his critical reading of this manuscript and his valuable comment on tyrosinase (Tyr) gene as well as Dr. Hong He of Melbourne University for her unpublished trigue observation on the albino PAK1-KO mice (C57B16 strain) which prompted us to initiate the present study.

References

1. Lee JH, Jang JY, Park C, Kim BW, Choi YH, Choi BT. Curcumin suppresses alpha-melanocyte stimulating hormone-stimulated melanogenesis in B16F10 cells. *Int J Mol Med.* 2010; 26:101-106.
2. Lee JY, Choi HJ, Chung TW, Kim CH, Jeong HS, Ha KT. Caffeic acid phenethyl ester inhibits alpha-melanocyte stimulating hormone-induced melanin synthesis through suppressing transactivation activity of microphthalmia-associated transcription factor. *J Nat Prod.* 2013; 76:1399-1405.
3. Maruta H. Herbal therapeutics that block the oncogenic kinase PAK1: A practical approach towards PAK1-dependent diseases and longevity. *Phytother Res.* 2014; 28:656-672.
4. Nguyen BCQ, Taira N, Tawata S. Several herbal compounds in Okinawa plants directly inhibit the oncogenic/aging kinase PAK1. *Drug Discov Ther.* 2014; 8:238-244.
5. Nguyen BCQ, Be Tu PT, Tawata S, Maruta H. Combination of immunoprecipitation (IP)-ATP_Glo kinase assay and melanogenesis for the assessment of potent and safe PAK1-blockers in cell culture. *Drug*

- Discov Ther. 2015; 9:289-295.
6. He H, Maruta H. Oncogenicity of PAKs and their substrates. In: PAKs, RAC/CDC42 (p21)-activated kinases: Towards the cure of cancers and other PAK-dependent diseases (Maruta H, ed.). Elsevier, Oxford, 2013; pp. 23-51.
 7. Widlund HR, Horstmann MA, Price ER, Cui J, Lessnick SL, Wu M, He X, Fisher DE. β -Catenin-induced melanoma growth requires the downstream target *Microphthalmia*-associated transcription factor. J Cell Biol. 2002; 158:1079-1087.
 8. Yun CY, You ST, Kim JH, Chung JH, Han SB, Shin EY, Kim EG. p21-activated kinase 4 critically regulates melanogenesis *via* activation of the CREB/MITF and β -catenin/MITF pathways. J Invest Dermatol. 2015; 135:1385-1394.
 9. Huynh N, Liu KH, Baldwin GS, He H. P21-activated kinase 1 stimulates colon cancer cell growth and migration/invasion *via* ERK- and AKT-dependent pathways. Biochim Biophys Acta. 2010; 1803:1106-1113.
 10. Tagliati F, Bottoni A, Bosetti A, Zatelli MC, degli Uberti EC. Utilization of luminescent technology to develop a kinase assay: Cdk4 as a model system. J Pharm Biomed Anal. 2005; 39:811-814.
 11. Yoon NY, Eom TK, Kim MM, Kim SK. Inhibitory effect of phlorotannins isolated from *Ecklonia cava* on mushroom tyrosinase activity and melanin formation in mouse B16F10 melanoma cells. J Agric Food Chem. 2009; 57:4124-4129.
 12. Li X, Guo L, Sun Y, Zhou J, Gu Y, Li Y. Baicalein inhibits melanogenesis through activation of the ERK signaling pathway. Int J Mol Med. 2010; 25:923-927.
 13. He H, Levitzki A, Zhu HJ, Walker F, Burgess A, Maruta H. Platelet-derived growth factor requires epidermal growth factor receptor to activate p21-activated kinase family kinases. J Biol Chem. 2001; 276:26741-26744.
 14. Saito Y, Haendeler J, Hojo Y, Yamamoto K, Berk BC. Receptor hetero-dimerization: Essential mechanism for platelet-derived growth factor-induced epidermal growth factor receptor transactivation. Mol Cell Biol. 2001; 21:6387-6394.
 15. Hirobe T, Shibata T, Fujiwara R, Sato K. Platelet-derived growth factor regulates the proliferation and differentiation of human melanocytes in a differentiation-stage-specific manner. J Dermatol Sci. 2016; 83:200-209.
 16. Garcez RC, Teixeira BL, Schmitt Sdos S, Alvarez-Silva M, Trentin AG. Epidermal growth factor (EGF) promotes the *in vitro* differentiation of neural crest cells to neurons and melanocytes. Cell Mol Neurobiol. 2009; 29:1087-1091.
 17. Roig J, Traugh JA. p21-activated protein kinase gamma-PAK is activated by ionizing radiation and other DNA-damaging agents. Similarities and differences to alpha-PAK. J Biol Chem. 1999; 274:31119-31122.
 18. Buggy JJ. Binding of alpha-melanocyte-stimulating hormone to its G-protein-coupled receptor on B-lymphocytes activates the Jak/STAT pathway. Biochem J. 1998; 331:211-216.
 19. Hammer A, Oladimeji P, De Las Casas LE, Diakonova M. Phosphorylation of tyrosine 285 of PAK1 facilitates β PIX/GIT1 binding and adhesion turnover. FASEB J. 2015; 29:943-959.
 20. Blaskovich MA, Sun J, Cantor A, Turkson J, Jove R, Sebt SM. Discovery of JSI-124 (cucurbitacin I), a selective Janus kinase/signal transducer and activator of transcription 3 signaling pathway inhibitor with potent antitumor activity against human and murine cancer cells in mice. Cancer Res. 2003; 63:1270-1279.
 21. Yeo D, Huynh N, Beutler JA, Christophi C, Shulkes A, Baldwin GS, Nikfarjam M, He H. Glaucaurubinone and gemcitabine synergistically reduce pancreatic cancer growth *via* down-regulation of p21-activated kinases. Cancer Lett. 2014; 346:264-272.
 22. Dan C, Kelly A, Bernard O, Minden A. Cytoskeletal changes regulated by the PAK4 serine/threonine kinase are mediated by LIM kinase 1 and cofilin. J Biol Chem. 2001; 276:32115-32121.
 23. Yang EJ, Yoon JH, Min DS, Chung KC. LIM kinase 1 activates cAMP-responsive element-binding protein during the neuronal differentiation of immortalized hippocampal progenitor cells. J Biol Chem. 2004; 279:8903-8910.

(Received September 15, 2016; Revised September 29, 2016; Re-revised October 8, 2016; Accepted October 8, 2016)

Effect of astigmatism on refraction in children with high hyperopia

Hao Hu¹, Jinhui Dai^{2,3,*}, Minjie Chen^{2,3}, Lanting Chen^{4,5,6}, Lingli Jiang¹, Ran Lin¹, Ling Wang^{4,5,6,*}

¹Department of Ophthalmology, The First People's Hospital of Wenling, Wenling, Zhejiang, China;

²Department of Ophthalmology, EYE and ENT Hospital of Fudan University, Shanghai, China;

³The Key Laboratory of myopia of the Chinese Health Ministry, Shanghai, China;

⁴Laboratory for Reproductive Immunology, Hospital & Institute of Obstetrics and Gynecology, IBS, Fudan University Shanghai Medical College, Shanghai, China;

⁵The Academy of Integrative Medicine of Fudan University, Shanghai, China;

⁶Shanghai Key Laboratory of Female Reproductive Endocrine Related Diseases, Shanghai, China.

Summary

The aim of this study was to evaluate primitively whether the extent and component of astigmatism influences regression in degree of spherical (DS) and the best corrected visual acuity (BCVA) of children with hyperopia of +5.00 diopters (D) or greater. Children were screened from the outpatient refraction database in the Wenling No. 1 People's Hospital in Zhejiang province and in Eye & ENT Hospital of Fudan University between June 2005 and December 2015. Eligible eyes were divided into three groups according to the extent of astigmatism: group of astigmatism ≤ -2 D of cylinder, group without astigmatism or with astigmatism ≥ -0.5 D of cylinder, and the group with astigmatism ≥ -0.75 D and ≤ -1.75 D of cylinder. For the component of astigmatism, eyes with astigmatism as ≤ -0.75 D of cylinder were divided into 3 groups: with the rule (WTR), against the rule (ATR) and the group with the oblique. Differences in the changes of BCVA and refractive error (RE) during follow-up terms were compared within and among groups. Differences in the mean DS or BCVA were not statistically significant between groups according to the extent of the astigmatism at the last visit ($p = 0.2396$ and $p = 0.2131$, respectively). As for the component of astigmatism, the group with oblique astigmatism had more severe hyperopia than the group of WTR ($p < 0.0001$) and mean BCVA in the group of ATR were better than that of the other two groups ($p < 0.0001$) at the first visit. However, the among-group changes were not significant at the end of the observation ($p > 0.1$). The regression of DS and improvement of the BCVA in children with hyperopia of +5.00D or greater may be irrespective of the component and the extent of astigmatism.

Keywords: Astigmatism, high hyperopia, refraction, child

1. Introduction

The refraction in infants is usually hyperopic, and generally develops gradually toward emmetropia during

the first years of life (1). However, Cambridge photo-screening program indicates that hyperopia more than +3.5 D in one or more meridians would be the most frequent refractive anomaly (5-6%) observed in a population at 9 months of age. Moreover, it is associated with a higher risk of amblyopia (almost 7 times that of the control group) and strabismus (21% versus 1.6%) at 4 years of age (2,3). Besides, further study concludes that young children with hyperopia greater than 5.00 D are prone to suffer from amblyopia and strabismus (4). Due to regression of typical neonatal hyperopia, ease of correction with spectacle lenses, and rare association with blinding disease, studies concerning the prevalence,

Released online in J-STAGE as advance publication November 27, 2016.

*Address correspondence to:

Dr. Jinhui Dai, Eye & ENT Hospital of Fudan University, 83 Fenyang Road, Shanghai 200031, China.
E-mail: daijinhui8@126.com

Dr. Ling Wang, Obstetrics & Gynecology Hospital of Fudan University, 413 Zhaozhou Road, Shanghai 200011, China.
E-mail: dr.wangling@fudan.edu.cn

incidence, and natural history of high hyperopia, and subsequent complications in children are limited (3,5) though subsequent amblyopia affects approximately 2-4% of the population (6).

During the process of emmetropization, there has been some controversy about the role of astigmatism in visual development. For one thing, some researchers speculated that persistent astigmatism may impede emmetropization with formation of a blurred image on the retina (7-11). Animal results in monkeys and chicks showed astigmatic defocus caused young eyes to grow slightly toward hyperopia (10). However, others hold the opposite view. Fulton and Shih *et al.* have suggested that an astigmatic blur induced myopia (7-9). Among which, against-the-rule astigmatism is agreed to predict later development of myopia and faster progression of existing myopia (8). So, if astigmatism has an effect on myopia on-set or its progression, then its role on emmetropization is obviously important. Nevertheless, clear signs of either hyperopic or myopic was both presented in cylinder-lens-reared monkeys (11).

Though numerous reports intend to disclose the role of astigmatism in visual development, no studies can well document this yet. Recently, studies have been carried out that astigmatism and high hyperopia are both risk factors for bilateral decreased visual acuity (12). For another, researchers found that changes in the cylinder power were almost independent of spherical equivalent over the period from 9 to 20 months in hyperopic children (1). Considerably less attention has been devoted to the association between astigmatism and the refractive development in children with high hyperopia. For this purpose, the present study was conducted to determine the influence of the extent and component of astigmatism on regression of typical neonatal refraction in children with hyperopia of +5.00 D or greater.

2. Materials and Methods

2.1. Patients

This study was conducted in accordance with the Declaration of Helsinki. Ethics Committee of Eye and ENT Hospital of Fudan University and Wenling No. 1 People's Hospital specifically approved this study. The patients included in this study were screened from outpatient refraction database in the Wenling No. 1 People's Hospital in Zhejiang province and in Eye & ENT Hospital of Fudan University between June 2005 and December 2015. Eligible children of either sex had to be no more than 10 years of age at the first visit and had hyperopia of +5.00 D or greater in at least one eye on cycloplegic refraction. We excluded patients who had glaucoma, retinal detachment, congenital cataract, nystagmus, retinopathy of prematurity or any previous ocular surgeries including laser therapy, refractive surgery, cataract surgery, and strabismus surgery, as

well as those unable to cooperate with cycloplegic refraction. Finally, 890 children (1,514 eyes) were enrolled retrospectively and eligible for analysis. All children were prescribed with spectacle correction of hyperopia.

2.2. Treatment

Subjective cycloplegic refraction (CV-3000, Topcon, Tokyo, Japan) was checked with experienced optometrists half an hour after instilling a drop of tropicamide 0.5% (Shenyang Xingqi Pharmaceutical co., Ltd., Shenyang, China) three times with five minute intervals or an hour after instilling a drop of tropicamide 0.5% five times with five minute intervals. Others were administered with atropine 0.1% (Shenyang Xingqi Pharmaceutical co., Ltd.) eye gel three times a day for three days before subjective refraction. All refractions were written using the minus cylinder convention. The axis of any cylindrical component was classified as with-the-rule (WTR) if the minus cylinder axis was within 15° of 180°, against-the-rule (ATR) for minus cylinder axis within 15° of 90°, or oblique (other than WTR or ATR) (13). In agreement with other studies, the standard Refractive Error in School-age Children (RESC) definitions of refractive errors were used: astigmatism as ≤ -0.75 D of cylinder in at least one eye (14).

2.3. Follow-up and data collection

Eligible eyes were divided into three groups according to the extent of the astigmatism: group of astigmatism ≤ -2 D of cylinder, group without astigmatism or with astigmatism ≥ -0.5 D of cylinder, and the group with astigmatism ≥ -0.75 D and ≤ -1.75 D of cylinder. For the component of astigmatism, eyes with astigmatism as ≤ -0.75 D of cylinder were divided into 3 groups: group of WTR, group of ATR and the group with the oblique.

Eligible patients had been followed up for at least 3 years. Measurements of refractive status and the BCVA were performed at least twice. The refraction data of the first and the last visit were collected, from which the changes of BCVA and DS between the two visits were included for analysis. Differences in changes of BCVA and DS were compared between groups. The data were collected and analyzed anonymously.

2.4. Statistical analysis

Analyses were performed with Stata software (Version 11.0). Both eyes were selected as the study eye when they were in accordance with the inclusion criteria. Visual acuities were converted to logarithm of minimal angle of resolution (log MAR) for data analysis. The numerical data were expressed as the mean \pm S.D. Changes within groups from the first visit were analyzed using the Wilcoxon signed ranks test.

Comparisons between the group were performed using Kruskal-Wallis test or covariance analysis. A p value of < 0.05 was considered statistically significant.

3. Results

Of all the patients reviewed, 890 children (1,514 eyes) (age range, 2.47 to 10 years; mean age \pm standard deviation, 6.39 ± 1.70 years) were eligible for analysis. At the first visit, the mean RE was 7.16 ± 1.70 D and the mean logarithm of BCVA was 0.23 ± 0.25 (Snellen equivalent, 0.66 ± 0.26). They had a mean follow-up time of 4.00 years (range, 3.06 to 5.3 years). Overall, there was a significant decrease of 1.91 D at the last visit in the mean DS ($p < 0.0001$) and obvious increase of 0.17 (Snellen equivalent, 0.24) in the logarithm of BCVA at the last visit ($p < 0.0001$). The mean reduction of DS was 0.48 D per year in the present study.

Figure 1 and 2 demonstrate schematically the mean DS and the mean logarithm of BCVA in the first and last visits for three groups according to the extent of the astigmatism. No statistically significant differences were seen among groups in the DS and BCVA at the first visit ($p = 0.1425$ and $p = 0.0646$, respectively). Notable improvements in the mean DS and BCVA were found for all three groups compared with the first visit ($p < 0.0001$). However, there was no favorable difference among groups either in the mean DS or in the mean BCVA ($p = 0.2396$ and $p = 0.2131$, respectively).

Of the 1,063 eyes with astigmatism as ≤ -0.75 D of cylinder, 871 eyes (81.9%) had WTR astigmatism while 23 eyes (2.2%) had ATR astigmatism. At the first visit, a significant difference was seen in the DS among groups ($p = 0.0008$). Of which, the group with the oblique astigmatism had more severe hyperopia than the group of WTR ($p < 0.0001$). Nevertheless, the

differences were statistically insignificant for the group of ATR compared to the group with the oblique ($p = 0.692$) and the group of WTR ($p < 0.0001$). Both groups achieved a great reduction in mean RE at the last visit ($p < 0.0001$). However, the differences among groups were not significant ($p > 0.3$) (Figure 3).

Statistically significant differences were found in the mean BCVA at the first visit ($p = 0.0005$). Mean BCVA in the group of ATR were better than that of the other two groups ($p < 0.0001$), however, it was uncomparable between the group of WTR and group with the oblique ($p = 0.467$). Though there were significant differences in the mean BCVA within groups from the first visit ($p < 0.001$), the among-group changes at the last visit were not notable ($p > 0.1$). (Figure 4).

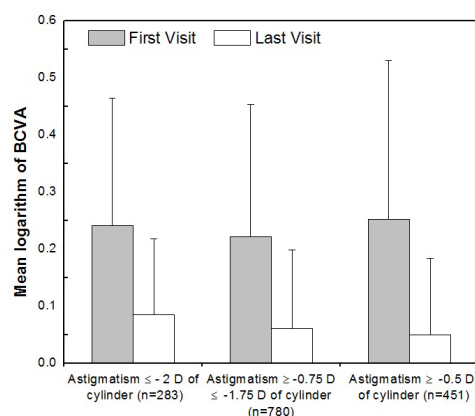


Figure 2. The BCVA improvement during the follow-up terms in all three groups divided according to the extent of astigmatism. Eligible eyes were divided into three groups according to the extent of the astigmatism. The refraction data of the first and the last visit were collected from 890 children (1,514 eyes) before and after the follow-up term. The changes of BCVA between the two visits were included for analysis. Data are expressed as the mean \pm S.D (N for number of eyes).

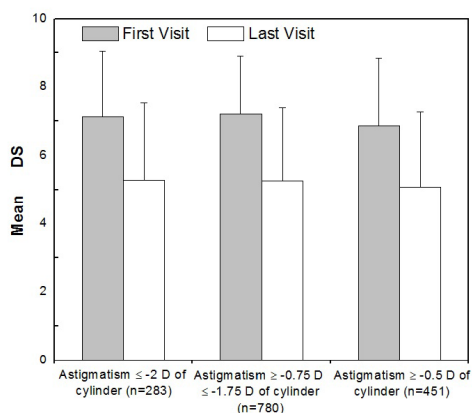


Figure 1. DS significantly decreased during follow-up terms. Eligible eyes were divided into three groups according to the extent of the astigmatism. The refraction data of the first and the last visit were collected from 890 children (1,514 eyes) before and after the follow-up term. Data are expressed as the mean \pm S.D. (N for number of eyes).

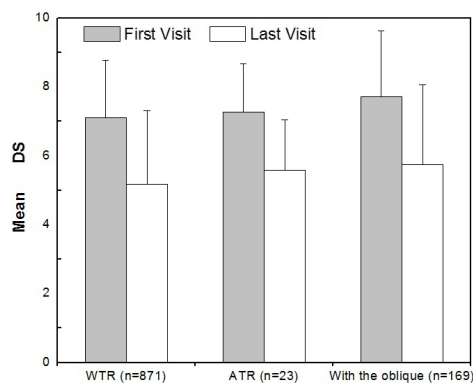


Figure 3. The group with oblique astigmatism had more severe hyperopia. The groups were divided according to the component of astigmatism into group of WTR, group of ATR and group with the oblique. The refraction data of the first and the last visit were collected from 1,063 eligible eyes with astigmatism before and after the follow-up term. Data are expressed as the mean \pm S.D (N for number of eyes).

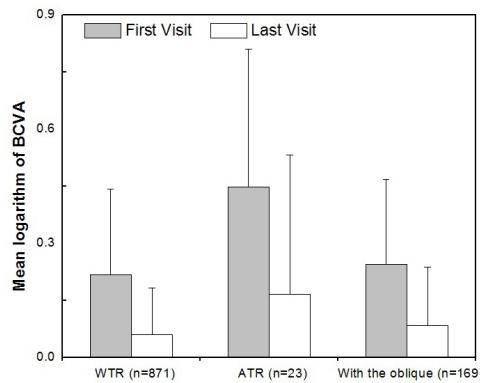


Figure 4. The group with ATR had better BCVA at the first visit but the differences become insignificant by the last visit. The groups were divided according to the component of the astigmatism into group of WTR, group of ATR and group with the oblique. The refraction data of the first and the last visit were collected from 1,063 eligible eyes with astigmatism before and after the follow-up term. Data are expressed as the mean \pm S.D (N for number of eyes).

4. Discussion

In our study, for the group as a whole, a substantial alleviation of hyperopia occurs in the children, which is consistent with previous studies (2). Consequently, the process of emmetropization in children with high hyperopia can also be considered as a convergence of refractions toward a low hyperopic value. It was supposed that eyes with high hyperopia may reflect an intrinsic tendency to undergo less emmetropization (15). The mean reduction of DS was 0.48 D every year in this research. However, no comparable studies were available, thus we could not reach a final verdict in this study that whether eyes with high hyperopia may undergo less emmetropization. On the other hand, evident improvements in the BCVA were also noticed in the study, though high hyperopia (5.25 D) still existed. An achievement of 0.9 at the last visit demonstrated a definitive development of visual acuity independent of existing high hyperopia.

With regards to the extent of astigmatism, no statistical differences among groups were seen in this study. From studies concerning the response of the eye to blur imposed by cylindrical lenses, little attention was drawn to the influence of the extent of astigmatism on refractive development. For one thing, it was hypothesized that chicks with highly astigmatic lenses with their image quality sufficiently degraded might experience form deprivation effects (myopia shift) (16). Also, some researchers showed that higher astigmatism was associated with more myopic refraction and more myopic shift, but also suggested that astigmatism was related to longer axial length and axial length growth (17). For another, a study of hyperopic children found that changes in the cylinder power were almost independent of spherical equivalent over the period

from 9 to 20 months of each other, indicating the extent of the astigmatism would not interfere with the regression of hyperopia in the early months of life (1). As it is worth noting that even though the subjects here are much older than those in the published paper, similar results were observed consistent with Ehrlich's conclusion. This suggests that the amount of astigmatic defocus could not produce any difference in the DS and BCVA, or even in the process of emmetropization in the children with high hyperopia. In contrast, numerous reports have linked the component of astigmatism to refractive development and emmetropization. As in most reports, WTR astigmatism occupied the major portion in preschool children (1,17), which was also applicable to children with high hyperopia in the present study. For animal experiments with different orientation of the imposed astigmatism in chicks and monkeys, no consistent conclusion was obtained about the influence of a component of astigmatism on emmetropization as signs of either hyperopic or myopic growth were both shown (12,16). In fact, the association between astigmatism and myopia is controversial. On one hand, Fulton *et al.* described the relations between increasing myopic spherical equivalent refraction (SER) and an increase in astigmatism in their study of 298 children (aged from 0-10 years) (7). On the other hand, the results in older children (> 10 years) from Parssinen did not support the causal relation between astigmatism and myopic progression (18). However, the disparity of age may account for the dispute because the development of the older children was more or less completed. One finding determined that the outcome of amblyopia treatment seems to be less favorable in patients with either hyperopic or myopic ATR astigmatism (19). In their study, there was statistically significant less line gain of BCVA among patients with hyperopic ATR astigmatism compared with patients with hyperopic WTR astigmatism and myopic ATR patients compared with myopic WTR patients. A number of factors may have affected our results differently from the previous study (19). Of which, the enrolled patients all had unilateral amblyopia due to anisometropia without strabismus, whereas we did not gather systematic data. Further research should be directed concerning those parameters. However, Mutti and associates held the opinion that astigmatism in infancy appeared to be unrelated to emmetropization of spherical equivalent refractive error (20). Though we experienced a large age range (2.47-10 years), the regression of children's high hyperopia should be irrespective of the component and the extent of astigmatism.

This study has a number of limitations. First, the study was retrospective, resulting in incomplete data including information on spectacle correction. A review of the ophthalmic literature fails to show any consistent guidelines for the level of hyperopic refractive error that warrants a prescription. Whether spectacle wear

would impede emmetropization or not is not well established yet. Although Smith and Hung noted that fully correcting the hyperopic refractive errors of juvenile monkeys induced a hyperopic shift (21). In a randomized clinical trial, Atkinson *et al.* found that refractive error correction for +3.50 D or more of hyperopia significantly reduces the risk of strabismus and amblyopia, and they also found that refractive error correction does not alter the emmetropization process in hyperopic children (2). Nevertheless, they cannot be sure how refractive correction might affect the development of very large hyperopic errors, which showed very variable degrees of emmetropization in their observations. Of note, children with hyperopic refractive errors with or more than +5 D would be taken into consideration for optical correction as general guidelines for most practitioners to improve visual acuity (22). Therefore, it would have been instructive to have studied matched groups of children with corrected and uncorrected refraction who have high hyperopic refractive errors. Second, our study's lack of information on amblyopic training prevented us from definitively evaluating the role that astigmatism may play in altering the natural history of hyperopia. Children with confirmed 3.75 D hyperopia usually had a high prevalence and incidence of amblyopia and strabismus (3) and called for treatment of occlusions and special trainings which could interfere with the reduction of refractive errors and improvement of the BCVA.

Notwithstanding the above limitations, this report primitively documented that the regression of spherical refractive errors and improvement of the BCVA in children with hyperopia of +5.00 D or greater may be irrespective of the component and the extent of astigmatism.

Acknowledgements

This work was supported by Grants 81070750 from the National Natural Science Foundation of China. This work was supported by the National Natural Science Foundation of China No. 31571196 (to Ling Wang), the Science and Technology Commission of Shanghai Municipality 2015 YIXUEYINGDAO project No. 15401932200 (to Ling Wang), the FY2008 JSPS Postdoctoral Fellowship for Foreign Researchers P08471 (to Ling Wang), the National Natural Science Foundation of China No. 30801502 (to Ling Wang), the Shanghai Pujiang Program No. 11PJ1401900 (to Ling Wang), and Development Project of Shanghai Peak Disciplines-Integrative Medicine No.20150407.

References

- Ehrlich DL, Atkinson J, Braddick O, Bobier W, Durden K. Reduction of infant myopia: A longitudinal cycloplegic study. *Vision Res.* 1995; 35:1313-1324.
- Atkinson J, Anker S, Bobier W, Braddick O, Durden K, Nardini M, Watson P. Normal emmetropization in infants with spectacle correction for hyperopia. *Invest Ophthalmol Vis Sci.* 2000; 41:3726-3731.
- Colburn JD, Morrison DG, Estes RL, Li C, Lu P, Donahue SP. Longitudinal follow-up of hypermetropic children identified during preschool vision screening. *J AAPOS.* 2010; 14:211-215.
- Wutthiphphan S. Guidelines for prescribing optical correction in children. *J Med Assoc Thai.* 2005; 88 (Suppl 9):S163-169.
- Saw SM. Refraction and refractive errors: Theory and practice. In: *Pediatric ophthalmology and strabismus* (Taylor D, Hoyt CS, editors, eds.). Elsevier Saunders, St. Louis, USA, 2005.
- Chang CH, Tsai RK, Sheu MM. Screening amblyopia of preschool children with uncorrected vision and stereopsis tests in Eastern Taiwan. *Eye (Lond).* 2007; 21:1482-1488.
- Fulton AB, Hansen RM, Petersen RA. The relation of myopia and astigmatism in developing eyes. *Ophthalmology.* 1982; 89:298-302.
- Gwiazda J, Grice K, Held R, McLellan J, Thorn F. Astigmatism and the development of myopia in children. *Vision Res.* 2000; 40:1019-1026.
- Shih YF, Ho TC, Chen MS, Lin LL, Wang PC, Hou PK. Experimental myopia in chickens induced by corneal astigmatism. *Acta Ophthalmol (Copenh).* 1994; 72:597-601.
- McLean RC, Wallman J. Severe astigmatic blur does not interfere with spectacle lens compensation. *Invest Ophthalmol Vis Sci.* 2003; 44:449-457.
- Kee CS, Hung LF, Qiao-Grider Y, Roorda A, Smith EL, 3rd. Effects of optically imposed astigmatism on emmetropization in infant monkeys. *Invest Ophthalmol Vis Sci.* 2004; 45:1647-1659.
- Tarczy-Hornoch K, Varma R, Cotter SA, *et al.* Risk factors for decreased visual acuity in preschool children: The multi-ethnic pediatric eye disease and Baltimore pediatric eye disease studies. *Ophthalmology.* 2011; 118:2262-2273.
- Gwiazda J, Scheiman M, Mohindra I, Held R. Astigmatism in children: Changes in axis and amount from birth to six years. *Invest Ophthalmol Vis Sci.* 1984; 25:88-92.
- Negrel AD, Maul E, Pokharel GP, Zhao J, Ellwein LB. Refractive Error Study in Children: Sampling and measurement methods for a multi-country survey. *Am J Ophthalmol.* 2000; 129:421-426.
- Lambert SR, Lynn MJ. Longitudinal changes in the spherical equivalent refractive error of children with accommodative esotropia. *Br J Ophthalmol.* 2006; 90:357-361.
- Schmid K, Wildsoet CF. Natural and imposed astigmatism and their relation to emmetropization in the chick. *Exp Eye Res.* 1997; 64:837-847.
- Fan DS, Rao SK, Cheung EY, Islam M, Chew S, Lam DS. Astigmatism in Chinese preschool children: Prevalence, change, and effect on refractive development. *Br J Ophthalmol.* 2004; 88:938-941.
- Parssinen O. Astigmatism and school myopia. *Acta Ophthalmol (Copenh).* 1991; 69:786-790.
- Somer D, Budak K, Demirci S, Duman S. Against-the-rule (ATR) astigmatism as a predicting factor for the

- outcome of amblyopia treatment. *Am J Ophthalmol.* 2002; 133:741-745.
20. Mutti DO, Mitchell GL, Jones LA, Friedman NE, Frane SL, Lin WK, Moeschberger ML, Zadnik K. Refractive astigmatism and the toricity of ocular components in human infants. *Optom Vis Sci.* 2004; 81:753-761.
21. Smith EL, 3rd, Hung LF. The role of optical defocus in regulating refractive development in infant monkeys. *Vision Res.* 1999; 39:1415-1435.
22. Lyons SA, Jones LA, Walline JJ, Bartolone AG, Carlson NB, Kattouf V, Harris M, Moore B, Mutti DO, Twelker JD. A survey of clinical prescribing philosophies for hyperopia. *Optom Vis Sci.* 2004; 81:233-237.

(Received September 4, 2016; Revised October 16, 2016; Accepted October 22, 2016)

The use of mannitol in HIV-infected patients with symptomatic cryptococcal meningitis

Zhiliang Hu, Yongfeng Yang, Jian cheng, Cong Cheng, Yun Chi, Hongxia Wei*

Department of Infectious Diseases, the Second Affiliated Hospital of Medical School of the Southeast University, Nanjing, Jiangsu, China.

Summary

Cryptococcal meningitis (CM) is a common opportunistic infection with a high mortality rate in human immunodeficiency virus (HIV)-infected patients. It is unclear whether mannitol could be used to manage neurological symptoms in HIV-associated CM. Here, we retrospectively analyzed the clinical data of 33 patients with HIV-associated symptomatic CM at our hospital where mannitol was used to relieve neurologic symptoms. With the empirical mannitol therapy, patients had a median of 2 episodes (range, 1-6 episodes) of headaches the day at the starting of anti-cryptococcal therapy. The median score of pain intensity assessed by numerical rating scales was 7-point (range, 4-8 points). After the administration of mannitol, the score of pain intensity was reduced to 3-point or less. Three weeks after anti-cryptococcal therapy, 75.8% (25/33) of the patients did not report headaches. During the initial 3 weeks of anti-cryptococcal therapy, 13 patients had a total of 42 episodes of seizures. 97.6% (41/42) of the episodes of seizures were controlled after the administration of mannitol. Overall, 87.9% (29/33) of the patients survived more than 10 weeks without the need of therapeutic cerebrospinal fluid drainage. Mannitol was used for median of 26 days (range, 1-85 days) in these 29 patients. One patient had permanent vision loss. This study indicates that mannitol may possibly relieve neurologic symptoms in HIV-associated CM. It is worth re-evaluating the role of mannitol administration as a symptom control strategy in mild cases of HIV-associated CM.

Keywords: HIV, cryptococcal meningitis, intracranial pressure, mannitol

1. Introduction

Cryptococcal meningitis (CM) is a common opportunistic infection with a high mortality rate in human immunodeficiency virus (HIV)-infected patients. It is estimated that about 1 million cases occur yearly and lead to more than 0.6 million deaths (1). Treatment of HIV-associated CM includes effective antifungal therapy and aggressive management of the elevated intracranial pressure (ICP) (2,3). The mechanism underlying the elevated ICP in HIV-associated CM

has not been well-defined. Cerebrospinal fluid (CSF) inflammatory responses tend to be modest therefore may be a less important contributor to elevated ICP in many cases of HIV-associated CM (4,5). At least, in severe cases, accumulation of fungal elements in arachnoid granulations, which causes CSF outflow obstruction, leads to the raised ICP (6,7). Based on these findings, therapeutic lumbar puncture is recommended to control elevated ICP, although the optimal frequency of therapeutic lumbar puncture and the amount of CSF to be removed need to be further evaluated (8-10).

For many reasons, repeated therapeutic lumbar punctures are not performed in our clinical center. Patients with neurological symptoms (such as headache, seizures and confusion) associated with elevated ICP are routinely treated with mannitol, a hyperosmotic drug used for controlling elevated ICP caused by many other reasons (11-13). Here, we retrospectively analyzed the clinical and laboratory data of the patients with HIV-

Released online in J-STAGE as advance publication October 11, 2016.

*Address correspondence to:

Dr. Hongxia Wei, Department of Infectious Diseases, the Second Affiliated Hospital of Medical School of the Southeast University, 1-1 Zhongfu Road, Nanjing, 210003, China.
E-mail: wghongxia@163.com

associated CM at our hospital to evaluate the prognosis of the patients and the adverse effects that may be related to mannitol administration.

2. Patients and Methods

HIV-infected patients with symptomatic CM in the Second Affiliated Hospital of the Southeast University from December 2010 to September 2014 were retrospectively analyzed. We collected the following data of the patients, such as age, sex, weight, CD4 count, clinical features, CSF parameters, biochemistry parameters, treatment, and outcome. Patients were followed with regular clinic visits and by telephone. This retrospective study was approved by the Ethics Committee of the Second Affiliated Hospital of the Southeast University.

HIV infection was documented by ELISA and confirmed with a Western blot. CM was diagnosed with at least one or more of the following: isolation of cryptococci in the CSF by staining methods (India ink preparation or alcian blue staining), a positive CSF culture for *Cryptococcus* spp. or a positive CSF cryptococcal antigen test (IMMY, Latex-Cryptococcus Antigen Detection System). ICP was measured with an intravenous tube attached to a metered stick, as described elsewhere (14).

Anti-fungal treatment of CM followed the recommended clinical practice guidelines (9), which included an initial induction therapy with amphotericin B (0.7 mg/kg per day intravenously) plus flucytosine (100 mg/kg per day orally) for more than 2 weeks, followed by fluconazole 400 mg/d for a minimum of 8 weeks as consolidation therapy, and then suppressive therapy with fluconazole 200 mg/d. We generally added 1-2 mg dexamethasone to amphotericin B during the first 1 to 2 weeks for the purpose of reducing infusion-related toxicities of amphotericin B. After initiation of anti-cryptococcal therapy, lumbar punctures were performed every 1 to 2 weeks to monitor CSF parameters.

For patients with neurological symptoms such as headache, seizures and confusion, they were treated with 20% mannitol intravenously infused over 15-30 minutes. As a general rule, symptomatic patients were usually started with 125ml or 250 mL 20% mannitol every eight to six hours. The dosage of mannitol was adjusted according to the frequencies of headache or seizures at the discretion of treating physicians. If symptoms persisted, the daily dosage of mannitol was increased. If patients' clinical condition was improved, and there was no new episode of headache or seizures, the daily dosage of mannitol was gradually reduced. Patients were hospitalized until they did not need intravenous therapy. The pain intensity was assessed by numerical rating scales that 0 represent no pain and 10 represent the worst pain imaginable (15).

3. Results

3.1. Patient characteristics

During December 2010 to September 2014, 39 cases of HIV-associated CM were identified in the Second Affiliated Hospital of Nanjing. Two patients early gave up therapy (within 2 days of admission) due to economic reasons, therefore were excluded from analysis. Four cases of CM with good prognosis were early diagnosed before the onset of any neurologic symptoms. The patients were screened for cryptococcus infection because of the presence of pulmonary cavitory nodules, which were regarded as common lesions of HIV-associated pulmonary cryptococcosis (16). As mannitol was not used, these four patients were excluded from analysis. The remaining 33 symptomatic patients with headaches who had received at least one dosage of mannitol were included in the case-referent analysis, including one patient with coexisting tuberculosis meningitis. At admission, 69.7% (23/33) of the patients also had fever and 30.3% (10/33) of the patients had seizures or confusion.

Of the 33 studied patients, 26 were men; median age was 34 years (range, 12-71 years); median body weight was 54.5 kg (range, 30-71 kg); median CD4 cell count was 16 cells/ μ L (range, 2-280 cells/ μ L), and 87.9% (29/33) of the patients had CD4 count less than 100 cells/ μ L. Eight patients were on anti-retroviral therapy (ART) for a median of 2.3 months (range, 25 days to 25 months) at the time of CM confirmation. Virologic failure was confirmed in two patients who had received ART for 12 months and 25 months, respectively. Short courses of corticosteroids (about 2 weeks) were used in 4 patients that newly initiated ART. One patient on ART with suppressed HIV viral load received corticosteroids due to coexisting tuberculosis meningitis and CM.

For the baseline CSF parameters, the median CSF opening pressure was 230 mm H₂O (range, 60-900 mmH₂O); median white cell count was 6 cells/ μ L (range, 1-56 cells/ μ L); median sugar level was 2.6 mmol/L (range, 0.4-4.3 mmol/L); median protein level was 418.7mg/L (range, 171.2-993 mg/L).

3.2. Patients' outcome and mannitol administration

After initiation of anti-cryptococcal therapy, the survival rates at 2 weeks and 10 weeks were 93.9% (31/33) and 90.9% (30/33), respectively. One patient had permanent vision loss. Of the 3 patients that died within 10 weeks, 1 patient died of respiratory failure 4 days after the diagnosis of CM, 1 patient gave up therapy after 10 days' anti-cryptococcal therapy and the other patient developed brain herniation after a lumbar puncture when she had received anti-cryptococcal therapy for about 2 weeks. That patient with brain herniation survived another 2 weeks with her respiration controlled by a

ventilator. Of the 30 patients that survived more than 10 weeks, one patient received closed continuous lumbar drainage of CSF after 52 days' anti-cryptococcal therapy, and he died 86 days later due to neurological damages. Taken together, 87.9% (29/33) patients recovered from acute stage of CM without the need of therapeutic serial lumbar punctures or surgical interventions such as ventriculoperitoneal shunt. Mannitol was used for median of 26 days (range, 1-85 days) in these 29 patients.

The median daily dosage of mannitol at the starting of anti-cryptococcal therapy was 4 times (range, 1-12 times). To maximally limit the frequency of headache or seizure, varying dosages of mannitol were added (Figure 1). Overall, 54.5% (18/33) of the patients had at least once received more than 4 times of mannitol administration in a day during hospitalization. Two weeks after the initiation of anti-cryptococcal therapy, 66.7% (22/33) of the patients' condition was stabilized that no more than 4 times of mannitol was administered every day and there was no increase of mannitol dosage thereafter (Figure 1). Nevertheless, 18.2% (6/33) of the patients still need 7 times or more mannitol administration, of whom 33% (2/6) finally died of CM.

With the empirical mannitol therapy, patients still had a median of 2 episodes (range, 1-6 episodes) of headaches the day at the starting of anti-cryptococcal therapy. The median score of pain intensity assessed by numerical rating scales was 7-point (range, 4-8 points). Fifteen minutes after the finish of mannitol administration, the score of pain intensity was reduced to 3-point or less. After 1 week's anti-cryptococcal therapy, 36.4% (12/33) of the patients did not report

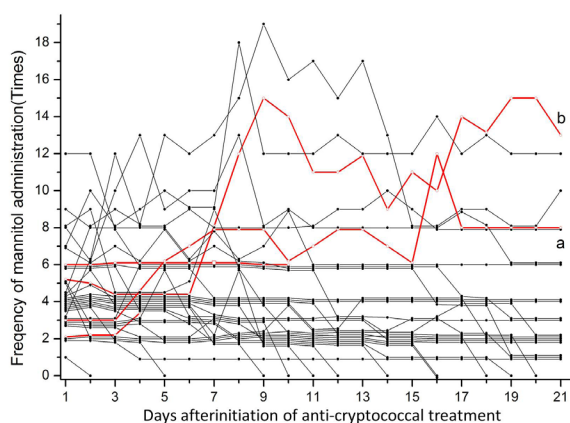


Figure 1. Dynamic of mannitol dosages after initiation of anti-cryptococcal therapy. To maximally limit the frequency of neurologic symptoms such as headache and seizures, varying dosages of mannitol were administered. Of the 4 patients (marked with red color) that were not saved by mannitol treatment, 2 patients died within 2 weeks of anti-cryptococcal therapy, 1 patient (a) developed cerebral herniation after having received anti-cryptococcal therapy for about 2 weeks and died 2 weeks later, and 1 patient (b) finally received closed continuous lumbar drainage of CSF after 52 days of anti-cryptococcal therapy and died 86 days later. In this figure, overlapped points were displayed with Y offset by manually changing the Y values.

headaches. After 3 weeks' anti-cryptococcal therapy, 75.8% (25/33) of the patients did not report headaches.

During the initial 3 weeks of anti-cryptococcal therapy, 13 patients had a total of 42 episodes of seizures (median 3 episodes; range, 1-10 episodes), accompanied by loss of consciousness. 97.6% (41/42) of the episodes of seizures were controlled after the administration of mannitol. Sudden cardiopulmonary arrest occurred after one episode of seizure that mannitol treatment was considered unsuccessful. This patient with suspected brain herniation survived another 2 weeks with her respiration controlled by a ventilator, as above mentioned. At the time of starting anti-cryptococcal therapy, 6 patients had different degrees of confusion. The mental status gradually recovered in 5 of those 6 patients after a median of 5 days (range, 2 to 14 days), however, mental status in one patient continued to progress even though he was aggressively treated with mannitol. After 10 days' anti-cryptococcal therapy, the patient, who had become unconsciousness for 1 day, gave up therapy and was considered to be dead.

3.3. Monitoring of laboratory parameters

Hyponatremia, defined as serum sodium level of less than 135 mmol/L, was detected at least once in 72.7% (24/33), 43.8% (14/32) and 32.3% (10/31) of the patients during the first, second and third week, respectively. Serum sodium level of less than 130 mmol/L was detected at least once in 36.4% (12/33), 25% (8/32) and 12.9% of the patients during the first, second and third week, respectively. Serum sodium level of less than 125 mmol/L was detected at least once in 9.1% (3/33), 9.4% (3/32) and 3.2% (1/31) of the patients during the first, second and third week, respectively.

Hypokalemia, defined as serum potassium level of less than 3.5 mmol/L, was detected at least once in 18.2% (6/33), 21.9% (7/32) and 45.2% (14/31) of the patients during the first, second and third week after the initiation of anti-cryptococcal therapy, respectively. Serum potassium level of less than 3.0 mmol/L was detected at least once in 3.0% (1/33), 3.1% (1/32) and 12.9% (4/31) of the patients during the first, second and third week after the initiation of anti-cryptococcal therapy, respectively. Serum potassium level of less than 2.5 mmol/L was only seen in one patient during the third week. During the initial 3 weeks of anti-cryptococcal therapy, elevated serum blood urea nitrogen (BUN) level (more than 8.3 $\mu\text{mol/L}$) and/or elevated serum creatinine level (more than 97 $\mu\text{mol/L}$) was detected at least once in 18.2% (6/33) and 12.1% (4/33) of the patients, respectively. None of the patients had a serum creatinine level exceeding 220 $\mu\text{mol/L}$ during hospitalization.

4. Discussion

Elevated ICP often leads to developing neurological

symptoms such as headache, altered mental status, and coma (2). Higher pretreatment ICP in HIV-associated CM is associated decreased short-term survival (7). Lumbar puncture drainage is an effective strategy to reduce the ICP and it also helps to remove fungal elements (7). There are accumulated evidences that therapeutic lumbar puncture in HIV associated CM is associated with improvement in survival, and non-adherence to this strategy may in part lead to neurological injury (14,17,18). Despite of survival benefit, therapeutic lumbar puncture is not performed in some patients, which may be due to limited awareness of the importance of ICP management (7,17,18).

In our clinical center, for the following reasons, mannitol is routinely used to manage neurological symptoms associated with CM in HIV-infected patients. At first, Mannitol is used to manage elevated ICP in various conditions such as bacterial meningitis, tuberculosis meningitis, and brain injury (11,19-21). In China, mannitol administration is still one of the recommended choices for the management of HIV-associated CM based on expert opinions (22). Finally, there is still lack of physicians to manage HIV-infected patients in our center. It is not possible to perform a lumbar puncture drainage whenever the patient has a headache episode, especially at night or during the weekend. Our study suggests that mannitol administration may be efficacious to relieve headaches and perhaps seizures associated with CM. With anti-cryptococcal therapy and adjunctive mannitol therapy for symptom control, 87.9% (29/33) of the patients survived more than 10 weeks without the need of therapeutic CSF drainage. The prognosis seems to be not bad as compared to a recently well-controlled clinical trial performed in Asian population (23). This is the most important reason why mannitol is still being used in our clinical center to managing neurological symptoms associated with CM. It should be noted that varying dosages of mannitol were needed to control neurological symptoms (Figure 1). This may reflect different extent of CSF reabsorption impairment due to accumulation of cryptococcal elements in the arachnoid granulations. 54.5% (18/33) of the patients had at least once received more than 4 times of mannitol administration in a day during hospitalization. Patients with pre-exist cardiac diseases may not tolerate frequent intravenous mannitol injection. Massive administration of mannitol warrants more frequent monitoring of renal function and electrolytes.

The findings in our study have several clinical implications. Firstly, although capable to reduce ICP, repeated lumbar punctures are not always effective to relieve headaches, and may even increase headaches in a minority of patients (7). In this condition, mannitol administration may be a possible choice to relieve headaches. Secondly, compared with therapeutic lumbar puncture, mannitol therapy is relatively less invasive and easier to perform. For patients not willing to receive

lumbar puncture, especially those with mild neurologic symptoms, mannitol may be used to relieve headaches. Finally, mannitol may be a choice in settings where therapeutic lumbar puncture is unavailable.

This study was limited by relatively small sample size with retrospective nature and no control was included. In our study, during the first 1 to 2 weeks, 1-2 mg dexamethasone was added to amphotericin B to reduce the infusion-related toxicities of amphotericin B. A recent study showed that dexamethasone is harmful in HIV-associated CM (24). Nevertheless, the dose of dexamethasone in our clinical practice was very small and the duration was relatively short, therefore in our opinion, the negative effects of dexamethasone were negligible. The causes of the laboratory abnormalities in our study were multifactorial. Both mannitol and amphotericin B may induce renal damage and electrolyte disturbance. Poor appetite and vomiting associated with CM may also contribute to electrolyte disturbance. Although the prognosis of patients receiving mannitol administration as a symptom control strategy seems not to be greatly impaired in our studied patients, it should not be regarded as that mannitol is as effective as standard therapeutic lumbar puncture drainage. For the patients that need massive mannitol administration, they would better receive therapeutic lumbar puncture drainage or perhaps ventriculoperitoneal shunting (25), although this was not performed in our patients. Of note, adult human produces 500-600 mL CSF every day (26), while usually less than 30 mL CSF is removed by a lumbar puncture drainage (14). If one lumbar puncture is performed each day, 94-95% of the CSF still needs to be reabsorbed by meninge. It suggests that for most of the patients with CM, CSF outflow obstruction may be not severe. Perhaps, only in this condition, mannitol administration would not severely impair the outcome of HIV-associated CM.

In conclusion, although it is not known whether mannitol could reduce the ICP in HIV-associated CM, mannitol administration may be used to relieve neurologic symptoms in HIV-associated CM. Of great interesting, the prognosis of patients receiving mannitol administration as a symptom control strategy seems not to be greatly impaired. It is worth re-evaluating the role of mannitol administration as a symptom control strategy in mild cases of HIV-associated CM.

Acknowledgements

This work is supported by clinical special grant BL-2013003 from Department of Science and Technique, Jiangsu.

References

1. Park BJ, Wannemuehler KA, Marston BJ, Govender N, Pappas PG, Chiller TM. Estimation of the current global

- burden of cryptococcal meningitis among persons living with HIV/AIDS. *Aids*. 2009; 23:525-530.
2. Abassi M, Boulware DR, Rhein J. Cryptococcal Meningitis: Diagnosis and Management Update. *Curr Trop Med Rep*. 2015; 2:90-99.
 3. Pappas PG. Managing cryptococcal meningitis is about handling the pressure. *Clin Infect Dis*. 2005; 40:480-482.
 4. Bratton EW, El Husseini N, Chastain CA, Lee MS, Poole C, Sturmer T, Juliano JJ, Weber DJ, Perfect JR. Comparison and temporal trends of three groups with cryptococcosis: HIV-infected, solid organ transplant, and HIV-negative/non-transplant. *PLoS One*. 2012; 7:e43582.
 5. Heyderman RS, Gangaidzo IT, Hakim JG, Mielke J, Taziwa A, Musvaire P, Robertson VJ, Mason PR. Cryptococcal meningitis in human immunodeficiency virus-infected patients in Harare, Zimbabwe. *Clin Infect Dis*. 1998; 26:284-289.
 6. Loyse A, Wainwright H, Jarvis JN, Bicanic T, Rebe K, Meintjes G, Harrison TS. Histopathology of the arachnoid granulations and brain in HIV-associated cryptococcal meningitis: Correlation with cerebrospinal fluid pressure. *AIDS*. 2010; 24:405-410.
 7. Graybill JR, Sobel J, Saag M, van Der Horst C, Powderly W, Cloud G, Riser L, Hamill R, Dismukes W. Diagnosis and management of increased intracranial pressure in patients with AIDS and cryptococcal meningitis. The NIAID Mycoses Study Group and AIDS Cooperative Treatment Groups. *Clin Infect Dis*. 2000; 30:47-54.
 8. Govender N, Meintjes G, Bicanic T, Dawood H, Harrison T, Jarvis J, Karstaedt A, Maartens G, McCarthy K, Rabie H. Guideline for the prevention, diagnosis and management of cryptococcal meningitis among HIV-infected persons: 2013 update. *S Afr J HIV Med*. 2013; 14:76-86.
 9. Perfect JR, Dismukes WE, Dromer F, Goldman DL, Graybill JR, Hamill RJ, Harrison TS, Larsen RA, Lortholary O, Nguyen MH, Pappas PG, Powderly WG, Singh N, Sobel JD, Sorrell TC. Clinical practice guidelines for the management of cryptococcal disease: 2010 update by the infectious diseases society of america. *Clin Infect Dis*. 2010; 50:291-322.
 10. Pappas PG. Editorial commentary: An expanded role for therapeutic lumbar punctures in newly diagnosed AIDS-associated cryptococcal meningitis? *Clin Infect Dis*. 2014; 59:1615-1617.
 11. Glimaker M, Johansson B, Halldorsdottir H, Wanecek M, Elmi-Terander A, Ghatan PH, Lindquist L, Bellander BM. Neuro-intensive treatment targeting intracranial hypertension improves outcome in severe bacterial meningitis: An intervention-control study. *PLoS One*. 2014; 9:e91976.
 12. Lescot T, Abdennour L, Boch AL, Puybasset L. Treatment of intracranial hypertension. *Curr Opin Crit Care*. 2008; 14:129-134.
 13. Hays AN, Lazaridis C, Neyens R, Nicholas J, Gay S, Chalela JA. Osmotherapy: Use among neurointensivists. *Neurocrit Care*. 2011; 14:222-228.
 14. Meda J, Kalluvya S, Downs JA, Chofle AA, Seni J, Kidenya B, Fitzgerald DW, Peck RN. Cryptococcal meningitis management in Tanzania with strict schedule of serial lumbar punctures using intravenous tubing sets: An operational research study. *J Acquir Immune Defic Syndr*. 2014; 66:e31-36.
 15. Hjermstad MJ, Fayers PM, Haugen DF, Caraceni A, Hanks GW, Loge JH, Fainsinger R, Aass N, Kaasa S, European Palliative Care Research C. Studies comparing Numerical Rating Scales, Verbal Rating Scales, and Visual Analogue Scales for assessment of pain intensity in adults: A systematic literature review. *J Pain Symptom Manage*. 2011; 41:1073-1093.
 16. Hu Z, Xu C, Wei H, Zhong Y, Bo C, Chi Y, Cheng C, Yang Y. Solitary cavitary pulmonary nodule may be a common CT finding in AIDS-associated pulmonary cryptococcosis. *Scand J Infect Dis*. 2013; 45:378-389.
 17. Rolfes MA, Hullsiek KH, Rhein J, Nabeta HW, Taseera K, Schutz C, Musubire A, Rajasingham R, Williams DA, Thienemann F, Muzoora C, Meintjes G, Meya DB, Boulware DR. The effect of therapeutic lumbar punctures on acute mortality from cryptococcal meningitis. *Clin Infect Dis*. 2014; 59:1607-1614.
 18. Shoham S, Cover C, Donegan N, Fulnecky E, Kumar P. *Cryptococcus neoformans* meningitis at 2 hospitals in Washington, D.C.: Adherence of health care providers to published practice guidelines for the management of cryptococcal disease. *Clin Infect Dis*. 2005; 40:477-479.
 19. Murthy JM. Management of intracranial pressure in tuberculous meningitis. *Neurocrit Care*. 2005; 2:306-312.
 20. Francony G, Fauvage B, Falcon D, Canet C, Dilou H, Lavagne P, Jacquot C, Payen JF. Equimolar doses of mannitol and hypertonic saline in the treatment of increased intracranial pressure. *Crit Care Med*. 2008; 36:795-800.
 21. Battison C, Andrews PJ, Graham C, Petty T. Randomized, controlled trial on the effect of a 20% mannitol solution and a 7.5% saline/6% dextran solution on increased intracranial pressure after brain injury. *Crit Care Med*. 2005; 33:196-202; discussion 257-198.
 22. AIDS Group SoID, Chinese Medical Association. Guideline of diagnosis and treatment of AIDS. *Chin J Clin Infect Dis*. 2011; 4:321-330.
 23. Day JN, Chau TT, Wolbers M, *et al*. Combination antifungal therapy for cryptococcal meningitis. *N Engl J Med*. 2013; 368:1291-1302.
 24. Beardsley J, Wolbers M, Kibengo FM, *et al*. Adjunctive Dexamethasone in HIV-Associated Cryptococcal Meningitis. *N Engl J Med*. 2016; 374:542-554.
 25. Liu L, Zhang R, Tang Y, Lu H. The use of ventriculoperitoneal shunts for uncontrollable intracranial hypertension in patients with HIV-associated cryptococcal meningitis with or without hydrocephalus. *Biosci Trends*. 2014; 8:327-332.
 26. Johanson CE, Duncan JA, 3rd, Klinge PM, Brinker T, Stopa EG, Silverberg GD. Multiplicity of cerebrospinal fluid functions: New challenges in health and disease. *Cerebrospinal Fluid Res*. 2008; 5:10.

(Received August 27, 2016; Revised September 28, 2016; Accepted October 5, 2016)

A newborn with hemorrhagic meningoencephalitis due to *Proteus mirabilis*

Yesim Coskun^{1*}, Ipek Akman¹, Canan Yildirim¹, Mustafa Kemal Demir²

¹Department of Pediatrics, Goztepe Medicalpark Hospital, Bahcesehir University School of Medicine, Istanbul, Turkey;

²Department of Radiology, Goztepe Medicalpark Hospital, Bahcesehir University School of Medicine, Istanbul, Turkey.

Summary Neonatal meningoencephalitis is a severe condition for the developing brain of a newborn. Radiologic findings of necrosis and liquefaction due to hemorrhagic meningoencephalitis may be confused with brain abscess. In this article, we report a neonate having liquefaction necrosis due to hemorrhagic meningoencephalitis mimicing intracranial abscess due to *Proteus mirabilis*. We would like to describe the clinical course and evolution of brain imaging and emphasize the importance of the serial MR imaging (MRI).

Keywords: Brain abscess, hemorrhagic meningoencephalitis, newborn, serial MR imaging

1. Introduction

Although *Proteus mirabilis* is a common cause of urinary tract infections, it has been reported that approximately 4% of neonatal meningitis may be caused by this microorganism and it also can cause hemorrhagic meningoencephalitis. Group B streptococcus and *Escherichia coli* are the most common causes of meningoencephalitis in the neonatal period. *Serratia marcescens* and *Citrobacter* may be considered a causal microorganism in cases of hemorrhagic meningoencephalitis. Necrosis and liquefaction are the complications of the hemorrhagic meningoencephalitis. The differential diagnosis of the brain abscess and the liquefaction necrosis should be done by serial magnetic resonance imaging (MRI).

In this article, we report a newborn with hemorrhagic meningoencephalitis due to *Proteus mirabilis*, whose cranial MRI findings mimic brain abscess. The authors also emphasize the importance of early and serial brain MRI for the differential diagnosis of brain abscess and sequelea of hemorrhagic meningoencephalitis.

2. Case Report

A 6-day old female was admitted to the emergency room for grunting for 2 days and poor feeding on the morning of the admission.

The baby was born full term by Caesareal section as the first child of 34-year-old mother. Her mother had no history of radiation exposure, drug ingestion, alcohol use, smoking during pregnancy, family history was unremarkable for congenital anomalies and there was no consanguinity. On the second day of the birth she was discharged from the hospital.

On presentation to the hospital, her body temperature was 36.3°C, with blood pressure of 65/40 mmHg, heart rate of 138 beats per minute, and respiratory rate of 64 breaths per minute. On physical exam, she was hypotonic, she had depressed reflexes and poor sucking and swallowing reflexes. Capillary refill time was 5 seconds. Her anterior fontanelle was soft and nonbulging. Her breath sounds were equal, she had grunting, nasal flaring, tachypnea, subcostal retraction, central cyanosis and the other system findings were normal. Laboratory data on admission showed a white blood cell count of 17.770 cell/ μ L with 72.4% neutrophils, the hemoglobin was 13.9 g/dL and platelet count was 187.000 cell/ μ L. C-reactive protein was 12.36 mg/dL (N:0-8.2 mg/dL). Cerebrospinal fluid (CSF) had glucose of < 5 mg/dL, protein of 299.9 mg/dL and 6,500 leucocytes. Gram stain of the CSF showed no bacteria. At 24 hours, the blood culture grew *Proteus mirabilis*, but the CSF culture, the urine culture and the endotracheal aspirate culture had no growth of

Released online in J-STAGE as advance publication December 18, 2016.

*Address correspondence to:

Dr. Yesim Coskun, Department of Pediatrics, Goztepe Medicalpark Hospital, Bahcesehir University School of Medicine, E5 uzeri 23 Nisan sokak N0:17 34732 Merdivenkoy/Goztepe, Istanbul, Turkey.

E-mail: coskunyesim@yahoo.com

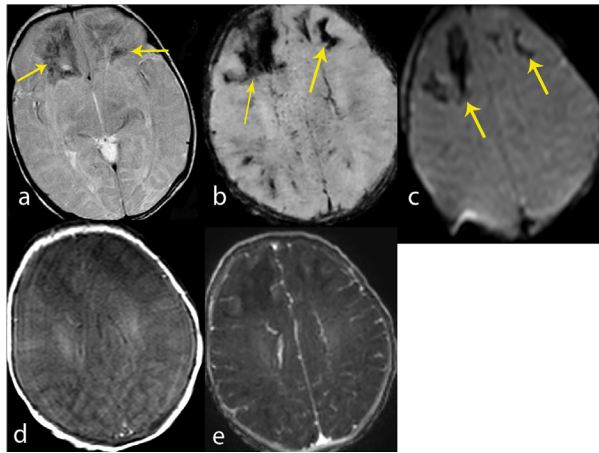


Figure 1. Acute phase of the proteus mirabilis hemorrhagic meningoencephalitis MRI findings. Axial T2W1 (a), SWI (b) and DWI (c) show dark signal intensities suggestive of hemorrhages within the frontal lobes (arrows). Unenhanced axial T1W1 (d) demonstrates hypointense signals in the frontal lobes with sulcal effacement. Contrast-enhanced axial T1W1 (e) shows diffuse leptomeningeal enhancement.

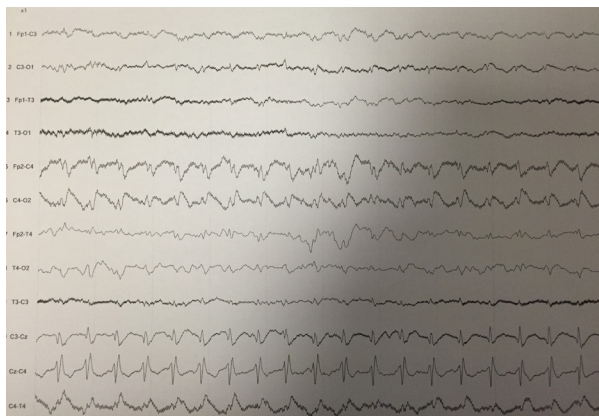


Figure 2. Electroencephalogram (EEG) findings. Background activity disorganization and epileptic activity in the central region.

bacteria.

Upon admission, patient was started on ampicilline and amicasin. While following up on continuous positive airway pressure (CPAP) mode, the blood gases revealed hypercarbia and respiratory acidosis. At the second hour of the admission, she was intubated because of respiratory failure. One hour later the patient had multifocal clonic seizure. The seizure was controlled with midazolam and phenobarbital. Her antibiotics were switched to vancomycine and meropenem. Acyclovir was added because the patients' mother had a herpes lesion on her lip. Blood and urine samples collected for metabolic disease screening. Cranial MRI findings showed acute phase of the *Proteus mirabilis* hemorrhagic meningoencephalitis. It showed dark signal intensities suggestive of hemorrhages within the frontal lobes, hypointense signals in the frontal lobes with sulcal effacement and diffuse leptomeningeal enhancement (Figure 1).

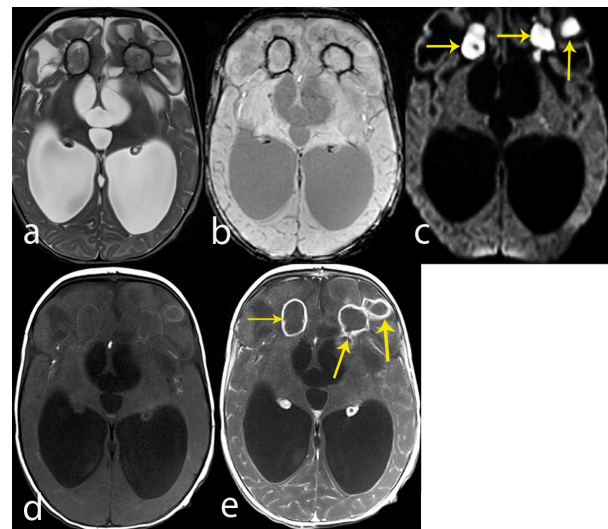


Figure 3. Intermediate phase of the proteus mirabilis hemorrhagic meningoencephalitis MRI findings. Axial T2W1 (a) and SWI (b) demonstrate severe hydrocephalus and subcortical white matter lesions that have peripheral hemosiderin deposits and central liquefactive necrosis within the atrophic frontal lobes. These lesions show high signals on DWI due to marked restricted diffusion (arrows) (c). They show peripheral high signals and central low signals on unenhanced axial T1W1 (d), and marked peripheral enhancement on contrast-enhanced axial T1W1 (arrows) (e). There is also ependymal and periventricular enhancement.

The electroencephalogram (EEG) findings showed background activity disorganization and epileptic activity in the central region (Figure 2). She was treated with antibioteraphy for 21 days for neonatal sepsis and meningitis. During the follow up she needed mechanical ventilaton for 11 days. On the 10th day of the treatment, she reached to full enteral feeding. According to the cranial ultrasound (USG) she didn't have hydrocephalus. EEG was normal at the second week of admission. At the 23th of her admission, she was discharged from the hospital with phenobarbital therapy. Two weeks after the discharge, she was feeding well and had a stable clinical course other than the rapidly increasing head circumference. A cranial MRI was performed when she was 1.5 months old. The cranial MRI findings showed the intermediate phase of the proteus mirabilis hemorrhagic meningoencephalitis. It demonstrated severe hydrocephalus and subcortical white matter lesions that have peripheral hemosiderin deposits and central liquefactive necrosis within the atrophic frontal lobes and ependymal and periventricular enhancement (Figure 3). In the differential diagnosis brain abscess couldn't be ruled out, CSF tap was performed. CSF had glucose of 24 mg/dL, protein of 730 mg/dL and no cells were seen. Gram strain of the CSF showed no bacteria. Vancomycine and meropenem was started untill the CSF culture was obtained as sterile for 7 days. With her physical examination, the cranial MRI findings and the sterile CSF culture, brain abscess was ruled out. During her follow ups, her head circumference increased 1 cm in 3 days. Her neurological examination showed

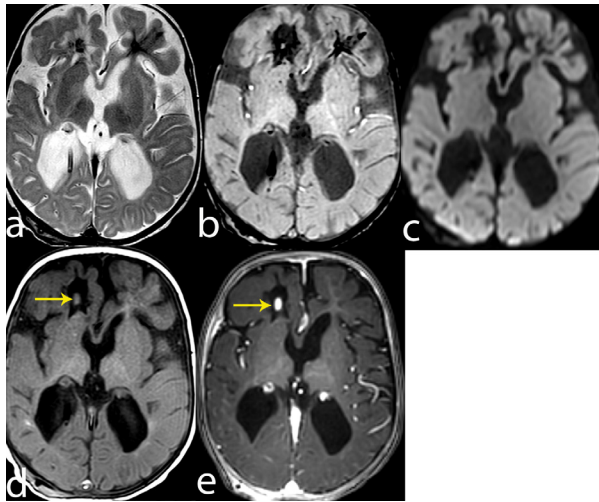


Figure 4. Late phase of the proteus mirabilis hemorrhagic meningoencephalitis MRI findings. Axial T2W1 (a) and SWI (b) demonstrate severe cerebral atrophy and encephalomalacia that contain chronic hemorrhagic signals in the frontal lobes. There is no restricted diffusion on DWI (c). Encephalomalacia on right frontal lobe contains a central hyperintensity on TIWI (arrow) (d) and shows only a nodular enhancement contrast-enhanced image due to regression (arrow) (e).

limited eye tracking, strabismus, axial hypotonia, increased deep tendon reflexes and clonus bilaterally. So ventriculoperitoneal shunt (VPS) placement was performed for her hydrocephalus when she was 69 days old. After VPS placement her head circumference remained stable and her neurological examination findings improved. Increased eye tracking, head control, decreased strabismus and mild hemiparesis were seen. When she was 4 months old, one more time cranial MRI was repeated to check the changes of the crainal pathology. The cranial MRI showed the late phase of the proteus mirabilis hemorrhagic meningoencephalitis. It demonstrated cerebral atrophy and encephalomalacia that contain chronic hemorrhagic signals in the frontal cerebral atrophy and encephalomalacia that contain chronic hemorrhagic signals in the frontal lobes (Figure 4).

3. Discussion

Neonatal sepsis is an important cause of mortality and morbidity among infants, with a incidence of culture-proven early-onset neonatal sepsis in the United States is estimated to be 0.77 to 1 per 1,000 live births (1). Acute bacterial meningitis is more frequent in the neonatal period than in any other time of life due to immaturity of humoral and cellular immunity, with the incidence of 0.8 and 6.1 cases every 1,000 live births (2,3). The absence of specific clinical sign and symptoms makes the diagnosis of neonatal meningitis more difficult (4). Brain abcess is a rare disorder in neonates (5). It is most commonly located periventricularly in the white matter of the frontal or

parieto-occipital region. In the neonatal period bacterial meningitis is commonly caused by group B streptococci and *Escherichia coli* and rarely complicated by the brain abscess, however bacterial meningitis due to infections with *Proteus* species, *Citrobacter diversus*, *Enterobacter sakazakii* and *S. marcescens* often complicated by intracranial abscess formation in up to 13% of cases (6,7). *Proteus mirabilis* is a non-lactose fermenting gram-negative bacillus. There are several species of *Proteus*, but *Proteus mirabilis* and *Proteus vulgaris* are more common among clinical isolates. It is the causative organism of urinary tract infections, osteomyelitis, mastoiditis and wound infection as well as neonatal gram-negative meningitis with an incidence of 4% (8). As a complication, intracranial abscess has an increased risk of neurologic sequelae, developmental delay, visual and audologic impairment or death (9).

Cranial imaging in neonates with meningitis is not routine, it is usually performed for complications. Each causitive organism for the neonatal meningitis has identifiable patterns of complications on MRI. Recognition of these patterns can help the radiologist propose the possible diagnosis and helps the clinician for the early management (10). Neuroimaging findings in pyogenic meningitis shows leptomeningeal enhancement as the most common finding present in 57% of the cases (11). Vasculitic infarcts, hydrocephalus and abscess formation are other common findings. Jaremko *et al.* reported that, during culture positive menengitis, 35% of patients had subdural collection, 32% patients had ventriculomegaly, 19% had ventriculitis and overall 86% had some parenchymal abnormality, including edema 43%, infarction 52%, parenchymal abscess 13%, hemorrhage 24% and sinus thrombosis 6% (9). In our patient, in the first cranial MRI (hemorrhagic phase) which was the early period MRI, dark signal intensities suggestive of hemorrhagies within the frontal lobes, hypointense signals in the frontal lobes with sulcal effacement and diffuse leptomeningeal enhancement was detected. The hemorrhagic focuses and ischemic areas were thought as the result of sepsis and septic trombus however the differential diagnosis was suggestive of hemorrhagic meningoencephalitis. In the second cranial MRI (liquefaction abscess phase) which was the intermediate phase, severe hydrocephalus and subcortical white matter lesions that have peripheral hemosiderin deposits and central liquefactive necrosis within the atrophic frontal lobes and ependymal and periventricular enhancement were detected. The necrosis and liquefaction areas in the frontal lobes seen in the second cranial MRI which look like the lessions seen in brain abscess was due to hemorrhagic meningoencephalitis. The third cranial MRI (encephalomalacia phase) which was taken during the late period, showed cerebral atrophy and encephalomalacia that contain chronic hemorrhagic signals in the frontal lobes. These findings revealed

the same lesions as the sequelae of the hemorrhagic meningoencephalitis.

In conclusion, *P. mirabilis* can cause liquefaction necrosis on the late-onset of severe hemorrhagic meningoencephalitis. We emphasize the importance of early and serial brain MRI imaging in neonates. In our opinion, cranial MRI is the imaging modality of choice in infants with the diseases of the central nervous system especially in the differential diagnosis of brain abscess and sequelae of hemorrhagic meningoencephalitis.

References

1. Simonsen KA, Anderson-Berry AL, Delair SF, Davies HD. Early-onset neonatal sepsis. *Clin Microbiol Rev.* 2014; 27:21-47.
2. De Louvois J. Acute bacterial meningitis in the newborn. *J Antimicrob Chemother.* 1994; 34:61-73.
3. Thaver D, Zaidi AK. Burden of neonatal infections in developing countries: A review of evidence from community-based studies. *Pediatr Infect Dis J.* 2009; 28:3-9.
4. Baud O, Aujard Y. Neonatal bacterial meningitis. *Handb Clin Neurol.* 2013; 112:1109-1113.
5. Obana WG, Cogen PH, Callen PW, Edwards MSB. Ultrasound-guided aspiration of a neonatal brain abscess. *Child's Nerv Syst.* 1991; 7:272-274.
6. Ries M, Deeg KH, Heininger U, Stehr K. Brain abscesses in neonates-report of three cases. *Eur J Pediatr.* 1993; 152:745-746.
7. Pong A, Bradley JS. Bacterial meningitis and the newborn infant. *Infect Dis Clin North Am.* 1999 ;13:711-733.
8. Phan H, Lehman D. Cerebral abscess complicating *Proteus mirabilis* meningitis in a newborn infant. *J Child Neurol.* 2012; 27:405-407.
9. Jaremko JL, Moon AS, Kumbla S. Patterns of complications of neonatal and infant meningitis on MRI by organism: A 10 year review. *Eur J Radiol.* 2011; 80:821-827.
10. Oliveira CR, Morriss MC, Mistrot JG, Cantey JB, Doern CD, Sanchez PJ. Brain magnetic resonance imaging of infants with bacterial meningitis. *J Pediatr.* 2014; 165:134-139.
11. Oliveira CR, Morriss MC, Mistrot JG, Cantey JB, Doern CD, Sánchez PJ. Brain magnetic resonance imaging of infants with bacterial meningitis. *J Pediatr.* 2014; 165:134-139.

(Received October 17, 2016; Revised December 1, 2016; Accepted December 11, 2016)

Biotin treatment causing erroneous immunoassay results: A word of caution for clinicians

Raashda Ainuddin Sulaiman^{1,2,*}

¹Department of Medical Genetics, King Faisal Specialist Hospital and Research center, Riyadh, Saudi Arabia;

²College of Medicine, Alfaisal University, Riyadh, Saudi Arabia.

Summary Biotin or vitamin B7 when ingested in high doses may cause immunoassay interference leading to false potentially misleading results. It is important that clinicians should always interpret laboratory results in the context of patient's clinical state as erroneous results may lead to misdiagnosis and injudicious treatment with adverse patient outcome.

Keywords: Biotin, immunoassay interference, erroneous results

Knowledge of biotin induced immunoassay interference is crucial for clinicians as not only biotin is used to treat certain inherited metabolic disorders and multiple sclerosis, it is also widely consumed as nutritional supplement. We recently had experience of erroneous thyroid function test (TFT) results in three adult patients receiving high doses of biotin (1-10 mg/kg body weight daily) to treat their inherited metabolic disorders. Two patients with biotin responsive basal ganglia disease had depression which triggered the request for TFT (1). Another patient with biotinidase deficiency brought in abnormal TFT results performed in another hospital. Although these patients were clinically euthyroid, their TFT persistently showed high free thyroxine (FT4): 26-56 nmol/L, (12-22 nmol/L), high free triiodothyronine (FT3): 5.2-7.8 nmol/L (1.3-3.1 nmol/L) with variable thyroid stimulating hormone (TSH) concentrations 0.03-0.24 mU/L (0.27-4.2 mU/L). One patient had high thyrotropin receptor antibody (TRAb) titer 30 IU/L (< 1.75 IU/L) as well. Subsequent Iodine-123 thyroid scan was normal in all patients. Discordance in laboratory results and clinical picture, as well as in physiologically dependent variables FT4, TSH, strongly suggested immunoassay interference. Blood samples were tested on Roche Modular Cobas 602 which uses biotin-streptavidin capture in immunoassay. Subsequent testing of samples on Abbott Architect I-2000 analyzer which does not use biotin-streptavidin capture,

showed normal FT4, FT3 and TSH results, confirming biotin induced immunoassay interference in Roche method. Since biotin is a water soluble vitamin and is rapidly cleared from the body, we repeated TFT of one patient 13 hours after the last dose of biotin, on Roche platform. There were significant changes in TFT as FT4 and TSH were normalized to 18.5 nmol/L and 0.51 mU/L respectively.

Biotin or vitamin B7 acts as a coenzyme for different carboxylases involved in gluconeogenesis, fatty acid synthesis and in certain amino acid catabolism. High concentration of biotin in blood interferes with the immunoassays which rely on the biotin streptavidin interaction as an immobilizing system (2). Henry *et al.* first described biotin interference in immunoassay yielding erroneous TSH and FT4 results of a newborn who was on biotin supplement (3). Biotin interference gives falsely high or low results in competitive or immunometric immunoassay respectively (4). It may cause falsely raised thyrotropin receptor antibodies (TRAb) as seen in one of our patients. This could lead to a misdiagnosis of Graves' disease. Biotin also interferes with the measurement of testosterone, oestradiol, dehydroepiandrosterone-sulfate (DHEAS), parathyroid hormone, ferritin and thyroglobulin, testosterone, thyroglobulin, leutinizing hormone (LH), follicle stimulating hormone (FSH), sex hormone binding globulin (SHBG), vitamin B12 and folate (4).

Clinicians should always interpret laboratory results in the context of patient's clinical state. A high index of clinical suspicion and good collaboration with the laboratory is essential to prevent and detect erroneous results which could otherwise lead to misdiagnosis, unnecessary, expensive additional laboratory and clinical

*Address correspondence to:

Dr. Raashda A Sulaiman, Department of Medical Genetics, MBC 75 King Faisal Specialist Hospital and Research Centre, PO Box No: 3354, Riyadh, 11211, Saudi Arabia.
E-mail: rsulaiman@kfshrc.edu.sa

investigations in addition to injudicious treatment with adverse patient outcome.

Acknowledgements

I am thankful to Ms Mariam Alfares, supervisor biochemistry laboratory at KFSHRC, Riyadh for organizing sample testing on different platform.

References

1. Bubshait DK, Rashid A, Al-Owain MA, Sulaiman RA. Depression in adult patients with biotin responsive basal ganglia disease. *Drug Discov Ther.* 2016; 10:223-225.
2. Kwok JS, Chan IH, Chan MH. Biotin interference on TSH and free thyroid hormone measurement. *Pathology.* 2012; 44:278-280.
3. Henry JG, Sobki S, Arafat N. Interference by biotin therapy on measurement of TSH and FT4 by enzyme immunoassay on Boehringer Mannheim ES700 analyser. *Ann Clin Biochem.* 1996; 33:162-163.
4. Wijeratne NG, Doery JC, Lu ZX. Positive and negative interference in immunoassays following biotin ingestion: a pharmacokinetic study. *Pathology.* 2012; 44:674-675.

(Received November 27, 2016; Accepted December 25, 2016)

Guide for Authors

1. Scope of Articles

Drug Discoveries & Therapeutics welcomes contributions in all fields of pharmaceutical and therapeutic research such as medicinal chemistry, pharmacology, pharmaceutical analysis, pharmaceuticals, pharmaceutical administration, and experimental and clinical studies of effects, mechanisms, or uses of various treatments. Studies in drug-related fields such as biology, biochemistry, physiology, microbiology, and immunology are also within the scope of this journal.

2. Submission Types

Original Articles should be well-documented, novel, and significant to the field as a whole. An Original Article should be arranged into the following sections: Title page, Abstract, Introduction, Materials and Methods, Results, Discussion, Acknowledgments, and References. Original articles should not exceed 5,000 words in length (excluding references) and should be limited to a maximum of 50 references. Articles may contain a maximum of 10 figures and/or tables.

Brief Reports definitively documenting either experimental results or informative clinical observations will be considered for publication in this category. Brief Reports are not intended for publication of incomplete or preliminary findings. Brief Reports should not exceed 3,000 words in length (excluding references) and should be limited to a maximum of 4 figures and/or tables and 30 references. A Brief Report contains the same sections as an Original Article, but the Results and Discussion sections should be combined.

Reviews should present a full and up-to-date account of recent developments within an area of research. Normally, reviews should not exceed 8,000 words in length (excluding references) and should be limited to a maximum of 100 references. Mini reviews are also accepted.

Policy Forum articles discuss research and policy issues in areas related to life science such as public health, the medical care system, and social science and may address governmental issues at district, national, and international levels of discourse. Policy Forum articles should not exceed 2,000 words in length (excluding references).

Case Reports should be detailed reports of the symptoms, signs, diagnosis, treatment, and follow-up of an individual patient. Case reports may contain a demographic profile of the patient but usually describe an unusual or novel occurrence. Unreported or unusual side effects or adverse interactions involving medications will also be considered. Case

Reports should not exceed 3,000 words in length (excluding references).

News articles should report the latest events in health sciences and medical research from around the world. News should not exceed 500 words in length.

Letters should present considered opinions in response to articles published in Drug Discoveries & Therapeutics in the last 6 months or issues of general interest. Letters should not exceed 800 words in length and may contain a maximum of 10 references.

3. Editorial Policies

Ethics: Drug Discoveries & Therapeutics requires that authors of reports of investigations in humans or animals indicate that those studies were formally approved by a relevant ethics committee or review board.

Conflict of Interest: All authors are required to disclose any actual or potential conflict of interest including financial interests or relationships with other people or organizations that might raise questions of bias in the work reported. If no conflict of interest exists for each author, please state "There is no conflict of interest to disclose".

Submission Declaration: When a manuscript is considered for submission to Drug Discoveries & Therapeutics, the authors should confirm that 1) no part of this manuscript is currently under consideration for publication elsewhere; 2) this manuscript does not contain the same information in whole or in part as manuscripts that have been published, accepted, or are under review elsewhere, except in the form of an abstract, a letter to the editor, or part of a published lecture or academic thesis; 3) authorization for publication has been obtained from the authors' employer or institution; and 4) all contributing authors have agreed to submit this manuscript.

Cover Letter: The manuscript must be accompanied by a cover letter signed by the corresponding author on behalf of all authors. The letter should indicate the basic findings of the work and their significance. The letter should also include a statement affirming that all authors concur with the submission and that the material submitted for publication has not been published previously or is not under consideration for publication elsewhere. The cover letter should be submitted in PDF format. For example of Cover Letter, please visit <http://www.ddtjournal.com/downloadcentre.php> (Download Centre).

Copyright: A signed JOURNAL PUBLISHING AGREEMENT (JPA) must be provided by post, fax, or as a scanned file before acceptance of the article. Only forms with a hand-written signature are accepted. This copyright will ensure the widest possible dissemination of information. A form facilitating transfer of copyright can be downloaded by clicking the appropriate link and can be returned to the e-mail address or fax number noted on the form (Please visit

Download Centre). Please note that your manuscript will not proceed to the next step in publication until the JPA form is received. In addition, if excerpts from other copyrighted works are included, the author(s) must obtain written permission from the copyright owners and credit the source(s) in the article.

Suggested Reviewers: A list of up to 3 reviewers who are qualified to assess the scientific merit of the study is welcomed. Reviewer information including names, affiliations, addresses, and e-mail should be provided at the same time the manuscript is submitted online. Please do not suggest reviewers with known conflicts of interest, including participants or anyone with a stake in the proposed research; anyone from the same institution; former students, advisors, or research collaborators (within the last three years); or close personal contacts. Please note that the Editor-in-Chief may accept one or more of the proposed reviewers or may request a review by other qualified persons.

Language Editing: Manuscripts prepared by authors whose native language is not English should have their work proofread by a native English speaker before submission. If not, this might delay the publication of your manuscript in Drug Discoveries & Therapeutics.

The Editing Support Organization can provide English proofreading, Japanese-English translation, and Chinese-English translation services to authors who want to publish in Drug Discoveries & Therapeutics and need assistance before submitting a manuscript. Authors can visit this organization directly at <http://www.iacmhr.com/iac-eso/support.php?lang=en>. IAC-ESO was established to facilitate manuscript preparation by researchers whose native language is not English and to help edit works intended for international academic journals.

4. Manuscript Preparation

Manuscripts should be written in clear, grammatically correct English and submitted as a Microsoft Word file in a single-column format. Manuscripts must be paginated and typed in 12-point Times New Roman font with 24-point line spacing. Please do not embed figures in the text. Abbreviations should be used as little as possible and should be explained at first mention unless the term is a well-known abbreviation (e.g. DNA). Single words should not be abbreviated.

Title page: The title page must include 1) the title of the paper (Please note the title should be short, informative, and contain the major key words); 2) full name(s) and affiliation(s) of the author(s); 3) abbreviated names of the author(s); 4) full name, mailing address, telephone/fax numbers, and e-mail address of the corresponding author; and 5) conflicts of interest (if you have an actual or potential conflict of interest to disclose, it must be included as a footnote on the title page of the manuscript; if no conflict of interest exists for each author, please state "There is no conflict of interest to disclose"). Please visit [Download Centre](#) and refer to the title page of the manuscript sample.

Abstract: The abstract should briefly state the purpose of the study, methods, main findings, and conclusions. For article types including Original Article, Brief Report, Review, Policy Forum, and Case Report, a one-paragraph abstract consisting of no more than 250 words must be included in the manuscript. For News and Letters, a brief summary of main content in 150 words or fewer should be included in the manuscript. Abbreviations must be kept to a minimum and non-standard abbreviations explained in brackets at first mention. References should be avoided in the abstract. Key words or phrases that do not occur in the title should be included in the Abstract page.

Introduction: The introduction should be a concise statement of the basis for the study and its scientific context.

Materials and Methods: The description should be brief but with sufficient detail to enable others to reproduce the experiments. Procedures that have been published previously should not be described in detail but appropriate references should simply be cited. Only new and significant modifications of previously published procedures require complete description. Names of products and manufacturers with their locations (city and state/country) should be given and sources of animals and cell lines should always be indicated. All clinical investigations must have been conducted in accordance with Declaration of Helsinki principles. All human and animal studies must have been approved by the appropriate institutional review board(s) and a specific declaration of approval must be made within this section.

Results: The description of the experimental results should be succinct but in sufficient detail to allow the experiments to be analyzed and interpreted by an independent reader. If necessary, subheadings may be used for an orderly presentation. All figures and tables must be referred to in the text.

Discussion: The data should be interpreted concisely without repeating material already presented in the Results section. Speculation is permissible, but it must be well-founded, and discussion of the wider implications of the findings is encouraged. Conclusions derived from the study should be included in this section.

Acknowledgments: All funding sources should be credited in the Acknowledgments section. In addition, people who contributed to the work but who do not meet the criteria for authors should be listed along with their contributions.

References: References should be numbered in the order in which they appear in the text. Citing of unpublished results, personal communications, conference abstracts, and theses in the reference list is not recommended but these sources may be mentioned in the text. In the reference list, cite the names of all authors when there are fifteen or fewer authors; if there are sixteen or more authors, list the first three followed by *et al.* Names of journals should

be abbreviated in the style used in PubMed. Authors are responsible for the accuracy of the references. Examples are given below:

Example 1 (Sample journal reference):
Nakata M, Tang W. Japan-China Joint Medical Workshop on Drug Discoveries and Therapeutics 2008: The need of Asian pharmaceutical researchers' cooperation. *Drug Discov Ther.* 2008; 2:262-263.

Example 2 (Sample journal reference with more than 15 authors):
Darby S, Hill D, Auvinen A, *et al.* Radon in homes and risk of lung cancer: Collaborative analysis of individual data from 13 European case-control studies. *BMJ.* 2005; 330:223.

Example 3 (Sample book reference):
Shalev AY. Post-traumatic stress disorder: Diagnosis, history and life course. In: *Post-traumatic Stress Disorder, Diagnosis, Management and Treatment* (Nutt DJ, Davidson JR, Zohar J, eds.). Martin Dunitz, London, UK, 2000; pp. 1-15.

Example 4 (Sample web page reference):
World Health Organization. The World Health Report 2008 – primary health care: Now more than ever. http://www.who.int/whr/2008/whr08_en.pdf (accessed September 23, 2010).

Tables: All tables should be prepared in Microsoft Word or Excel and should be arranged at the end of the manuscript after the References section. Please note that tables should not in image format. All tables should have a concise title and should be numbered consecutively with Arabic numerals. If necessary, additional information should be given below the table.

Figure Legend: The figure legend should be typed on a separate page of the main manuscript and should include a short title and explanation. The legend should be concise but comprehensive and should be understood without referring to the text. Symbols used in figures must be explained.

Figure Preparation: All figures should be clear and cited in numerical order in the text. Figures must fit a one- or two-column format on the journal page: 8.3 cm (3.3 in.) wide for a single column, 17.3 cm (6.8 in.) wide for a double column; maximum height: 24.0 cm (9.5 in.). Please make sure that artwork files are in an acceptable format (TIFF or JPEG) at minimum resolution (600 dpi for illustrations, graphs, and annotated artwork, and 300 dpi for micrographs and photographs). Please provide all figures as separate files. Please note that low-resolution images are one of the leading causes of article resubmission and schedule delays. All color figures will be reproduced in full color in the online edition of the journal at no cost to authors.

Units and Symbols: Units and symbols conforming to the International System of Units (SI) should be used for physicochemical quantities. Solidus notation (*e.g.* mg/kg, mg/mL, mol/mm²/min) should be used. Please refer to the SI Guide www.bipm.org/en/si/ for standard units.

Supplemental data: Supplemental data might be useful for supporting and enhancing your scientific research and Drug Discoveries & Therapeutics accepts the submission of these materials which will be only published online alongside the electronic version of your article. Supplemental files (figures, tables, and other text materials) should be prepared according to the above guidelines, numbered in Arabic numerals (*e.g.*, Figure S1, Figure S2, and Table S1, Table S2) and referred to in the text. All figures and tables should have titles and legends. All figure legends, tables and supplemental text materials should be placed at the end of the paper. Please note all of these supplemental data should be provided at the time of initial submission and note that the editors reserve the right to limit the size and length of Supplemental Data.

5. Submission Checklist

The Submission Checklist will be useful during the final checking of a manuscript prior to sending it to Drug Discoveries & Therapeutics for review. Please visit [Download Centre](#) and download the Submission Checklist file.

6. Online submission

Manuscripts should be submitted to Drug Discoveries & Therapeutics online at <http://www.ddtjournal.com>. The manuscript file should be smaller than 5 MB in size. If for any reason you are unable to submit a file online, please contact the Editorial Office by e-mail at office@ddtjournal.com

7. Accepted manuscripts

Proofs: Galley proofs in PDF format will be sent to the corresponding author *via* e-mail. Corrections must be returned to the editor (proof-editing@ddtjournal.com) within 3 working days.

Offprints: Authors will be provided with electronic offprints of their article. Paper offprints can be ordered at prices quoted on the order form that accompanies the proofs.

Page Charge: A page charge of \$140 will be assessed for each printed page of an accepted manuscript. The charge for printing color figures is \$340 for each page. Under exceptional circumstances, the author(s) may apply to the editorial office for a waiver of the publication charges at the time of submission.

(Revised February 2013)

Editorial and Head Office:

Pearl City Koishikawa 603
2-4-5 Kasuga, Bunkyo-ku
Tokyo 112-0003
Japan
Tel: +81-3-5840-9697
Fax: +81-3-5840-9698
E-mail: office@ddtjournal.com

JOURNAL PUBLISHING AGREEMENT (JPA)

Manuscript No.:

Title:

Corresponding author:

The International Advancement Center for Medicine & Health Research Co., Ltd. (IACMHR Co., Ltd.) is pleased to accept the above article for publication in Drug Discoveries & Therapeutics. The International Research and Cooperation Association for Bio & Socio-Sciences Advancement (IRCA-BSSA) reserves all rights to the published article. Your written acceptance of this JOURNAL PUBLISHING AGREEMENT is required before the article can be published. Please read this form carefully and sign it if you agree to its terms. The signed JOURNAL PUBLISHING AGREEMENT should be sent to the Drug Discoveries & Therapeutics office (Pearl City Koishikawa 603, 2-4-5 Kasuga, Bunkyo-ku, Tokyo 112-0003, Japan; E-mail: office@ddtjournal.com; Tel: +81-3-5840-9697; Fax: +81-3-5840-9698).

1. Authorship Criteria

As the corresponding author, I certify on behalf of all of the authors that:

- 1) The article is an original work and does not involve fraud, fabrication, or plagiarism.
- 2) The article has not been published previously and is not currently under consideration for publication elsewhere. If accepted by Drug Discoveries & Therapeutics, the article will not be submitted for publication to any other journal.
- 3) The article contains no libelous or other unlawful statements and does not contain any materials that infringes upon individual privacy or proprietary rights or any statutory copyright.
- 4) I have obtained written permission from copyright owners for any excerpts from copyrighted works that are included and have credited the sources in my article.
- 5) All authors have made significant contributions to the study including the conception and design of this work, the analysis of the data, and the writing of the manuscript.
- 6) All authors have reviewed this manuscript and take responsibility for its content and approve its publication.
- 7) I have informed all of the authors of the terms of this publishing agreement and I am signing on their behalf as their agent.

2. Copyright Transfer Agreement

I hereby assign and transfer to IACMHR Co., Ltd. all exclusive rights of copyright ownership to the above work in the journal Drug Discoveries & Therapeutics, including but not limited to the right 1) to publish, republish, derivate, distribute, transmit, sell, and otherwise use the work and other related material worldwide, in whole or in part, in all languages, in electronic, printed, or any other forms of media now known or hereafter developed and the right 2) to authorize or license third parties to do any of the above.

I understand that these exclusive rights will become the property of IACMHR Co., Ltd., from the date the article is accepted for publication in the journal Drug Discoveries & Therapeutics. I also understand that IACMHR Co., Ltd. as a copyright owner has sole authority to license and permit reproductions of the article.

I understand that except for copyright, other proprietary rights related to the Work (e.g. patent or other rights to any process or procedure) shall be retained by the authors. To reproduce any text, figures, tables, or illustrations from this Work in future works of their own, the authors must obtain written permission from IACMHR Co., Ltd.; such permission cannot be unreasonably withheld by IACMHR Co., Ltd.

3. Conflict of Interest Disclosure

I confirm that all funding sources supporting the work and all institutions or people who contributed to the work but who do not meet the criteria for authors are acknowledged. I also confirm that all commercial affiliations, stock ownership, equity interests, or patent-licensing arrangements that could be considered to pose a financial conflict of interest in connection with the article have been disclosed.

Corresponding Author's Name (Signature):

Date:

